HUMECTANTS TO AUGMENT CURRENT FROM METALLIZED ZINC CATHODIC PROTECTION SYSTEMS ON CONCRETE

Final Report

SPR 384

HUMECTANTS TO AUGMENT CURRENT
FROM METALLIZED ZINC CATHODIC PROTECTION
SYSTEMS ON CONCRETE

Final Report

SPR 384

by

Gordon R. Holcomb, Bernard S. Covino, Jr., Stephen D. Cramer,
James H. Russell, Sophie J. Bullard, and W. Keith Collins
Albany Research Center, U. S. Department of Energy, Albany OR 97321

Jack E. Bennett
J. E. Bennett Consulting, Inc., Chardon OH 44024

Steven M. Soltesz and H. Martin Laylor
Oregon Department of Transportation, Salem OR 97301

for

December 2002

1. Report No. FHWA-OR-RD-03-08	2. Government Accession No.	3. Recipient's Catalog No.
4. Title and Subtitle Humectants to Augment Current from Metallized Zinc Cathodic Protection Systems on Concrete		5. Report Date December 2002
		6. Performing Organization Code
7. Author(s) Gordon R. Holcomb, Bernard S. Covino, Jr., Stephen D. Cramer, James H. Russell, Sophie J. Bullard, and W. Keith Collins Albany Research Center, U. S. Department of Energy, Albany OR 97321 Jack E. Bennett, J. E. Bennett Consulting, Inc., Chardon OH 44024 Steven M. Soltesz and H. Martin Laylor, Oregon Department of Transportation, Salem OR 97301		8. Performing Organization Report No.
9. Performing Organization Name and Address Oregon Department of Transportation Research Group 200 Hawthorne Avenue SE, Suite B-240 Salem, Oregon 97301-5192		10. Work Unit No. (TRAIS)
		11. Contract or Grant No. SPR 384
12. Sponsoring Agency Name and Address Oregon Department of Transportation Federal Highway Administration Research Group and 400 Seventh Street S.W. 200 Hawthorne Avenue SE, Suite B-240 Washington, DC 20590 Salem, Oregon 97301-5192		13. Type of Report and Period Covered Final Report
		14. Sponsoring Agency Code
15. Supplementary Notes		

16. Abstract

Cathodic protection (CP) systems using thermal-sprayed zinc anodes are employed to mitigate the corrosion process in reinforced concrete structures. However, the performance of the anodes is improved by moisture at the anode-concrete interface. Research was conducted to investigate the effect of hydrophilic chemical additives, humectants, on the electrical performance and service life of zinc anodes. Lithium bromide and lithium nitrate were identified as feasible humectants with lithium bromide performing better under galvanic CP and lithium nitrate performing better under impressed current CP. Both humectants improved the electrical operating characteristics of the anode and increased the service life by up to three years.

17. Key Words Thermal-Spray, Zinc, Cathodic Protection, Yaquina Bay Bridge, Humectant, Lithium Bromide, Lithium Nitrate, Potassium Acetate, Corrosion	18. Distribution Statement Copies available from NTIS, and online at http://www.odot.state.or.us/tddresearch

| 19. Security Classification (of this report) Unclassified	20. Security Classification (of this page) Unclassified	21. No. of Pages 122 + Appendix	22. Price

Technical Report Form DOT F 1700.7 (8-72)   Reproduction of completed page authorized   ♻ Printed on recycled paper

SI* (MODERN METRIC) CONVERSION FACTORS

APPROXIMATE CONVERSIONS TO SI UNITS					APPROXIMATE CONVERSIONS FROM SI UNITS				
Symbol	When You Know	Multiply By	To Find	Symbol	Symbol	When You Know	Multiply By	To Find	Symbol
LENGTH					**LENGTH**				
in	inches	25.4	millimeters	Mm	mm	millimeters	0.039	inches	in
ft	feet	0.305	meters	M	m	meters	3.28	feet	ft
yd	yards	0.914	meters	M	m	meters	1.09	yards	yd
mi	miles	1.61	kilometers	Km	km	kilometers	0.621	miles	mi
AREA					**AREA**				
in^2	square inches	645.2	millimeters squared	mm^2	mm^2	millimeters squared	0.0016	square inches	in^2
ft^2	square feet	0.093	meters squared	m^2	m^2	meters squared	10.764	square feet	ft^2
yd^2	square yards	0.836	meters squared	m^2	ha	hectares	2.47	acres	ac
ac	acres	0.405	hectares	Ha	km^2	kilometers squared	0.386	square miles	mi^2
mi^2	square miles	2.59	kilometers squared	km^2	**VOLUME**				
VOLUME					mL	milliliters	0.034	fluid ounces	fl oz
fl oz	fluid ounces	29.57	milliliters	ML	L	liters	0.264	gallons	gal
gal	gallons	3.785	liters	L	m^3	meters cubed	35.315	cubic feet	ft^3
ft^3	cubic feet	0.028	meters cubed	m^3	m^3	meters cubed	1.308	cubic yards	yd^3
yd^3	cubic yards	0.765	meters cubed	m^3	**MASS**				
NOTE: Volumes greater than 1000 L shall be shown in m^3.					g	grams	0.035	ounces	oz
MASS					kg	kilograms	2.205	pounds	lb
oz	ounces	28.35	grams	g	Mg	megagrams	1.102	short tons (2000 lb)	T
lb	pounds	0.454	kilograms	kg	**CHARGE DENSITY**				
T	short tons (2000 lb)	0.907	megagrams	Mg	kC/m^2	kilocoulombs/m^2	0.02581	amp-hours per ft^2	A-hr/ft^2
CHARGE DENSITY					**TEMPERATURE (exact)**				
A-hr/ft^2	Amp-hours per ft^2	38.75	kilocoulombs/m^2	kC/m^2	°C	Celsius temperature	1.8C + 32	Fahrenheit	°F
TEMPERATURE (exact)									
°F	Fahrenheit temperature	5(F-32)/9	Celsius temperature	°C					
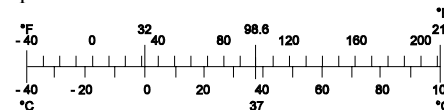
* SI is the symbol for the International System of Measurement

(4-7-94 jbp)

ACKNOWLEDGEMENTS

DISCLAIMER

This document is disseminated under the sponsorship of the Oregon Department of Transportation and the United States Department of Transportation in the interest of information exchange. The State of Oregon and the United States Government assume no liability of its contents or use thereof.

The contents of this report reflect the views of the authors, who are responsible for the facts and accuracy of the data presented herein. The contents do not necessarily reflect the official policies of the Oregon Department of Transportation or the United States Department of Transportation.

The State of Oregon and the United States Government do not endorse products of manufacturers. Trademarks or manufacturers' names appear herein only because they are considered essential to the object of this document.

This report does not constitute a standard, specification, or regulation.

HUMECTANTS TO AUGMENT CURRENT FROM METALLIZED ZINC CATHODIC PROTECTION SYSTEMS ON CONCRETE

TABLE OF CONTENTS

LIST OF TABLES

LIST OF PHOTOS/FIGURES

viii

1.0   INTRODUCTION

1.1   BACKGROUND

1.1.1   Bridge Rehabilitation with Cathodic Protection in Oregon

Reinforced concrete bridges exposed to chloride environments, such as on the Oregon coast, can undergo extensive corrosion damage. Chloride ions (Cl^-) deposited onto the concrete migrate in towards the reinforcing steel, where the ions disrupt the passive films that normally protect steel in concrete from corrosion. Subsequent corrosion of the steel results in a volume expansion that causes cracking and delamination of the concrete, which aids in further Cl^- transport to the steel. Section loss of the steel eventually results in loss of structural integrity of the structure.

Corrosion of bridges is a national problem. A report to the federal government reported that 15 percent of the nation's 583,000 bridges are structurally deficient, with corrosion of steel and steel reinforcement the primary cause (*Koch, et al. 2002*). The annual direct cost of corrosion for highway bridges was estimated at $8.3 billion per year. Indirect costs from traffic delays and lost productivity were estimated at more than ten times this amount. Costs for bridge maintenance, rehabilitation, and replacement are a necessary use of Department of Transportation (DOT) funds.

Beginning in the early 1990s, Oregon DOT started rehabilitating reinforced coastal bridges and protecting them with cathodic protection (CP) using thermal-sprayed (TS) zinc (Zn) anodes. These extensive rehabilitation and protection projects cost approximately 35 percent of that estimated for damaged section replacement (*Holcomb and Cryer 1998*). Table 1.1 shows the extent of Oregon's efforts in bridge rehabilitation and protection with TS Zn CP. Average costs, in 1997 dollars, for the first four projects, was $52/ft^2 ($556/m^2) based on total project costs, and $14/ft^2 ($151/m^2) based on the CP portion of the projects (*Holcomb and Cryer 1998*).

Table 1.1: Oregon's thermal-sprayed zinc cathodic protection systems on coastal bridges

PROJECT	YEAR BUILT	YEAR OF CP	CP SURFACE AREA ft^2 (m^2)	TOTAL COST*
Cape Creek	1931	1991	102,500 (9,520)	$2.5M
Yaquina Bay Arches	1934	1994	195,500 (18,160)	$10.8M
Depoe Bay	1927 (widened in 1939)	1995	67,000 (6,220)	$4.4M
Yaquina Bay South Approach	1934	1997	65,000 (6,040)	$2.4M
Big Creek Bridge	1931	1998	20,000 (1,860)	$2.1M
Rocky Creek Bridge	1927	2001	40,000 (3,720)	$3.9M
Cummins Creek Bridge	1931	2001	20,000 (1,860)	$1.7M
Rogue River Patterson Bridge	1930	2003	350,000 (32,520)	$18.4M

* Contract cost at the time of the CP project.

1.1.2 Cathodic Protection Processes

Cathodic Protection (CP) systems work by preferentially oxidizing the Zn anode in place of the steel rebar. This can be accomplished with either galvanic CP (GCP) or impressed current CP (ICCP). In GCP (also known as sacrificial CP or SACP) the Zn anode is electrically connected to the steel rebar. This allows for the naturally higher chemical potential of Zn, to drive the oxidation reactions to occur at the Zn anode as opposed to at the steel rebar. In comparison with ICCP, GCP has several advantages, ease of application and much less electrical hardware and system maintenance. Galvanic CP is extensively used in Florida for substructures in tidal and splash zones (*Scannell, Sohanghpurwala and Powers 1995*). In ICCP the Zn anode is connected to the steel rebar through a power supply. The power supply supplements the natural chemical potential between Zn and iron (Fe) with electrical potential. It offers the advantage of an assured amount of protection current. Most of the CP systems in Oregon are ICCP. Galvanic CP systems require high temperatures and humidity to maintain enough protection of the steel rebar.

In both GCP and ICCP systems, physical changes occur at the Zn-concrete interface with time (*Covino, et al. 1996a; Covino, et al. 1996b; Covino, et al. 2002; Holcomb, et al. 1996*). Zinc oxide (ZnO) reaction products accumulate at the interface between the TS Zn anode and the concrete, as the anode is consumed. Zinc oxide occupies a larger volume than Zn. As a consequence stresses can build up at the interface, leading to cracking and eventual delamination of the anode along the interface. Zinc oxide is also a relatively weak material. The accumulation of zinc oxide reaction products at the interface will eventually weaken the initial mechanical bond between the much stronger zinc anode and the concrete. To somewhat mitigate these effects, zinc ions (Zn^{2+}) have been shown to migrate into the cement paste and displace calcium (Ca) ions within the cement (*Covino, et al. 2002*). This migration and displacement results in secondary mineralization of the cement paste involving the zinc ions. To some extent, secondary mineralization of the Zn reaction products reduces the damaging effects of Zn oxide accumulation, by dissipating some of the oxidized Zn into the cement matrix.

The accumulation of ZnO at the Zn-concrete interface increases the electrical resistivity at the interface. Increased electrical resistivity can result in GCP systems not generating enough current to protect the rebar. In ICCP systems, the required voltage to maintain a constant protection current can increase beyond the compliance voltage of the power supplies, resulting in a lowering of the protection current.

Hence, the accumulation of ZnO at the Zn-concrete interface can result in three different failure modes of the CP system: 1) insertion of a weak intermediate layer between the anode and concrete to reduce bond strength, 2) delamination of the coating along the interface as the result of stresses produced in the reaction product layer, and 3) reduction of the protection current below needed levels by the growth of an insulating intermediate layer in the current path.

The presence of water at the Zn-concrete interface improves the performance of the CP system and increases its service life (*Bullard, et al. 1997a; Bullard, et al. 1998; Covino, et al. 2002*). Water accomplishes this by:

- Increasing the electrical conductivity of the CP system at the location where resistivities are highest. This increases the protection current in GCP systems and lowers the voltage needed to maintain a constant current in ICCP systems.

- Increasing the mobility of Zn^{2+} thereby delaying the buildup of the zinc oxide reaction layer. This delays the formation of the weak intermediate zinc oxide layer between the anode and concrete. It also allows for stress relief in the TS Zn coating because of increased secondary mineralization delaying delamination along the anode-concrete interface.

- Increasing the mobility of hydroxyl ions (OH^-), which allows the high pH pore water in the bulk cement to migrate to the anode-concrete interface, raises the pH from the low levels that are typically produced at the anode by CP (pH 6-8). This helps maintain a stronger bond between the TS Zn and the concrete, since concrete is known to lose much of its strength below a pH of 7-8 (*Mehta 1991*).

Accelerated ICCP laboratory tests comparing the effects of a dry environment with that of an environment with wet and dry cycles have confirmed that water increases adhesion life and decreases the voltage needed to maintain a constant ICCP current.

1.1.3 Humectants

Humectants, as used in this report, are water-soluble chemical additives that attract water. When applied to the surface of the concrete, the idea is that they will increase the amount of moisture at the Zn-concrete interface and thereby increase the lifetime of the CP system by the processes described above.

Three humectants, chosen on the basis of a screening experiment (*Bennett 1998*), were used in this study. They were lithium bromide (LiBr), lithium nitrate ($LiNO_3$), and potassium acetate ($KC_2H_3O_2$). During this study, it was found that $KC_2H_3O_2$ was not enhancing the performance of the CP system (and was at times detrimental). As a result it was dropped from further investigation. Adhesion strength results for $KC_2H_3O_2$ are given in the main body of this report, including cases of early anode delamination. Other results relating to $KC_2H_3O_2$ are found in the Appendix.

Related to this project, several publications have been written on laboratory and field study research in progress (*Bennett, et al. 2000; Bullard, et al. 2000; Bullard, et al. 2001; Covino, et al. 1999a; Covino, et al. 1999b; Covino, et al. 1999c; Holcomb, et al. 2000a; Holcomb, et al. 2000b*).

1.2 PROBLEM DEFINITION

Thermal-sprayed Zn anodes are being used increasingly in CP systems for steel-reinforced concrete structures. Recent research (SPR #364) by Oregon DOT and the U.S. Department of Energy (DOE) has examined the effects of electrochemical aging on the long-term performance of TS Zn anodes, primarily for ICCP systems (*Covino, et al. 2002*). Both laboratory and field

studies have shown that Zn anode reaction products accumulate at the Zn-concrete interface with increasing electrochemical age. These reaction products eventually: decrease the bond strength of the anode to the concrete, increase the driving voltage needed to maintain a specified level of protection for the rebar, decrease the permeability of the Zn-concrete interface to gases and precipitation, and alter the chemistry of the interface. The level of moisture at the Zn-concrete interface was of particular importance in assuring a long service life for the anode. Based on bond strength, the anode service life was projected to be in excess of 25 years when the anode was repeatedly wetted, but it decreased to roughly five years when not wetted. Equally important, driving voltages were substantially lower when the anode was wetted.

Sheltered areas on structures receive less moisture than those fully exposed to the environment. Humectants are chemical solutions that, when applied to a TS Zn anode, can maintain a high moisture level at the Zn-concrete interface regardless of weather conditions or the location on the structure. This elevated moisture level should help dissipate Zn reaction products, promote improved current flow, reduce operating voltages, maximize secondary mineralization of Zn anode dissolution products, and improve long-term anode bond strength.

1.3   STUDY OBJECTIVES

- Determine the effectiveness of humectants (chemical additives) for improving the performance and extending the service life of TS Zn anodes used in the CP of steel-reinforced concrete.

- Examine the impact of the choice of humectant on the performance of Zn anodes, and the relationship between periodic wetting of the anode surface, ambient humidity level, electrochemical aging, and prior electrochemical aging on anode performance.

- Develop an understanding of how humectants affect the overall performance of ICCP and GCP systems.

- Determine an estimate of the increased service life to be gained by using humectants.

- Perform life cycle cost calculations for anode systems with and without humectants.

- Provide recommendations and guidelines for the implementation of humectant treatments on TS Zn anode CP systems.

1.4   WORK PLAN SYNOPSIS

Three humectants (LiBr, $LiNO_3$, and $KC_2H_3O_2$) were examined for their usefulness in a variety of laboratory and field experiments. Due to poor results with $KC_2H_3O_2$, this humectant was dropped from consideration during testing. Limited results for $KC_2H_3O_2$ are given in the main text of this report; additional results are presented in the Appendix.

1.4.1 Long-term Laboratory Experiments (ARC)

Long-term laboratory experiments were conducted at the Albany Research Center (ARC). Humectants were applied to both new and previously-aged concrete slabs coated with TS Zn. New concrete slabs contain an expanded steel mesh and were thermal-sprayed with Zn. Slab surface preparations were according to Oregon DOT practices. Previously-aged slabs were selected from those used as part of SPR # 364 (*Covino, et al. 2002*). Accelerated aging of both types of slabs was done galvanostatically at a nominal current density of 2.5 mA/ft^2 (27 mA/m^2) (compared to 0.2 mA/ft^2 (2.2 mA/m^2) used by Oregon DOT) for up to 12 months. A smaller group of the new slabs were cyclically aged at 2.5 mA/ft^2 (27 mA/m^2) for 3 weeks, then 0.2 mA/ft^2 (2.2 mA/m^2) for 1 week. The purpose of the cyclic tests was to age the slabs rapidly to a given electrochemical age as an ICCP anode, and then determine the operating voltages at the current density used by Oregon DOT to protect its coastal bridges. Galvanic aging of a group of both new and previously aged slabs was done by shorting the Zn anode coating to the steel mesh cathode.

Measurements were made to determine the effect of the humectants on operating characteristics such as ICCP voltage requirements, GCP current flow, and bond strength. Anode bond strength was measured at periodic intervals during electrochemical aging. Depolarization from 0.2 mA/ft^2 (2.2 mA/m^2) on the cyclic slabs was measured. The chemistry of the Zn-concrete interface was characterized during the electrochemical aging using an analytical scanning electron microscope (ASEM) and an electron microprobe.

1.4.2 Short-Term Chamber Experiments (ARC)

A small humidity chamber was used for two types of experiments. Circuit resistance responses to temperature and humidity were measured on slabs prepared similarly to the new slabs described above after at least one month of equilibration at a constant temperature and humidity. Very low current levels of 0.02 mA/ft^2 (0.22 mA/m^2) were used, so as to eliminate any effects of electrochemical aging from test to test.

The other type of test measured mass changes as functions of temperature and humidity due to the humectants attracting water. Thin slices of concrete were cut from 3-inch (7.62 cm) diameter cylinders that were made with 2, 5, and 10 lb/yd^3 of NaCl (1.2, 3.0, and 5.9 kg/m^3). Half were thermal-sprayed with zinc. Humectants were applied with pipettes to allow an exact amount to be added to each slice. The humectant treated slices, along with the controls, were equilibrated at constant temperature and humidity. The mass of each slice was measured periodically during the equilibration process.

1.4.3 Long-Term Laboratory GCP Experiments (Ohio)

The effectiveness of each humectant was tested on thermal-sprayed Zn anodes as a function of environment (low RH, high RH, outdoor exposed, and outdoor sheltered) in Chardon Ohio. Concrete blocks were constructed with 5.1 lb/yd^3 (3.0 kg/m^3) of NaCl. They were then aged, sandblasted, thermal-sprayed with Zn, and humectant treated (except the controls). The galvanic current was monitored during the length of the test. Additional items were examined, including

the effects of reapplying the humectant and the concentration of Cl^- in the concrete, using additional blocks.

1.4.4 Yaquina Bay Bridge Field Trial (Oregon)

Four ICCP zones of the Yaquina Bay Bridge (located on the Pacific coast of Oregon) were selected for a field study. Two of the zones were untreated controls, one zone was treated with LiBr, and one zone was treated with $LiNO_3$. Operating current and voltage were monitored, and the interfacial chemistry was examined as part of the trial.

2.0   HUMECTANT SCREENING (OHIO)

Experience has shown that metallized Zn delivers a relatively large protective galvanic current when first connected to the steel, but the current decreases significantly with time (*Cramer, et al. 2002b*). The amount of current that flows is dependent on several factors, including the following: the resistivity of the concrete (largely a function of concrete quality and composition, Cl⁻ contamination, moisture content, and temperature), depth of cover over the reinforcement, charge history of the anode, and frequency of wetting. Studies have indicated that galvanic Zn anode performance is not likely to be adequate unless the anode is subjected to periodic direct wetting (*Powers, Sagues and Murase 1992; Sagues, et al. 1994*).

If a technique could be found to enhance the flow of GCP current, particularly in dryer environments, then the number of sites where simple GCP systems could be used to control corrosion could be greatly increased. The resulting reduction in installation, monitoring, and maintenance costs could encourage the acceptance of CP for reinforced concrete structures.

The choice of chemicals used in this report for use as humectants on Zn anodes for CP systems, on reinforced concrete, arose from a screening study by Bennett (*1998*). The results of this screening study are presented below.

2.1   SCREENING STUDY PROCEDURES

Thirty concrete blocks were constructed with dimensions of 12 x 9 x 2 inch (30.5 x 22.9 x 5.1 cm). The concrete contained a 3/16 diameter x 72-inch (0.5 diameter x 183 cm) long mild steel rod that was bent back and forth to form a layer at a depth of 1.5-inch (3.8 cm) from the top surface of the concrete block. The surface area of the steel rod was 0.29 ft^2 (0.027 m^2). The mix proportions for the concrete were as follows:

Type 1A Portland Cement -	715 lb/yd^3 (425 kg/m^3)
Lake Sand Fine Aggregate -	1010 lb/yd^3 (600 kg/m^3)
No.8 Marblehead Limestone -	1830 lb/yd^3 (1090 kg/m^3)
Water -	285 lb/yd^3 (170 kg/m^3)
NaCl -	0 and 8.2 lb/yd^3 (4.9 kg/m^3)
Entrained Air -	about 6%

Following a 24-hour mold curing period, the blocks were wrapped wet in plastic and allowed to cure for 28 days at room temperature. The top surfaces of the specimens were prepared by sandblasting to remove the cement paste layer, but care was taken not to expose too much coarse aggregate. The top surface of the concrete blocks was then coated with pure Zn by combustion spray using an oxy-acetylene flame. The blocks were not preheated. Zinc was hand-applied to a thickness of approximately 15 mil (0.38 mm). An electrical connection was made between the

metallized Zn and the embedded steel across a 10 Ω resistor to facilitate measurement of galvanic current. The blocks were then placed in a controlled room where the relative humidity (RH) was maintained between 55% and 60%. Temperature was maintained at 20°C ± 2°C.

Each block was then brush coated with a solution containing 300 g/l of a performance-enhancing chemical. Since metallized coatings are inherently porous, the solution was transported to the anode-concrete interface by capillary action. Two coats were applied resulting in a total application rate of about 30 ml/block. Control blocks were coated with distilled water with no chemical addition.

Current flowing between the Zn anode and the embedded steel was monitored and recorded for a period of 60 days. After 60 days the RH was raised to 80-85%. Current was then monitored and recorded under this condition for an additional 30-day period.

2.2   SCREENING STUDY RESULTS

At the start of the experiment the Zn anode was wet with distilled water, which produced a large galvanic current. Since these specimens were maintained at low humidity (55-60% RH), the current rapidly decayed with time. This current decay was much more pronounced for Cl⁻ free specimens than for specimens contaminated with 8.2 lbs NaCl/yd^3 (4.9 kg/m^3). After 11 days, distilled water was again applied to the Zn anode and galvanic current again surged to relatively high levels. Following wetting, the current again decayed and appeared to reach a stable value of approximately 1.4 mA/m^2 for the Cl⁻ contaminated specimen, and less than 0.1 mA/m^2 for the Cl⁻ free.

After 60 days the specimens were placed in an environment of about 80% RH and galvanic current increased to approximately 2.7 and 10.0 mA/m^2 for the Cl⁻ free and Cl⁻ contaminated specimens respectively. In the absence of direct periodic wetting of the anode, it is likely that these specimens would require impressed current to insure protection against corrosion of embedded steel.

A total of 13 chemicals were selected and investigated for their ability to enhance galvanic current from metallized Zn anodes on concrete. Chemicals were chosen primarily for their efficiency as humectants (chemicals that are either deliquescent or hygroscopic). Potassium (K)- and lithium (Li)-based chemicals were targeted since these are generally more deliquescent. In the case of Li-based chemicals, their ability to inhibit alkali-silica reaction (ASR) was also targeted. Results are summarized in Table 2.1. The most effective chemicals were bromides, acetates, chlorides, and nitrates. Several others, including certain organics, resulted in only slight improvement in galvanic current.

Table 2.1: Results of feasibility study of chemicals for use as humectants (*Bennett 1998*)

CHEMICAL	PERFORMANCE
Lithium Bromide	Exceptional improvement (galvanic current = 10-20 x control)
Potassium Acetate	Good improvement (galvanic current = 5-10 x control)
Lithium Acetate	Good improvement (galvanic current = 5-10 x control)
Sodium Chloride	Good improvement (galvanic current = 5-10 x control)
Calcium Chloride	Good improvement (galvanic current = 5-10 x control)
Lithium Nitrate	Good improvement (galvanic current = 5-10 x control)
Glycerol	Slight improvement (galvanic current = 1-2 x control)
Ethylene Glycol	Slight improvement (galvanic current = 1-2 x control)
Potassium Phosphate	Slight improvement (galvanic current = 1-2 x control)
Potassium Carbonate*	Slight improvement (galvanic current = 1-2 x control)
Potassium Nitrate*	Slight improvement (galvanic current = 1-2 x control)
Lithium Hydroxide	Slight improvement (galvanic current = 1-2 x control)
Potassium Borate*	Slight improvement (galvanic current = 1-2 x control)

* From a previous study conducted January, 1997

Lithium bromide (LiBr) was the best chemical tested from the standpoint of maximum galvanic current, about 15 times that of the control specimen at 55% RH. Even after equilibrating at 80% RH, galvanic current for the specimen treated with LiBr was about 7 times that of the control specimen.

Treatment with potassium acetate ($KC_2H_3O_2$) and lithium acetate ($LiC_2H_3O_2$) both increased the flow of galvanic current by a factor of approximately 7-9 at 55% RH, and by a factor of 2 at 80% RH. These chemicals are both readily available, non-toxic, and environmentally acceptable.

Lithium nitrate ($LiNO_3$) had some potential, increasing galvanic current by a factor of 7 at 55% RH. Sodium chloride (NaCl) was also an effective chemical for enhancing galvanic current, increasing current up to an order of magnitude at 55% RH and by a factor of about 2 at 80% RH. Calcium chloride ($CaCl_2$) was found to be about as effective as NaCl.

2.3   SELECTED HUMECTANTS

Application of solutions of potassium or lithium bromide, acetate, chloride or nitrate was shown to greatly enhance the flow of galvanic current for CP systems using metallized Zn anodes. Such chemicals were capable of increasing current by a factor of between 2 and 15, depending on RH and Cl^- contamination of the concrete.

The use of chlorides or bromides may be viewed with concern since both of these anions are capable of destroying the protective passive film that forms on steel in concrete. Again, it may be reasoned that electromigration will maintain these anions in the vicinity of the anode-concrete interface and away from the reinforcing steel, but this assumption is yet to be demonstrated. Acetates and nitrates are expected to raise no such concern.

It has been reported, and is generally accepted, that the presence of Li ions in the concrete will prevent or inhibit expansion due to ASR. It has been suggested that the lithium silicate reaction product does not have the capacity to expand, as do the sodium and potassium silicates. It has

been demonstrated that Li compounds mixed into fresh concrete as an admixture will prevent damage that would otherwise occur later due to ASR. It has also been shown that lithium cations can be injected into concrete during electrochemical chloride extraction and will prevent or inhibit damage due to ASR (*Bennett, et al. 1993*).

Based on this feasibility study, three chemicals were chosen for use as humectants for the research part of this project: Lithium Bromide (LiBr), Lithium Nitrate ($LiNO_3$), and Potassium Acetate ($KC_2H_3O_2$).

3.0   HUMECTANT THERMODYNAMICS

3.1   WATER ABSORPTION

Humectants lower the activity of water (which for an ideal solution is the RH above the solution) by retaining it within the system. If the cement-humectant-water ternary system is simplified to a humectant-water binary system, then Equation 3-1 can be used with the data in Table 3.1 to calculate the water activity, a_w, as a function of humectant molality, m_i (*Zaytsev and Aseyev 1992*). Molality is the number of moles dissolved in 1 kg of solvent.

$$\ln a_w = \frac{t m_i M_i}{55510 RT} \left\{ B_{1i} + a_i t + b_i t^2 + \frac{B_{2i} m_i M_i}{1000 + m_i M_i} \right\} \tag{3-1}$$

In Equation 3-1, t is the temperature in ºC, M_i is the molecular weight of the humectant, R is the gas constant (8.31441 J/kmol), T is the absolute temperature in K, and B_{1i}, a_i, b_i, and B_{2i} are constants which are given in Table 3.1.

Table 3.1: Parameters used in Equation 3-1 to calculate the activity of water in binary mixtures of humectant and water (*Zaytsev and Aseyev 1992*)

PARAMETER	LiBr		LiNO₃	
	0.293-4.78 *m*	5.05-15.9 *m*	0.297-5.48 *m*	5.91-19.54 *m*
M_i	86.845	86.845	68.946	68.946
B_{1i}	-7295.73	-8192.00	-4096.00	-6212.82
a_i	299.97	659.93	-128.00	-66.15
b_i	-2.36	-8.35	7.74	7.50
B_{2i}	-9213.91	-21117.89	-5573.42	-3683.06

Figure 3.1 shows the results of such calculations at 25ºC. The gaps between the molality ranges in Table 3.1 were smoothed and interpolated. Based on cold-water solubility limits (*Weast 1979*) of 1.45 kg/L (16.7 *m*) for LiBr and 0.898 kg/L (13.0 *m*) for LiNO₃, the calculated RH above saturated solutions will be 8% and 45%, respectively. This value for LiNO₃ closely agrees with an experimentally determined water activity of 0.47 above saturated LiNO₃•3H₂O at 25ºC (*Stokes and Robinson 1949; Robinson and Stokes 1959*). Figure 3.1 is useful in understanding how humectants work. For example, a saturated solution of LiBr (16.7 *m*) in an environment with a RH of 50% will absorb water until the concentration of LiBr is down to approximately 8 m (the concentration of LiBr in Figure 3.1 at a RH of 50%). Figure 3.1 also suggests that LiBr should be a more powerful humectant than LiNO₃, especially in dry environments, i.e., below a RH of 50%.
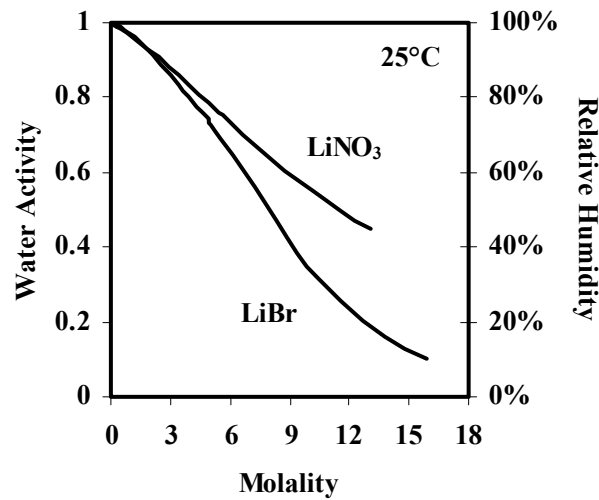
Figure 3.1: Water activity as a function of humectant molality at 25°C

Equilibration experiments, described in Section 4.2, used a humidity chamber to expose humectant-treated and control samples at fixed values of temperature and RH. Table 3.2 shows the results of using Equation 3-1, and the parameters in Table 3.1, to calculate humectant molality under these conditions.

Table 3.2: Calculated humectant molality at 90°F (32.2°C) at values of RH in equilibrium experiments

RH	CALCULTATED LiBr MOLALITY	CALCULATED LiNO$_3$ MOLALITY
35	9.9	13.0[a]
50	8.1	13.0[a]
70	5.8	10.7
80	4.4	7.7

[a]Saturated solution of LiNO$_3$ (using the solubility limit at 25ºC).

3.2   BROMIDE OXIDATION

Since the humectants are expected to reside in the Zn-concrete reaction zone, and this is the region of the highest voltage drop (*Orlova, et al. 1999*), it is possible that bromide ions (Br⁻) could be oxidized in LiBr-treated ICCP. Nitrate ions are already fully oxidized, so no such reactions are possible with LiNO$_3$ treatments. The potential-pH diagram (*Pourbaix 1974*) for Br in water at 25°C is shown in Figure 3.2. The reactions of interest in Figure 3.2 are shown in Table 3.3.
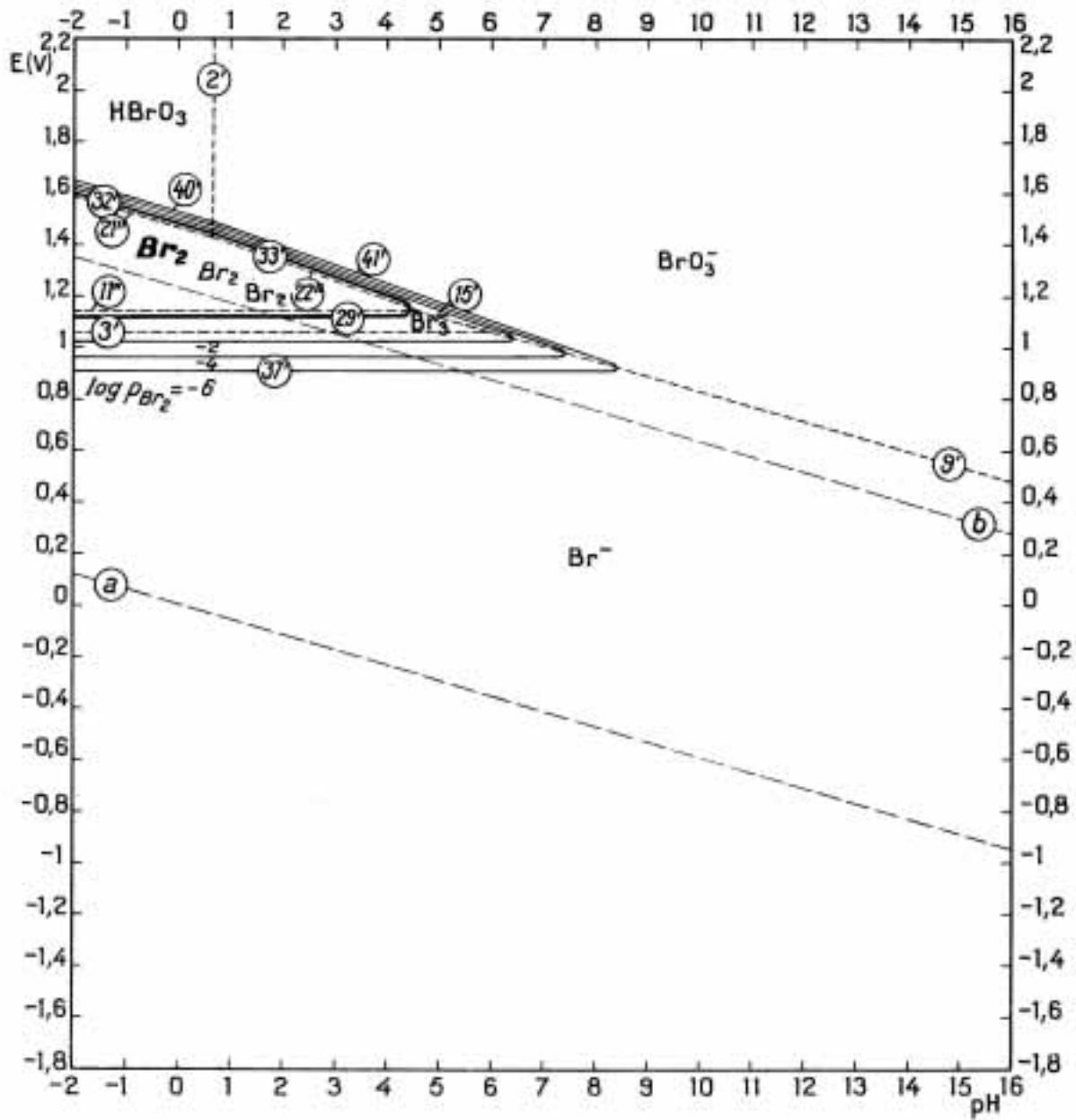
Figure 3.2: Potential-pH diagram at 25°C for Br in water (*Pourbaix 1974*)

Table 3.3: Selected oxidation reactions in the Br-H₂O system at 25°C (*Pourbaix 1974*)

OXIDATION REACTION	E_o, V	FIGURE 3.2 LINE	EQUATION
$2H_2O = 4H^+ + O_2 + 4e^-$	$1.228 - 0.0591pH + 0.0147\log P_{O_2}$	b	**3-2**
$2Br^- = Br_2 + 2e^-$	$1.082 \qquad\qquad + 0.0295\log(P_{Br_2} / C_{Br^-}{}^2)$	37'	**3-3**
$Br^- + 3H_2O = BrO_3^- + 6H^+ + 6e^-$	$1.423 - 0.0591pH + 0.0098\log(C_{BrO_3^-} / C_{Br^-})$	9'	**3-4**
$3Br^- = Br_3^- + 2e^-$	$1.051 \qquad\qquad + 0.0295\log(C_{Br_3^-} / C_{Br^-}{}^3)$	3'	**3-5**

Loss of Br from the system could occur by Br⁻ oxidizing to form Br_2 (Equation 3-3), which could then be released into the atmosphere. Figure 3.2 shows this as the "Br_2 nose" that extends up to a pH of 8. The pH of zinc anode-concrete interfaces from bridge ICCP systems were measured after electrochemical aging of about 3 years, and were found to be between 7 and 8 (*Covino, et al. 1997a; Covino, et al. 2002*). In the absence of a humectant it was surmised that Equation 3-2 was occurring, which lowered the interfacial pH. In Figure 3.2, the transition from O_2 evolution (line b, Equation 3-2) to Br_2 evolution (line 37', Equation 3-3) at a P_{Br_2} of 10^{-6} occurs at a pH of about 5.5, which is lower than the observed pH values.

It is possible, however, that the potentials of these reactions could differ in the more complex concrete-zinc system such that the oxidation to Br_2 occurs in preference to O_2 evolution. This would result in Br_2 production with pH values of up to 8. Such a situation occurs with Cl⁻ oxidation to Cl_2 in the presence of graphite. In this case, the overvoltage for oxygen evolution is much higher than that of Cl_2 evolution, and when anodically polarized, a graphite anode generates Cl_2 (*Wagner 1992; Cramer, et al. 2002a*).

Alternatively, if the pH at the Zn anode interface is greater than about 8, it is possible that Br⁻ will be oxidized to other oxygen derivatives of bromine, such as hypobromite (BrO⁻) or bromate (BrO₃⁻). Electrochemical generation of the latter species is especially likely (line 9' in Figure 3.2), and is the basis for a commercial process for production of both potassium bromate and sodium bromate (*Sugino 1964*). In this case, loss of Br from the system would not occur, but conversion to oxygen derivatives of Br would compromise the effectiveness of the chemical as a humectant.

4.0 EXPERIMENTAL PROCEDURES

The experiments conducted for this project can be divided into four main categories: long-term laboratory experiments performed at ARC, short-term experiments performed at ARC, long-term experiments performed in Ohio, and the field trial on the Yaquina Bay Bridge in Newport, Oregon.

4.1 LONG-TERM LABORATORY EXPERIMENTS (ARC)

The goal of the long-term laboratory experiments conducted at ARC was to test the effectiveness of each humectant on TS Zn anodes as a function of environment. Environmental conditions included low and high RH, electrochemical age (both new and a variety of initial electrochemical ages) and current density (both GCP and accelerated ICCP).

4.1.1 New Sample Preparation

Concrete slabs with an imbedded steel mesh were prepared to chemically, physically, and mechanically approximate a section of a reinforced concrete structure. The slab dimensions were 9 x 13 x 2 in (23 x 33 x 5 cm). Reinforcing steel was simulated with a layer of No. 16 expanded steel mesh and was cast with 1.25 in (3.2 cm) concrete cover. Wires were welded to the mesh at two corners and protruded beyond the top surface of the slab to provide electrical contact leads. The concrete mix design approximated that used in Oregon's coastal bridges that were constructed in the 1930s and had a water-cement ratio of 0.48. Sodium chloride (NaCl) was added to the concrete mix at 5.0 lb/yd^3 (3.0 kg/m^3) to approximate the present salt content of coastal bridges and to increase the electrical conductivity of the concrete. The slabs were cured for 28 days in a moist room, and then air-dried for one month. The top face of each slab was sandblasted to remove the weak laitance layer present on the surface and to produce a medium sandpaper surface with some aggregate exposed. The sandblasted surface was then air-blasted to remove dust. The areas around the two wire leads were masked with tape to a distance of 1 in (2.4 cm) to prevent shorting between the mesh and the Zn anode. The top surface of the slab was then thermally sprayed with 15±1 mil (0.38±0.02 mm) of zinc using multiple robotically-controlled x-y passes over the surface to produce uniformly coated concrete slabs, Figure 4.1. A twin wire arc-spray process with ⅛-inch (3.2 mm) diameter Zn wire was used to coat the slabs. These slabs are referred to as "new" slabs.

Figure 4.1: Thermal-spraying of zinc onto new slabs with robotic-controlled x-y passes

A few additional "new" slabs were cast with 2.0 and 10.0 lb/yd^3 (1.2 and 5.9 kg/m^3) of NaCl in the concrete mix. Since NaCl is a humectant, these were made to show the effects from NaCl.

4.1.2   Aged Sample Preparation

Zinc-coated concrete slabs from earlier studies (*Covino, et al. 1996a; Covino, et al. 1996b; Covino, et al. 2002; Holcomb, et al. 1996*), representing a broad range of electrochemical ages, were used to study humectant effects on aged anodes. They had 5.0 lb/yd^3 (3.0 kg/m^3) of NaCl. Pairs of slabs with initial electrochemical ages, based on the Oregon DOT ICCP current density of 0.2 mA/ft^2 (2.2 mA/m^2), of 1.6, 3, 5.1, 8, 12, 13.1, 16.1, and 19 years were selected. Slabs aged 3, 8, 13.1, and 19 years were used in the ICCP experiment and slabs aged 1.6, 5.1, 12, and 16.1 years were used in the GCP experiment. Each slab was cut into three pieces with each piece having approximately the same surface area. Electrical lead wires were welded to the exposed steel mesh to make an electrical contact and bare concrete areas were masked with epoxy paint. The surface area of zinc on each piece was then measured and recorded. These slabs are referred to as "aged" slabs and represent existing CP systems.

16

4.1.3   Humectant Application

Solutions containing 300 g/L of humectant (LiBr at 3.45M, LiNO$_3$ at 4.35M, and KC$_2$H$_3$O$_2$ at 3.06M) plus 10 ml/L of a commercially available surfactant were brush applied to both new and aged slabs in two applications on two different days. This resulted in approximately 86 g/m^2 (8 g/ft^2) of humectant on the anode surface. A control solution, containing only the surfactant, was applied to some of the new slabs as controls.

4.1.4   Environmental Conditions

Two enclosures were used to provide either a high or a low RH environment. Humidifiers and dehumidifiers controlled the RH. Heaters and air coolers controlled the temperature. Fans also provided air circulation. Mean values in the high RH enclosure were 81±5% RH and 26±2ºC (79±4ºF). Mean values in the low RH enclosure were 45±4% RH and 29±2ºC (84±4ºF). Figure 4.2 shows the samples in the high RH enclosure.

Figure 4.2: New and aged zinc slabs wired in series in the high RH enclosure

High-purity water was sprayed every day in the enclosures to simulate rainfall and to aid in maintaining the slab resistances low enough for each series of slabs to stay under the compliance voltages of their current sources.

4.1.5 Accelerated Impressed Current Cathodic Protection

Current was provided for the ICCP experiment using stable, constant, current sources with compliance voltages of either 100 or 300 V. Slabs were connected in series for each current source. Initially, all of the ICCP slabs had a nominal current density of 2.5 mA/ft^2 (27 mA/m^2). Soon after the experiment started, the compliance voltages of the current sources supplying the aged slabs, within the low RH enclosure, were limiting the current. Due to the limiting current of the supply sources, the current densities of the aged slabs were reduced to a nominal value of 0.9 mA/ft^2 (10 mA/m^2).

In the ICCP experiments, potentials and currents were monitored hourly using a data acquisition system. Potentials of the Zn anode were measured with respect to the steel cathode.

Differences in the current densities used in the experiments, and periods when the compliance voltage of the current sources were exceeded, combined together creating difficulties in comparing results in terms of voltage. Thus, circuit resistance was used (operating voltage/impressed current density) to better compare results at differing current densities (and with field installations). In this case, the current density was based on anode area and not cathode area. A lower circuit resistance means there is less polarization of the anode.

Later in this report, when mean circuit resistances are reported, the initial 204 kC/m^2 (3 years at Oregon DOT ICCP current densities) are not included in the mean so as to remove the initial low values of circuit resistance.

4.1.6 Cyclic Impressed Current Cathodic Protection

One of the concerns about accelerated electrochemical aging is the effect of higher current densities on the measured parameter slab polarization and the derived parameter circuit resistance. Higher current densities tend to produce greater values of polarization and circuit resistance. Accelerated aging is necessary, however, because it is not possible to conduct 20-30 year aging experiments in real time. To accomplish the accelerated aging while still minimizing its effects on parameters, a modified procedure was used on one set of slabs. Over a repeated 4-week cycle, one set of slabs was aged for three weeks at an accelerated rate of 2.5 mA/ft^2 (2.8 mA/m^2) identical to that of the rest of the slabs. At the start of the fourth week, the current density was decreased to 0.2 mA/ft^2 (2.2 mA/m^2), a value similar to that typically used by Oregon DOT on their coastal bridges. This was termed a cyclic ICCP procedure. The goal of cycling the slabs for one week to the lower current density was to allow the aged Zn-concrete interface to approach a steady-state value that was similar to that which would exist on a coastal bridge under ICCP. At the end of the fourth week, depolarization values were measured.

4.1.7 Galvanic Cathodic Protection

In the GCP experiments, the galvanic current was measured and recorded every hour. Resistors used to measure the current in the GCP experiment ranged from 3 to 4000Ω. The values of the resistors were chosen and maintained such that the potentials across them remained between 1.5 and 8 mV. This maximized the signal while keeping the voltage drop across the resistor small.

The usefulness of the anode is characterized by the current density, in mA/m^2, where the area is based on cathode area.

The new slabs have anode to cathode area ratios that are very close to one, so the distinction between anode and cathode areas is not necessary. Aged slabs, on the other hand, have anode to cathode area ratios that have a mean value of 0.8 and the distinction is necessary.

In cases where an average galvanic current is presented, it is called the long-term current density. The long-term current density is defined as the average current density for the experiment after removing the first year of current density values. This has the advantage of establishing the long-term protection current, which can be compared with the minimum current needed to protect the structure. It also ignores short periods of high galvanic current sometimes observed, especially in the initial days and months of GCP (*Cramer, et al. 2002b*).

The minimum current needed for protection is an empirically derived value and may well be different for different climates and chloride levels. For example, Oregon DOT has found that 0.2 mA/ft^2 (2.2 mA/m^2) is sufficient for their coastal thermal-sprayed zinc ICCP systems (*Bullard, et al. 1998; Covino, et al. 1997a; Covino, et al. 2002*), while Fontana and Greene (*1978, p. 207*) give 0.1-0.5 mA/ft^2 (1.1-5.4 mA/m^2) as sufficient for protecting reinforcing bars in concrete.

4.1.8 Depolarization

Depolarization was measured on the cyclic ICCP slabs at various times throughout the experiment. Prior to depolarization, the impressed current was reduced to 0.2 mA/ft^2 (2.2 mA/m^2) to reduce the polarization caused by the accelerated aging experiment. A $Cu/CuSO_4$ reference electrode was used with a wet sponge between the reference electrode and an area of bare concrete (without Zn) on the sample. For the new slabs the reference electrode was contacted to the underside of the sample. On the aged slabs the reference electrode made contact in an area without Zn left from prior adhesion strength pull tests, Figure 4.3.

Figure 4.3: Aged zinc slabs wired in series in the high RH enclosure. Note the reference electrode holders (PVC pipe) mounted in areas without zinc left from prior adhesion strength pull tests.

Measurements of the potential between the steel mesh and the reference electrode were made every minute for 30 minutes. The impressed current was then removed and the potential was recorded every minute for 2 hours. After that, the potential was recorded every hour for an additional 22 hours. The reported value of depolarization was the difference between the "instant off" potential (measured immediately after the impressed current was removed) and the potential measured at a later time during depolarization, typically 24 hours.

4.1.9   Microscopy

The TS Zn surface of selected ICCP slabs was stabilized by a coating of clear epoxy so that cutting, grinding and polishing could be performed without separating the anode from the concrete. The slabs were cross-sectioned to expose the anode-concrete interface. The cross-sections were mounted in epoxy, ground and polished to a 1 µm diamond finish. To prevent charging, the polished cross-sections were lightly coated with Palladium in a vacuum coating unit. The moisture in the concrete samples required substantial pumping to achieve the vacuum necessary for coating and for examination in the scanning electron microscope (SEM). SEM images were obtained with back-scattered electrons (BSE). Back-scattered electron images exhibit contrast based on average atomic number, so that cross-section composition can be qualitatively observed (low atomic number elements are darker). Analytical SEM (ASEM) was used to determine the composition of the Zn-concrete interface. The following elements were included in all analyses: Zn, Ca, Mg, Na, K, S, Cl, O, Fe, and Al. Line scans were done using x-ray fluorescence microanalyses and a wavelength dispersive spectrometer (WDS) with four crystals. Line scans across the anode-concrete interface typically contained 100 to 150 individual point analyses along the line. Data acquisition times for each element at each point on the line scan were typically 20 s. Element x-ray maps were all obtained using an energy dispersive spectrometer (EDS) to qualitatively show the distribution of individual elements in the cross-section.

The Br L_α (8.374Å) and Al K_α (8.329 Å) peaks overlap and cannot be distinguished by EDS when both elements are present. EDS could determine Br only in the Zn anode and in anode mineral products not containing cement paste. The Br L_β peak, which is separate and identifiable from other peaks by WDS, was used to quantify Br concentrations for the line scans.

Lithium is a light element that cannot be detected by either EDS or WDS. While Ti K_α and N K_α peaks overlap, there was insufficient Ti in the cement paste (as rutile or other Ti oxide) to prevent analysis for N. However, the polished slab cross-sections were not analyzed for N.

A line scan across an electrochemically aged Zn anode can be simplified into zones representing: the unreacted anode, a growing mineral reaction layer characterized largely as ZnO or $Zn(OH)_2$, altered cement paste containing varying levels of Zn from anode dissolution, and unaltered cement paste. Anions migrate to the anode under the influence of the ICCP potential gradient (*Covino, et al. 2002*). The total mass of Cl and Br in the different zones was found by integrating the ASEM line scan across the cross-section. There was about a 20% error in these calculations, a tolerable error given that the line scans represent a single traverse across an anode-concrete interface fractions of a millimeter wide (the analysis volume was roughly 5 µm in diameter).

4.1.10 AC Resistance and Circuit Resistance

Circuit resistance, as measured by the operating voltage divided by impressed current density, includes both ohmic resistances across the anode-cement-cathode electrochemical cell, and the effects of polarization of the steel cathode and zinc anode (*Covino, et al. 2002*). An attempt was made to separate the ohmic and polarization components. This was attempted by making alternating current (AC) resistance measurements between the zinc anode and the steel cathode; and then comparing them with the circuit resistance measurements.

The procedure was to obtain a mean value for the circuit resistance over the last 24 hours of impressed current. A subsequent 60 Hz AC resistance measurement was made between the steel mesh and the zinc coating. On some slabs the AC measurements were made as early as one day after the impressed current ended, and on other slabs as much as 320 days elapsed. In all cases the slabs were stored in the same humidity enclosure where the impressed current tests were performed. Measurements were taken on both new and aged slabs, from high and low RH enclosures, and from control and humectant-treated slabs. The humectant-treated slabs included $KC_2H_3O_2$-treated slabs removed from the main study.

4.1.11 Adhesion Strength

Slabs were removed from the electrochemical aging experiment at regular time intervals. The slabs were equilibrated with dry air for one day, and prepared for bond strength measurements by attaching aluminum dollies to the Zn coating using epoxy. For the new slabs the dollies were attached at six predetermined locations, and dollies were 50 mm (1.9 in) in diameter. For the aged slabs, which had much less Zn surface remaining from prior adhesion tests, smaller dollies were used that were 19 mm (0.75 in) in diameter. A high viscosity, high strength, short cure time (300 s) epoxy was used to eliminate failures at the epoxy-dolly interface and to prevent epoxy penetration through the coating to the concrete. Zn bond strength measurements were made using a universal testing machine (*Bullard, et al. 1997a; Covino, et al. 1995; Covino, et al. 1997b; Covino, et al. 2002*).

4.2   SHORT-TERM CHAMBER EXPERIMENTS (ARC)

The short-term chamber experiments used a small humidity and temperature-controlled chamber to equilibrate sixty 2-inch diameter concrete slices and four TS concrete slabs at specific conditions. Equilibration lasted a minimum of 50 days. Half of the slices were TS with Zn and half were not. Three NaCl levels were used in the slices, each containing 2.0, 5.0, and 10.0 lb/yd^3 (1.2, 3.0, 5.9 kg/m^3) of NaCl. Humectants in surfactant solutions were applied to some of the slices, surfactants without humectants were applied to some slices, and some slices were left untreated as controls. All of the slabs were TS with Zn. Three of the slabs were humectant treated and one was untreated for a control.

Mass changes of the slices were periodically recorded throughout the experiment. The TS concrete slabs underwent ICCP at very low current densities for 24 hours and the applied voltage was recorded and converted into circuit resistance. Very low current densities were used to

minimize any effects from electrochemical aging of the anode. After the ICCP the RH of the chamber was changed and a new equilibration was begun.

4.2.1   Sample Preparation

The sample preparations for the slabs were the same as for the long-term laboratory experiments (indoor) and are described in Section 4.1.2.

Nominally 0.25-inch (0.635 cm) thick slices were cut from 3-inch (7.62 cm) diameter cylinders. The cylinders were cast with a sand to cement ratio of 3 to 1 (by weight). The sand was partially absorbed with water (1.1%). After allowing for the sand to be fully absorbed with water (4.5%), the water to cement ratio was calculated to be 0.43. Added to the mix was NaCl at 2.0, 5.0, and 10.0 lb/yd^3 (1.2, 3.0, and 5.9 kg/m^3). The cylinders were cured in a high humidity chamber for four weeks prior to slicing.

Half of the slices were TS with 15 mil (0.38 mm) of Zn using the twin-wire arc-spray process used for the slabs (Section 4.1.2).

The slices without zinc were divided into 5 groups: those humectant-treated with $LiNO_3$, LiBr, and $KC_2H_3O_2$, those treated with just the surfactant, and those left untreated (as controls). The slices with zinc had the same arrangement except without $KC_2H_3O_2$. The humectants were brush applied to each side of the slice with each side receiving two applications. The solutions were made from 300 g/L of humectant with 1% surfactant. Solution was measured out with a pipette for 0.65 ml per side per application. This resulted in a total of 0.7854 g of humectant on each slice. Table 4.1 lists the number of slices for each condition.

Table 4.1: Number of slices for each condition

HUMECTANT	No Zn			TS Zn		
	2.0 1b/yd^3 (1.2 kg/m^3) NaCl	5.0 1b/yd^3 (3.0 kg/m^3) NaCl	10.0 1b/yd^3 (5.9 kg/m^3) NaCl	2.0 1b/yd^3 (1.2 kg/m^3) NaCl	5.0 1b/yd^3 (3.0 kg/m^3) NaCl	10.0 1b/yd^3 (5.9 kg/m^3) NaCl
LiNO$_3$	2	2	2	3	3	3
LiBr	2	2	2	3	3	3
Surfactant	2	2	2	2	2	2
Control	2	2	2	2	2	2
KC$_2$H$_3$O$_2$	2	2	2			

4.2.2   Equilibrium Procedures

Prior to the experiments, the humidity chamber was calibrated with saturated solutions of NaCl (75.3% RH at 25ºC) and lithium chloride (LiCl) (11.3% RH at 25ºC). After removing the calibration solutions, the slices and slabs were placed on racks so that both faces were free of obstruction. All of the samples were kept in the humidity chamber at 90ºF (32.2ºC) and at a fixed RH. The initial RH was 70% and was held for 89 days. Subsequent conditions were 50% RH for 51 days, 35% RH for 52 days, 80% RH for 72 days, and then 70% RH for 94 days.

Slice masses were periodically monitored and used to decide when the samples had equilibrated. The voltage and circuit resistance response to ICCP was measured at the end of each RH period.

4.2.3 Mass Change Response to Temperature and Humidity

The procedures used to measure the mass changes in the slices were as follows:

1) Remove the rack containing the slices from the chamber.

2) Weigh each slice to the nearest 0.1 mg. The slices were weighed in the same order each time; with the first two slices weighed again after all 60 slices were weighed. The rack and samples were then placed back into the humidity chamber.

3) Since the slices were outside the humidity chamber during weighing, the masses in the first two slices (that were also weighed again after all 60 slices were weighed) tended to dry a bit and decrease in mass by 10-20 mg. This change was used to correct (increase) the masses of the slices with a linear correction factor, proportional to the sequence number of that slice.

The mass change response was measured for the first four RH conditions (70%, 50%, 35% and 80% RH).

4.2.4 Circuit Resistance Response to Temperature and Humidity

The slabs were connected in series to a constant current power supply, with the anode (TS Zn) of one slab connected to the cathode (steel mesh) of the next. After the mass changes of the slices had been deemed good enough for equilibration, the chamber was allowed to be at the set temperature and RH for one more day. Then a constant current of 0.015 mA (0.020 mA/ft^2, 0.22 mA/m^2) was applied for 24 hours. The voltage drop across each slab was monitored. The voltage was recorded every minute for the first 10-15 minutes (when the voltage was changing rapidly). It was then recorded every few hours (with a longer gap overnight). A final reading was taken after 24 hours. The voltages were then converted into circuit resistance (kΩ-m^2) using the surface area of the TS zinc anode and the applied current density.

4.3 LONG-TERM LABORATORY GCP EXPERIMENTS (OHIO)

The goal of these long-term laboratory experiments was to test the effectiveness of each humectant on thermal-sprayed zinc anodes as a function of environment (low RH, high RH, outdoor sheltered and outdoor exposed), concrete chloride levels, and reapplication. The experiments were conducted in Chardon, Ohio (near Cleveland).

Thirty-six concrete blocks were constructed with dimensions of 12 x 9 x 2 inch (30.5 x 22.9 x 5.1 cm). The concrete contained a $^1/_{16}$-inch thick mild steel mesh (1.25-inch LWD x 0.5-inch SWD) at a depth of 1.5-inch (3.8 cm) from the top surface of the concrete block. The steel mesh provided a surface area of about 1 ft^2 steel/ft^2 of concrete. The mix proportions for the concrete were as follows:

Type 1A Portland Cement - 715 lb/yd^3 (425 kg/m^3)

Lake Sand Fine Aggregate - 1010 lb/yd^3 (600 kg/m^3)

No.8 Marblehead Limestone- 1830 lb/yd^3 (1090 kg/m^3)

Water - 285 lb/yd^3 (170 kg/m^3)

NaCl - 5.1 lb/yd^3 (3.0 kg/m^3)

Entrained Air - about 6%

Following a 24-hour mold curing period, the blocks were wrapped wet in plastic and allowed to cure for 28-days at room temperature.

The top surfaces of the specimens were prepared by sandblasting to remove the cement paste layer, but care was taken not to expose too much coarse aggregate. The blocks were then coated on their top surface with a pure zinc anode by the twin-wire arc-spray process to a thickness of about 15 mil (0.38 mm). Zinc was applied using a robot to insure consistency between applications. The blocks were not preheated. Electrical connection was made between the metallized Zn and the embedded steel across a 10 Ω resistor to facilitate measurement of galvanic current.

Each block was then brush coated with a solution containing 300 g/L of humectant plus 10 ml/L of a commercially available surfactant. Since metallized coatings are inherently porous, the solution was transported to the anode-concrete interface by capillary action. Three coats were applied resulting in a total application rate of about 30 ml/block. Control blocks were coated with distilled water with no chemical addition. Exact amounts of chemical applied to groups of blocks are shown in Table 4.2.

Table 4.2: Humectant and Operating Environment for the Blocks

BLOCK	OPERATING ENVIRONMENT	CHEMICAL APPLIED g/m^2 (g/ft^2)
1, 2, 3	80% RH, No Wetting	Distilled Water (Control)
4, 5, 6	80% RH, No Wetting	78.5 (7.29) KC$_2$H$_3$O$_2$
7, 8, 9	80% RH, No Wetting	82.9 (7.70) LiNO$_3$
10, 11, 12	80% RH, No Wetting	81.5 (7.57) LiBr
15, 16, 17	55% RH, No Wetting	Distilled Water (Control)
18, 19, 20	55% RH, No Wetting	87.3 (8.11) KC$_2$H$_3$O$_2$
21, 22, 23	55% RH, No Wetting	99.2 (9.22) LiNO$_3$
24, 25, 26	55% RH, No Wetting	99.1 (9.21) LiBr
29, 30	Outdoors (Exposed, Covered)	Distilled Water (Control)
31, 32	Outdoors (Exposed, Covered)	72.0 (6.69) KC$_2$H$_3$O$_2$
33, 34	Outdoors (Exposed, Covered)	76.7 (7.13) LiNO$_3$
35, 36	Outdoors (Exposed, Covered)	77.8 (7.23) LiBr

As shown on the table above, blocks were placed in one of three operating environments: 80% RH, 55% RH, and outdoors. Blocks placed indoors in 80% and 55% RH were never wetted, and therefore became relatively dry. Indoor blocks were maintained at a temperature of 20°C ± 2°C. The outdoor blocks were maintained outdoors in northeast Ohio in one of two conditions:

exposed (placed at a 45° angle and exposed to all natural precipitation), and covered (receiving no direct precipitation, but experiencing natural excursions of temperature and humidity). Blocks placed in 80% and 55% RH were energized on January 23, 1998. Blocks placed outdoors were energized on April 1, 1998.

In addition to the treatment above, the blocks listed in Table 4.3 were subjected to a second chemical treatment after 230 days of operation. Blocks receiving a second treatment were placed back into the same operating environment from which they were taken.

Table 4.3: Second humectant treatments and operating environments

BLOCK	OPERATING ENVIRONMENT	CHEMICAL APPLIED, g/m^2 (g/ft^2)
2	80% RH, No Wetting	Distilled Water (Control)
5	80% RH, No Wetting	105.3 (9.78) $KC_2H_3O_2$
8	80% RH, No Wetting	116.2 (10.80) $LiNO_3$
11	80% RH, No Wetting	87.5 (8.13) LiBr
16	55% RH, No Wetting	Distilled Water (Control)
19	55% RH, No Wetting	92.4 (8.58) $KC_2H_3O_2$
22	55% RH, No Wetting	122.1 (11.34) $LiNO_3$
25	55% RH, No Wetting	96.3 (8.95) LiBr

The blocks described in Tables 4.2 and 4.3 were constructed with an admixed salt content of 3.0 kg/m^3 (5.1 lb/yd^3) NaCl. In early 1999 it was decided to examine the effect of chloride ion content on performance. Twenty-seven blocks were therefore constructed containing 4.9, 7.3, and 9.8 kg/m^3 (8.2, 12.4, and 16.5 lb/yd^3) of NaCl. Otherwise, construction of the blocks was the same as that described above for the original blocks. These blocks received chemical treatment as shown in Table 4.4.

Table 4.4: Humectant treatments and operating environments for blocks of different NaCl contents

BLOCK	NaCl CONTENT kg/m^3 (lb/yd^3)	OPERATING ENVIRONMENT	CHEMICAL APPLIED g/m^2 (g/ft^2)
-1	4.9 (8.2)	55% RH, No Wetting	Distilled Water (Control)
-2	4.9 (8.2)	55% RH, No Wetting	150.3 (13.96) LiNO$_3$
-3	4.9 (8.2)	55% RH, No Wetting	154.7 (14.37) LiBr
-4	7.3 (12.4)	55% RH, No Wetting	Distilled Water (Control)
-5	7.3 (12.4)	55% RH, No Wetting	144.1 (13.39) LiNO$_3$
-6	7.3 (12.4)	55% RH, No Wetting	147.7 (13.72) LiBr
-7	9.8 (16.5)	55% RH, No Wetting	Distilled Water (Control)
-8	9.8 (16.5)	55% RH, No Wetting	141.4 (13.14) LiNO$_3$
-9	9.8 (16.5)	55% RH, No Wetting	166.0 (15.42) LiBr
-10	4.9 (8.2)	80% RH, No Wetting	Distilled Water (Control)
-11	4.9 (8.2)	80% RH, No Wetting	151.3 (14.06) LiNO$_3$
-12	4.9 (8.2)	80% RH, No Wetting	166.0 (15.42) LiBr
-13	7.3 (12.4)	80% RH, No Wetting	Distilled Water (Control)
-14	7.3 (12.4)	80% RH, No Wetting	145.6 (13.53) LiNO$_3$
-15	7.3 (12.4)	80% RH, No Wetting	143.5 (13.33) LiBr
-16	9.8 (16.5)	80% RH, No Wetting	Distilled Water (Control)
-17	9.8 (16.5)	80% RH, No Wetting	152.8 (14.20) LiNO$_3$
-18	9.8 (16.5)	80% RH, No Wetting	157.6 (14.64) LiBr
-19	4.9 (8.2)	Outdoors Covered	Distilled Water (Control)
-20	4.9 (8.2)	Outdoors Covered	156.5 (14.54) LiNO$_3$
-21	4.9 (8.2)	Outdoors Covered	170.2 (15.81) LiBr
-22	7.3 (12.4)	Outdoors Covered	Distilled Water (Control)
-23	7.3 (12.4)	Outdoors Covered	156.0 (14.49) LiNO$_3$
-24	7.3 (12.4)	Outdoors Covered	143.5 (13.33) LiBr
-25	9.8 (16.5)	Outdoors Covered	Distilled Water (Control)
-26	9.8 (16.5)	Outdoors Covered	144.0 (13.38) LiNO$_3$
-27	9.8 (16.5)	Outdoors Covered	149.1 (13.85) LiBr

4.4 YAQUINA BAY BRIDGE FIELD TRIAL (OREGON)

Field installation of humectants under the south approach of the Yaquina Bay Bridge in Newport, Oregon took place in October 1999. Four large under-deck, thermal-sprayed, zinc ICCP Zones, with areas of approximately 5000 ft^2 (465 m^2), were chosen for this two-year field trial. The two center zones had humectants applied to them, one with LiBr and one with LiNO$_3$. The two zones on each side of the treated zones were controls and had nothing applied to them. Concrete core samples and Cl$^-$ depth profiles were taken and analyzed at the start of the trial.

4.4.1 Bridge and Zone Description

The south approach of the Yaquina Bay Bridge was chosen to be the site of an ICCP field trial of the humectants. Four zones (ICCP Zones 10, 11, 13, and 14) were selected to be part of the trial, Figure 4.4.

Figure 4.4: The four field test zones on the Yaquina Bay Bridge. Each zone includes column and soffit areas. Zone 14 is closest to Yaquina Bay. The closer a zone is to the ocean, the higher the expected Cl⁻ level and the lower the expected circuit resistance.

All four zones are part of the approach and are not over water. The ICCP Zones are numbered beginning at the south end of the bridge, so the higher the zone number, the closer it is to Yaquina Bay. Zone 10 was 131 m (429 ft) from the bay, Zone 11 was 113 m (370 ft) from the bay, Zone 13 was 94 m (308 ft) from the bay, and Zone 14 was 73 m (239 ft) from the bay. The LiBr humectant was applied to Zone 11, $LiNO_3$ to Zone 13, and Zones 10 and 14 were used as controls. The surface areas of Zones 10, 11, 13, and 14 were 556.7 m² (5992 ft²), 443.3 m² (4771 ft²), 451.7 m² (4862 ft²), and 556.7 m² (5992 ft²), respectively.

4.4.2   Chloride Depth Profiling

The concentration of chloride ion (Cl⁻), as a function of depth, was measured on the four Yaquina Bay Bridge test zones prior to the application of humectants. The Cl⁻ profiles were taken from beams in the soffits supporting the roadbed. Thus, they were taken from areas sheltered from direct precipitation, but fully exposed to wind, fog, and dew formation. As a comparison, Cl⁻ profiles from the west side of the base of Bent 3N, on the north side of the bridge were also measured; one from the north face and one from the south face. The north side of Bent 3N is much more sheltered from wind and rain than the south side.

Chloride samples, taken as powdered concrete, were taken at 0.5 inches (1.27 cm) depth increments into the concrete. Precautions were taken to avoid sample cross-contamination. The procedures for sampling are described in detail in the report on Project SPR 364 (*Covino 2002, Appendix C*). Chloride analysis was performed following AASHTO T260-94 *(AASHTO 1995)* for both total and water-soluble Cl⁻. More detailed procedures for Cl⁻ analyses are described in the report on Project SPR 364 (*Covino 2002, Appendix D*).

27

4.4.3　Microscopy

Concrete core samples 5 cm (2 inches) in diameter were taken from the two humectant-treated zones and from the two control zones immediately after the humectant treatment (10-22-99) and again after about 2 years of service (12-5-01). The cores were prepared, cross-sectioned, ground and polished as was done for the concrete slabs, Section 4.1.9. SEM examination of the cores was the same as for the concrete slabs. In performing the line scans, the core from Zone 13 receiving the $LiNO_3$ treatment was analyzed for nitrogen using the N K_α line. The core from the control Zone 10 was analyzed for Br and N, as well as the usual elements, to determine their background levels. Data acquisition times for N and Br during the line scans were increased from 20 s to 60 s to improve signal-to-noise ratios.

4.4.4　Humectant Application Procedures

Humectants were applied to the Yaquina Bay Bridge in a scaled up version of the procedures described in Section 4.1.3 for the laboratory studies. Solutions were prepared with 300 g/L of humectant with 10 ml/L of surfactant. The surfaces were hand sprayed as shown in Figures 4.5 and 4.6. There was no surface preparation prior to spraying. Unlike the controls in the laboratory studies (that received water with surfactant), the controls here received no treatment at all.

Figure 4.5: Application of humectants under the deck of the Yaquina Bay Bridge

Figure 4.6: Application of humectants to the base of a bent on the Yaquina Bay Bridge

4.4.5 Monitoring Procedures

The humectant test covered four ICCP Zones: 10, 11, 13, and 14. The rectifiers operate in the constant-voltage, current-limited mode. The Yaquina Bay Bridge data acquisition system (DAS) was a CORD-4 System by Corexco. The system monitored the output voltage and current on an hourly basis. Depolarization measurements were made versus a graphite electrode. The integrity of the graphite electrodes was monitored with comparisons to silver/silver chloride electrodes.

The data was retrieved from the DAS by two methods. The first was by downloading the stored hourly data from the DAS, the "ON" reports. The "ON" reports were retrieved at the bridge several times each year. The second method was to manually download instantaneous data from the station reports that were available to be viewed from a remote location, the "SRP" reports. The "SRP" reports were retrieved daily. The "ON" reports have greater precision than the "SRP" reports, so the "ON" reports were used in preference to the "SRP" reports. However, between 2/26/98 to 11/06/98, 11/26/98 to 2/25/99, 4/18/00 to 7/21/00, and 7/25/01 to 11/26/01, the data recorder malfunctioned. Some, but not all of the "ON" data was recovered by the manufacturer by downloading the information and decoding it. Data from the "SRP" reports

were used to fill gaps in the data. This resulted in differences in the observed noise in the data since the "SRP" and "ON" data had different formats and precisions.

On 5/3/01 the voltage and currents in the four zones increased sharply by up to seven times the intended set points. This was discovered on 11/21/01 by an inspection of the rectifier cabinets. This rise was traced to failures of the potentiometers in the rectifiers, which caused the voltages/currents to drift upward. The voltages and currents were 2 to 7 times higher than the intended set points. This problem was corrected on 12/30/01 and the voltages/currents were reduced to the correct set values.

4.5   CONTROLS

There are minor differences in terms of what is meant by control samples or control zones between the four main categories of experiments. In the long-term experiments at ARC and Ohio, the surfactant was applied to the control samples. In the short-term experiments at ARC and in the Yaquina Bay Bridge field trial, the controls had nothing applied to them. The short-term experiments at ARC also had some samples with just a surfactant treatment; thus it essentially had two types of controls (differentiated as "controls" and "surfactant-treated").

4.6   NaCl CONCENTRATIONS

A variety of NaCl concentrations were used in the laboratory experiments. For ease of comparison, Table 4.5 presents these various concentrations in terms of both NaCl and Cl concentrations in commonly used units.

Table 4.5: NaCl and Cl concentrations used in the laboratory experiments

EXPERIMENT	NaCl		Cl	
	lb/yd^3	kg/m^3	lb/yd^3	kg/m^3
ARC Long Term (Primary)	5.0	3.0	3.0	1.8
ARC Long Term (Secondary)	2.0	1.2	1.2	0.7
ARC Long Term (Secondary)	10.0	5.9	6.1	3.6
ARC Short Term	2.0	1.2	1.2	0.7
ARC Short Term	5.0	5.9	3.0	1.8
ARC Short Term	10.0	3.0	6.1	3.6
Ohio Long Term (Primary)	5.1	3.0	3.1	1.8
Ohio Long Term (Secondary)	8.2	4.9	5.0	3.0
Ohio Long Term (Secondary)	12.4	7.3	7.5	4.4
Ohio Long Term (Secondary)	16.5	9.8	10.0	5.9
Screening Experiments	8.2	4.9	5.0	3.0

5.0   RESULTS AND ANALYSIS

5.1   LONG-TERM LABORATORY EXPERIMENTS (ARC)

5.1.1   Accelerated Impressed Current Cathodic Protection

The circuit resistances of the new ICCP slabs are shown in Figure 5.1 for high RH conditions and in Figure 5.2 for low RH conditions. In high RH conditions the $LiNO_3$-treated slabs had consistently lower values of circuit resistance than either the LiBr-treated slabs or the controls. This indicates an improvement with $LiNO_3$. The LiBr-treated slabs showed much the same response as the control slabs. In low RH conditions, Figure 5.2, the circuit resistances of the $LiNO_3$-treated slabs were again the lowest. However, in this case the LiBr-treated slabs had circuit resistances lower than the control slabs, which were removed from the experiment at an early date due to their large voltages.
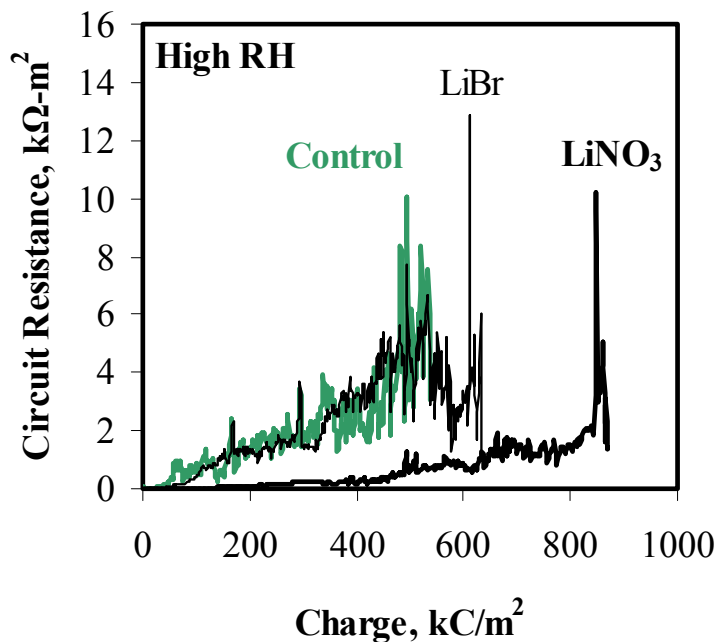

Figure 5.1: Circuit resistances of new ICCP slabs in high RH conditions
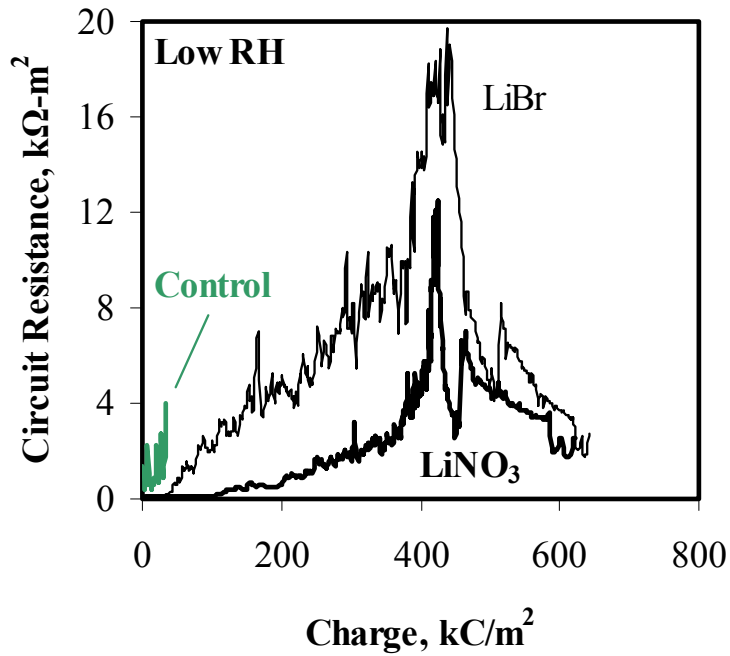
31

Figure 5.2: Circuit resistances of new ICCP slabs in low RH conditions

The sharp decreases in the circuit resistances in Figure 5.2 at around 400 kC/m^2 and the sharp increases following shortly thereafter, are artifacts from the curves representing an average of three slabs, then two slabs, and then just one slab. When the slabs with very high circuit resistance were removed (for both LiBr and LiNO$_3$) the plotted circuit resistance fell. Then when the next slabs were removed (with the lowest circuit resistances), the plotted circuit resistances rose.

The circuit resistances of the aged ICCP slabs are shown in Figure 5.3 for high RH conditions and in Figure 5.4 for low RH conditions. In general, the higher the initial electrochemical age, the higher the circuit resistance. In high RH conditions (Figure 5.3) up to an additional charge of approximately 700 kC/m^2 the LiNO$_3$-treated slabs had lower circuit resistances than the LiBr-treated slabs. In low RH conditions, Figure 5.4, the differences were similar: LiNO$_3$-treated slabs had lower circuit resistances for the first 300 kC/m^2 of additional charge. Overall the circuit resistances were higher in low RH conditions than in high RH conditions.
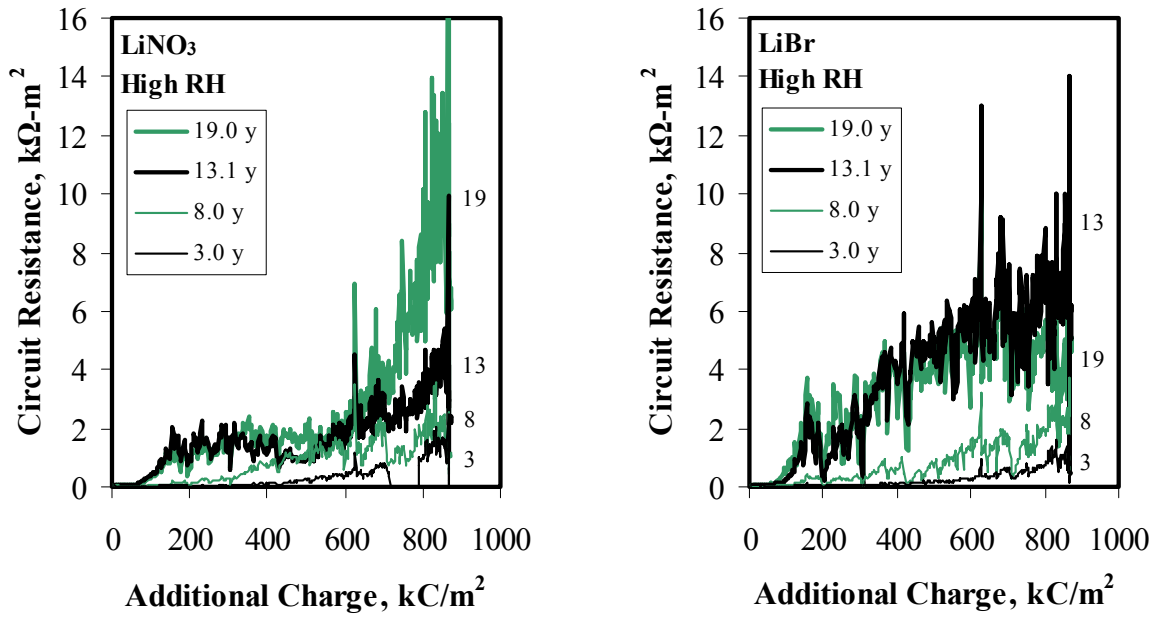
Figure 5.3: Circuit resistances of aged ICCP slabs in high RH conditions for LiNO$_3$ (left) and LiBr (right)
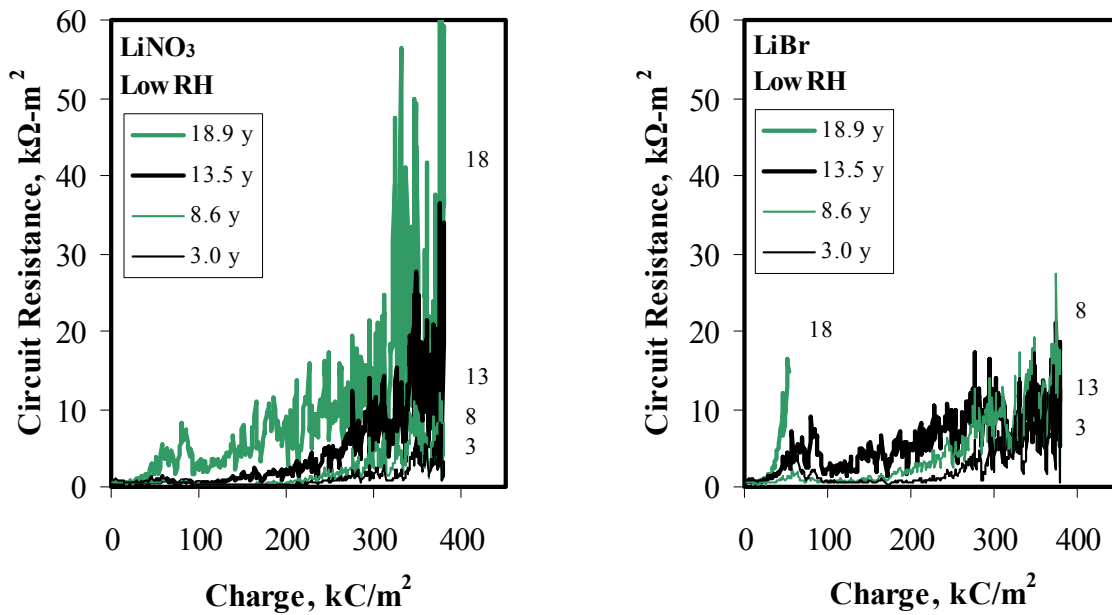

Figure 5.4: Circuit resistances of aged ICCP slabs in low RH conditions for LiNO$_3$ (left) and LiBr (right)

Mean values of circuit resistance of humectant-treated slabs are shown in Figure 5.5 for high RH conditions (left) and low RH conditions (right). To discount the low initial circuit resistances obtained during aging (Figures 5.1-5.4), the mean circuit resistance was calculated ignoring the first 204 kC/m^2 of charge, equivalent to 3 years of aging at 0.2 mA/ft^2 (2.2 mA/m^2). Thus, the mean values represent the mean circuit resistances from 3 to 11.7 years of aging in high RH conditions and from 3 to 5.1 years in low RH conditions. Results from an earlier study without humectants in a high RH environment were converted[1] to the same data format and shown in Figure 5.5 as "No Humectant" (*Bullard, et al. 1998; Covino, et al. 2002*). Humectant-treated slabs in high RH conditions had much lower circuit resistances than the untreated slabs. In both RH conditions the LiNO$_3$-treated slabs tended to have lower circuit resistances than the LiBr-treated slabs.
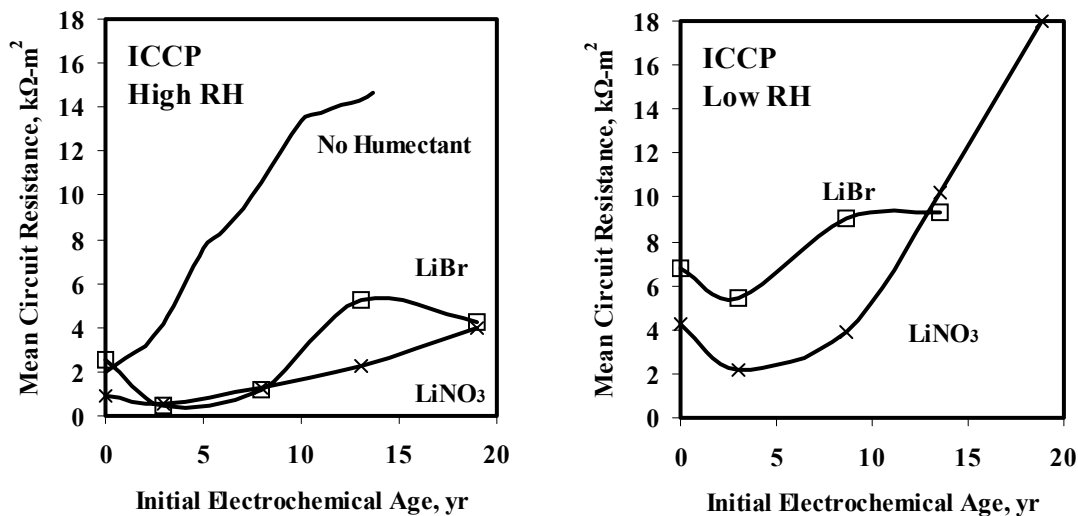

Figure 5.5: Mean circuit resistances of new and aged slabs after an additional 3 years of aging in high (left) and low (right) RH conditions. The "No Humectant" data are from an earlier study (*Bullard et al. 1998; Covino et al. 2002*).

5.1.2 Cyclic Impressed Current Cathodic Protection

The results for the experiments where the impressed current alternated between accelerated aging (high currents) and normal aging (low currents) are shown in Figure 5.6 for high RH conditions and in Figure 5.7 for low RH conditions. For these figures, low currents are defined as being from 0.10 to 0.16 mA (1.4 to 2.3 mA/m^2); and high currents are defined as being above 0.50 mA (7.2 mA/m^2). The gaps in Figure 5.7 result from currents having intermediate values. In terms of voltage (the left side in Figures 5.6-5.7) the higher currents resulted in higher voltage values. These differences disappeared when examined in terms of circuit resistance (the right side in Figures 5.6-5.7). Both humectants resulted in much lower voltages and circuit resistances than

---

[1] For a given electrochemical age (referred to as the initial electrochemical age in Figure 5.5), the mean circuit resistance was calculated from circuit resistance values between 3 and 10 years of additional electrochemical charge.

the slabs without humectants (control results). In general the $LiNO_3$-treated slabs had lower circuit resistances than the LiBr-treated slabs, which is consistent with the non-cyclic results. The circuit resistance values for the cyclic and non-cyclic tests were similar, as shown in Figures 5.1 and 5.6 for high RH conditions and in Figures 5.2 and 5.7 for low RH conditions.

The sharp decreases in voltages and circuit resistances in Figure 5.7 at around 450 and 500 kC/m^2 are artifacts from the curves representing an average of three slabs, then two slabs, and then just 1 slab. When the slabs with very high circuit resistance were removed (for both LiBr and $LiNO_3$) the plotted voltages and circuit resistances fell. Then when the next slabs were removed (again with the highest circuit resistances), the plotted circuit resistances decreased.
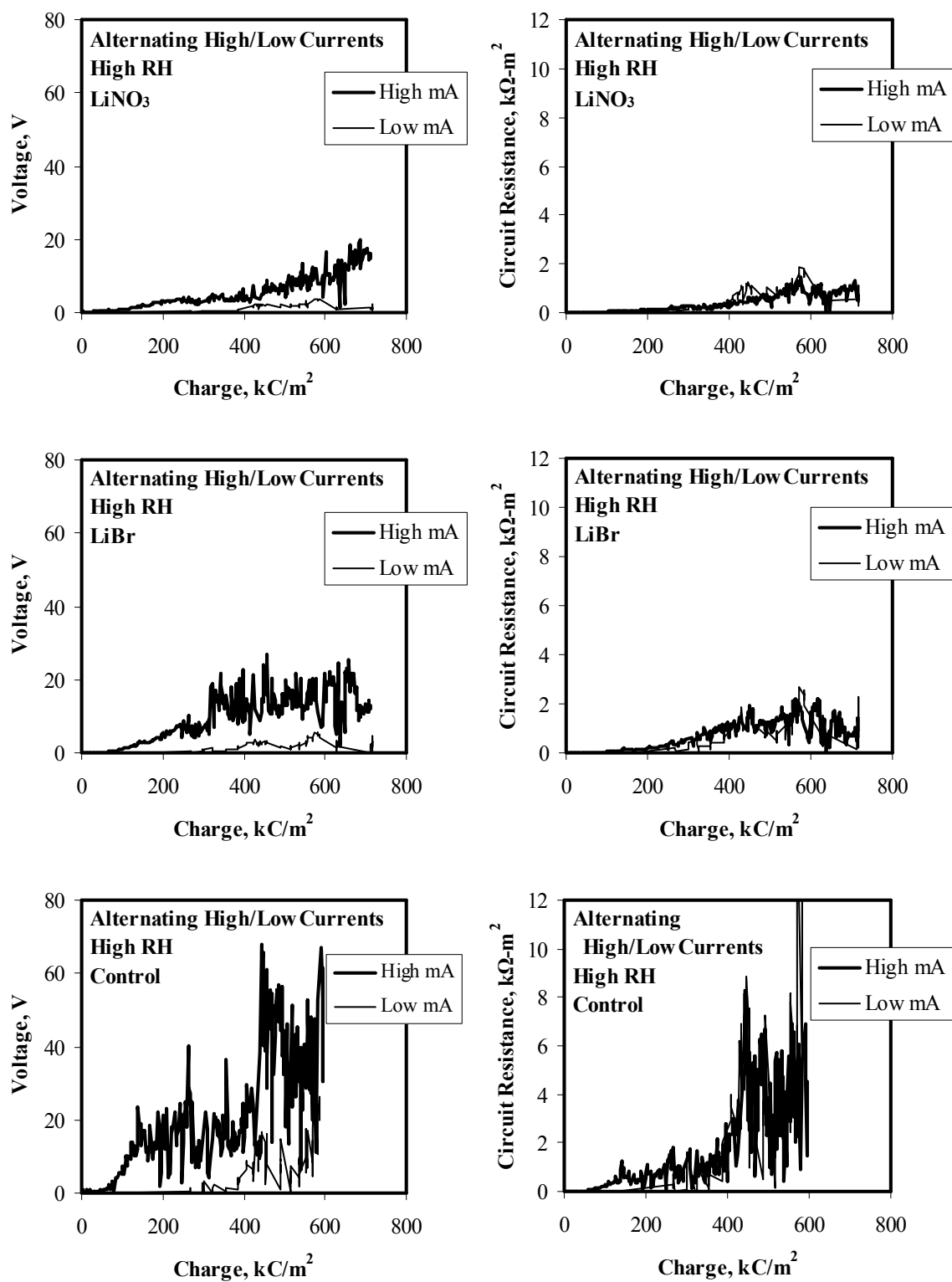
Figure 5.6: Cyclic ICCP voltages (left) and circuit resistances (right) for $LiNO_3$ (top), LiBr (middle), and control (bottom) in high RH conditions.
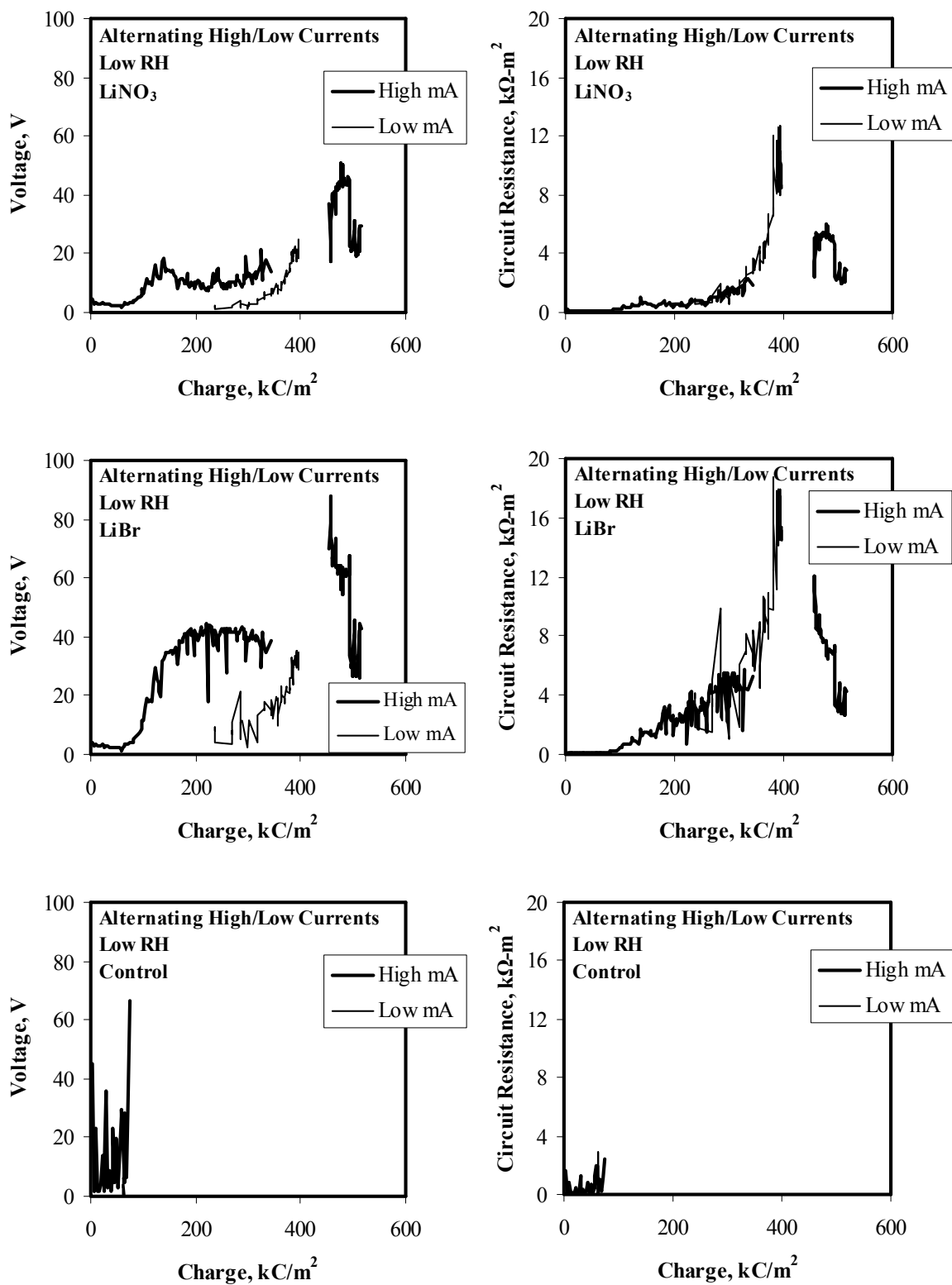
36

Figure 5.7: Cyclic ICCP voltages (left) and circuit resistances (right) for LiNO$_3$ (top), LiBr (middle), and control (bottom) in low RH conditions. Gaps are from intermediate current levels.

37

5.1.3 Galvanic Cathodic Protection

In interpreting GCP results, the desired galvanic current needs to be above the minimum needed for protection. The minimum current needed for protection is an empirically derived value and may well be different for different climates and chloride levels. For example, Oregon DOT has found that 0.2 mA/ft^2 (2.2 mA/m^2) is sufficient for their coastal thermal-sprayed zinc ICCP systems (*Bullard, et al. 1998; Covino, et al. 1997a; Covino, et al. 2002*); while Fontana and Greene (*1978, p. 207*) give 0.1-0.5 mA/ft^2 (1.1-5.4 mA/m^2) as sufficient for protect reinforcing bars in concrete.

Galvanic currents in excess of the required current are not beneficial. Excess current results in loss of zinc and accelerated electrochemical aging that provide no additional CP benefits and may lead to earlier anode replacement.

The results for the GCP experiments are shown in Figures 5.8-5.13 in terms of galvanic current density based on the cathode surface area (SA). Figure 5.8 is for new and aged LiNO$_3$-treated slabs in high RH conditions; Figure 5.9 is for new and aged LiBr-treated slabs in high RH conditions; Figure 5.10 is for new and aged LiNO$_3$-treated slabs in low RH conditions; Figure 5.11 is for new and aged LiBr-treated slabs in low RH conditions; Figure 5.12 is for the control in high RH conditions; and Figure 5.13 is for the control in low RH conditions.

In high RH conditions (Figures 5.8, 5.9, and 5.12), the galvanic currents were initially very high and sufficient to protect the steel. In all cases the currents decreased in value with time and in some cases dropped below the minimum current needed for protection. In general the LiBr-treated slabs had higher galvanic currents than the LiNO$_3$-treated slabs, which in turn were higher than the control slab.

In low RH conditions (Figures 5.10, 5.11, and 5.13), the galvanic currents started near the minimum required current density. Compared with the high RH conditions, galvanic currents did not drop nearly as much (even in terms of relative values). Again the LiBr-treated slabs had higher galvanic currents than the LiNO$_3$-treated slabs, which in turn were higher than the control slab (except for the new LiNO$_3$-treated slab in comparison with the control).

The galvanic currents in the controls, Figures 5.12-5.13, show a faster decline in current compared to the humectant-treated slabs.
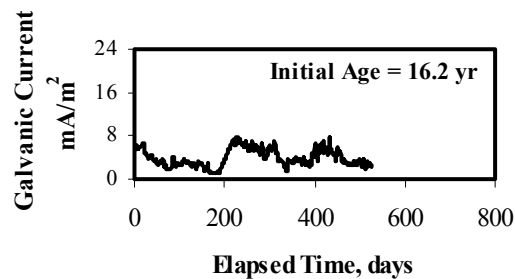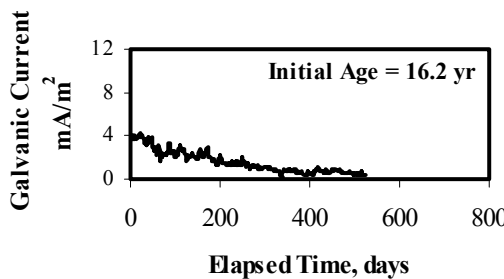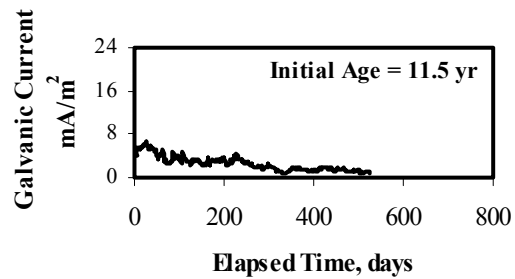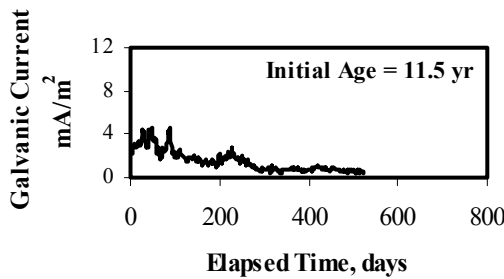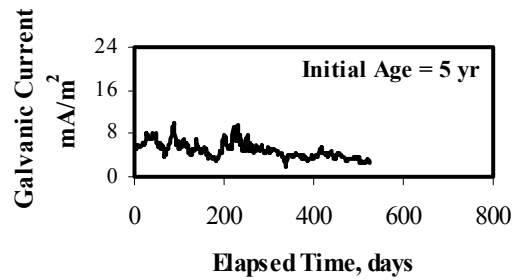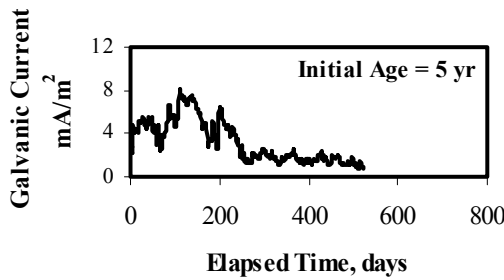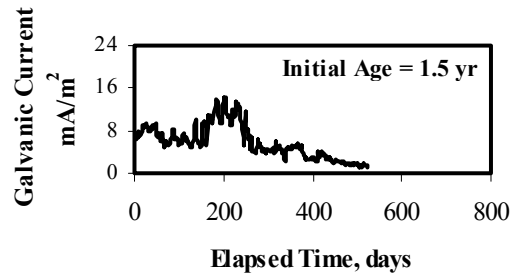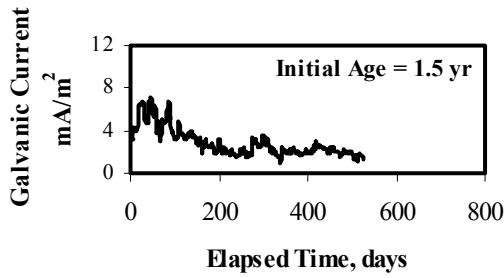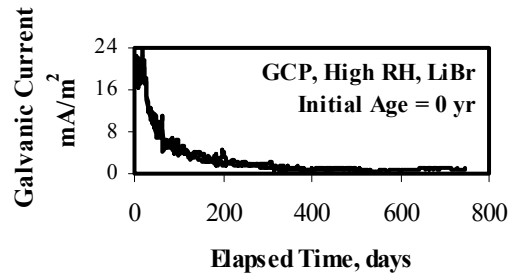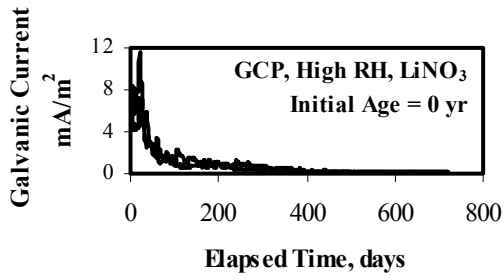
Figure 5.8: Galvanic currents for new and aged slabs with LiNO₃ in high RH conditions

Figure 5.9: Galvanic currents for new and aged slabs with LiBr in high RH conditions
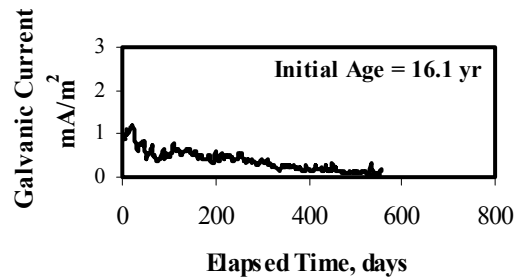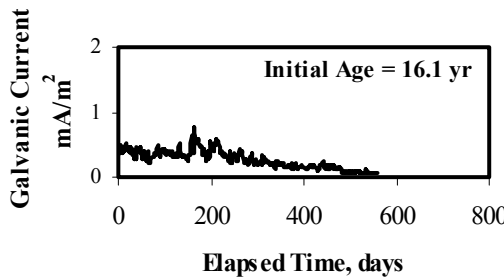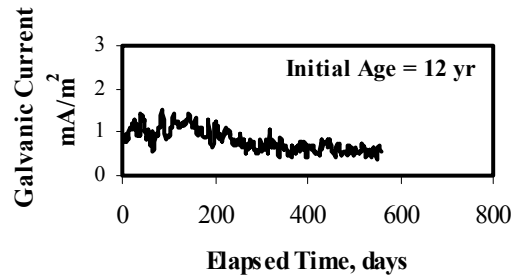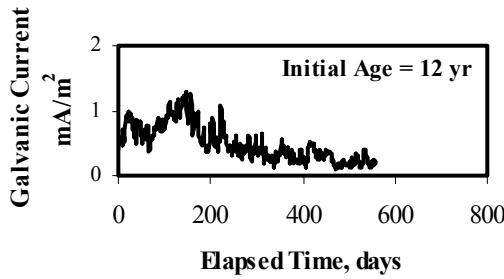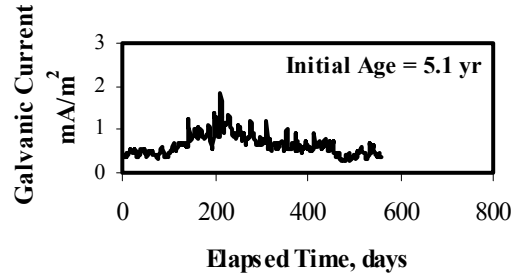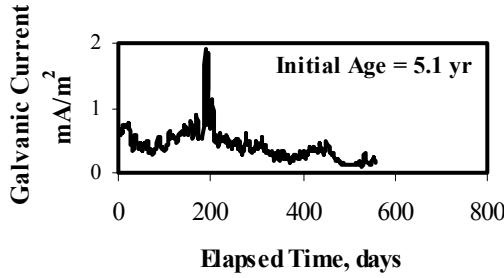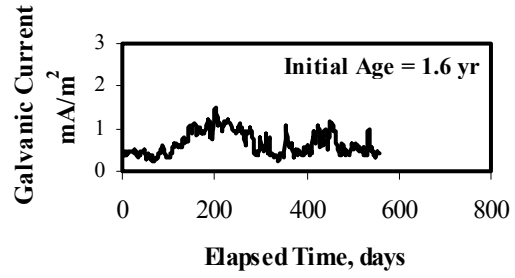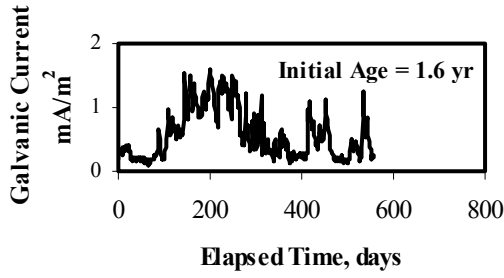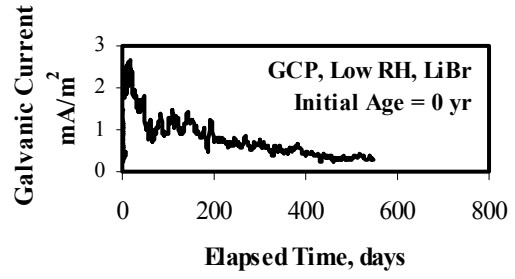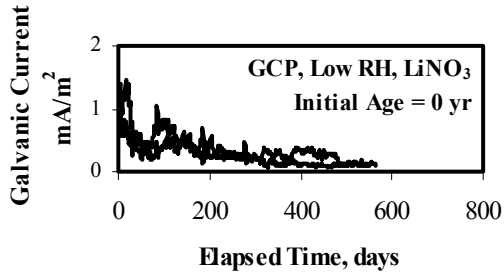
Figure 5.10: Galvanic currents for new and aged
slabs with LiNO$_3$ in low RH conditions

Figure 5.11: Galvanic currents for new and aged
slabs with LiBr in low RH conditions
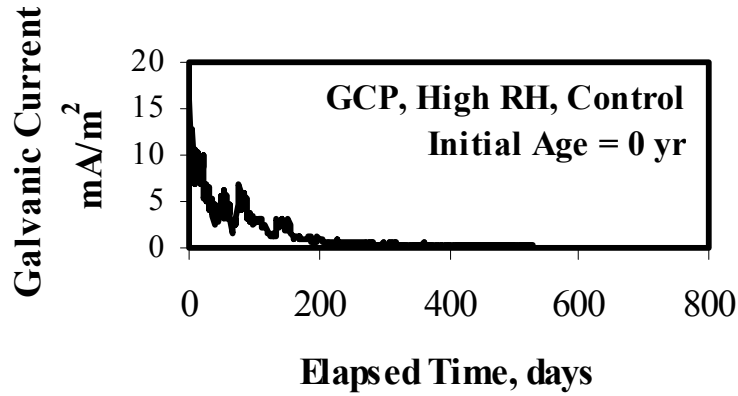
Figure 5.12: Galvanic currents for the new control slab in high RH conditions
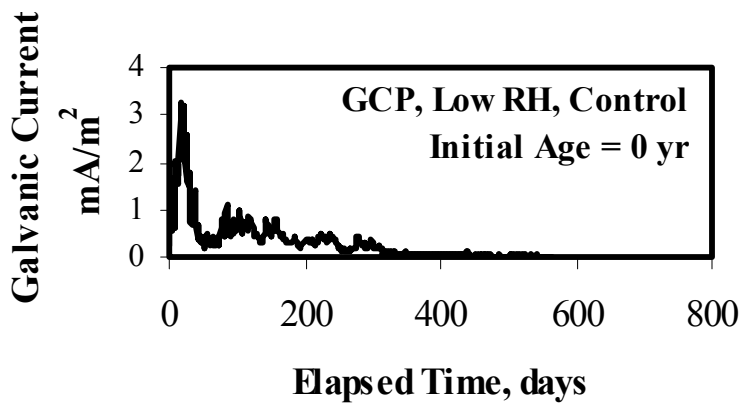
Figure 5.13: Galvanic currents for the new control slab in low RH conditions

Long-term galvanic current densities (the average current density after 1 year) in Figure 5.14 for high RH conditions show LiBr to provide more protection current than $LiNO_3$ for both new and aged slabs. Even the $LiNO_3$-treated slabs have sufficient current to protect the steel. However, the downward trends in current densities shown in Figures 5.8-5.13 suggest that LiBr-treatment may retain galvanic current densities above the minimum longer than $LiNO_3$-treatment.
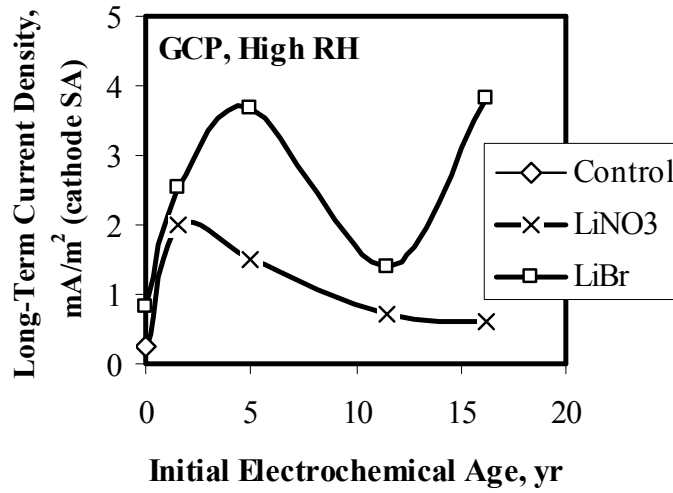
Figure 5.14: Long-term current densities for new and aged GCP slabs in high RH conditions
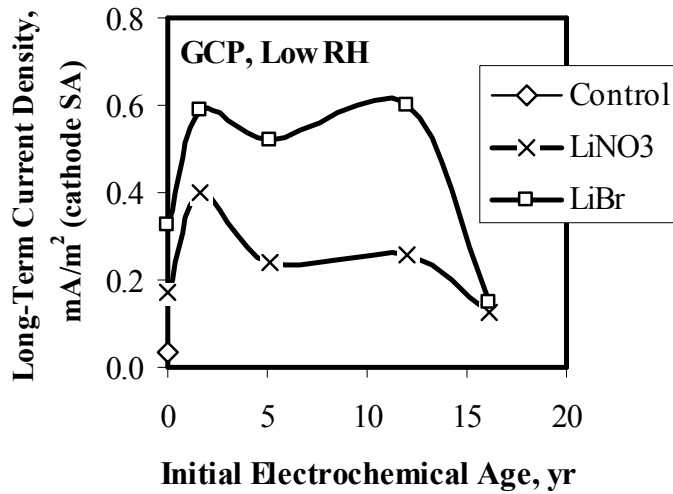
Figure 5.15: Long-term current densities for new and aged GCP slabs in low RH conditions

The long-term galvanic current densities in Figure 5.15 for low RH conditions show low values of current density. As in high RH conditions, LiBr resulted in higher currents than $LiNO_3$. Both were superior to untreated controls, yet were still below protective current density thresholds 1.1 to 5.4 mA/m^2 (*Fontana and Greene 1978*) or 2.2 mA/m^2 used for Oregon DOT ICCP systems (*Covino, et al. 2002*).

5.1.4 Depolarization

A common criterion for effective CP is depolarization of at least 100 mV. More than 100 mV indicates that the steel is completely protected, while less than 100 mV indicates that the steel protection may be incomplete. Note that the tests on slabs with ICCP were depolarized after a week at 0.2 mA/ft^2 (2.2 mA/m^2); the value used by Oregon DOT on coastal bridges, and not the larger accelerated current density used in most of the laboratory study.

The amount of depolarization that occurred after 24 hours is shown in Figure 5.16 for the ICCP slabs in both low RH conditions (top) and high RH conditions (bottom). The equivalent age is the combined age from both the initial electrochemical age (if any) and the electrochemical age from this study just prior to depolarization. Most of the depolarization values were above 100 mV. The exceptions were some of the LiBr-treated slabs in low RH conditions and some of the LiNO$_3$-treated slabs in high RH conditions. The linear regression lines show a slight downward trend with equivalent age. LiNO$_3$-treated slabs had, on average, higher depolarization values than LiBr-treated slabs.

Depolarization for GCP slabs is shown in Figure 5.17 in both low RH conditions (top) and high RH conditions (bottom). In contrast, with the ICCP results (Figure 5.16) there was a very distinct downward trend with equivalent age. Many depolarization values were below 100 mV, indicating insufficient protection. LiBr-treated slabs, on average had higher depolarization values under high RH conditions; the reverse was found under low RH conditions. The low depolarization values beyond an electrochemical age of 3-5 years correspond to the decreased current output from GCP anodes older than 5 years, Figure 5.14.
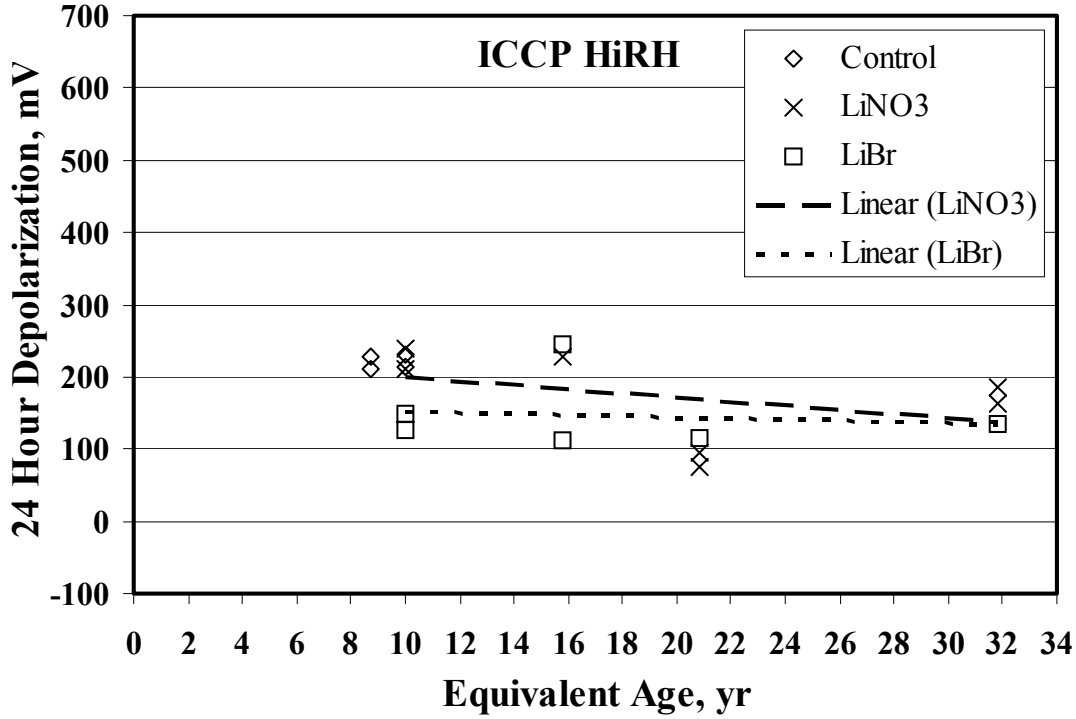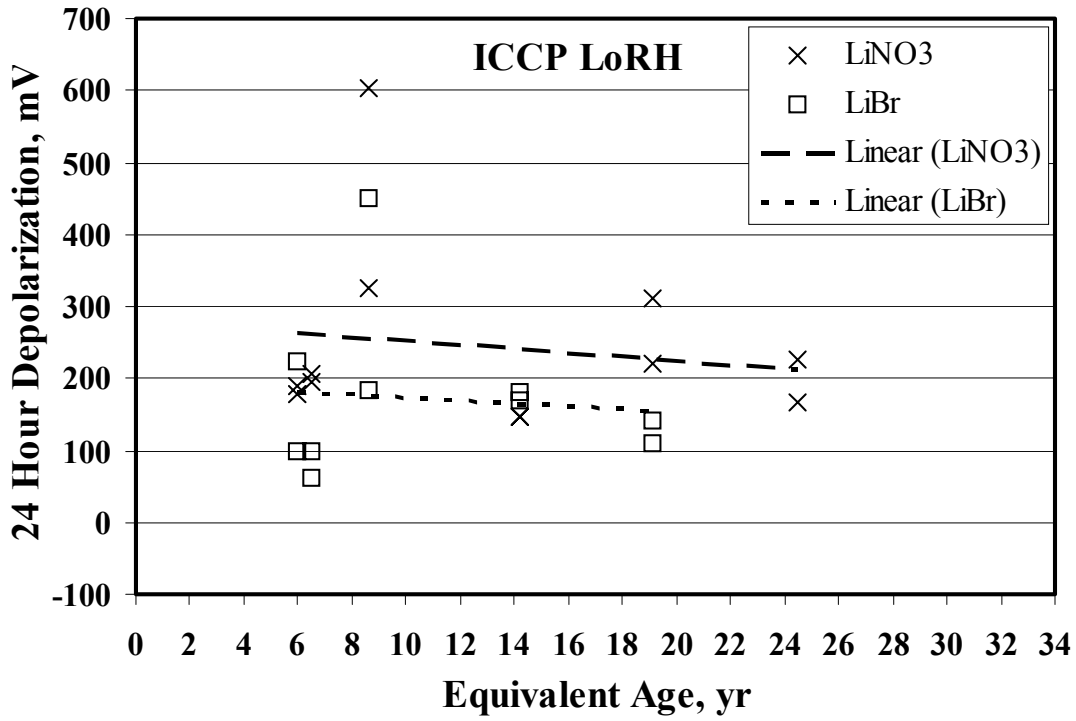
Figure 5.16: 24-hour depolarization voltages for long-term laboratory ICCP samples in low RH (top) and high RH (bottom) conditions
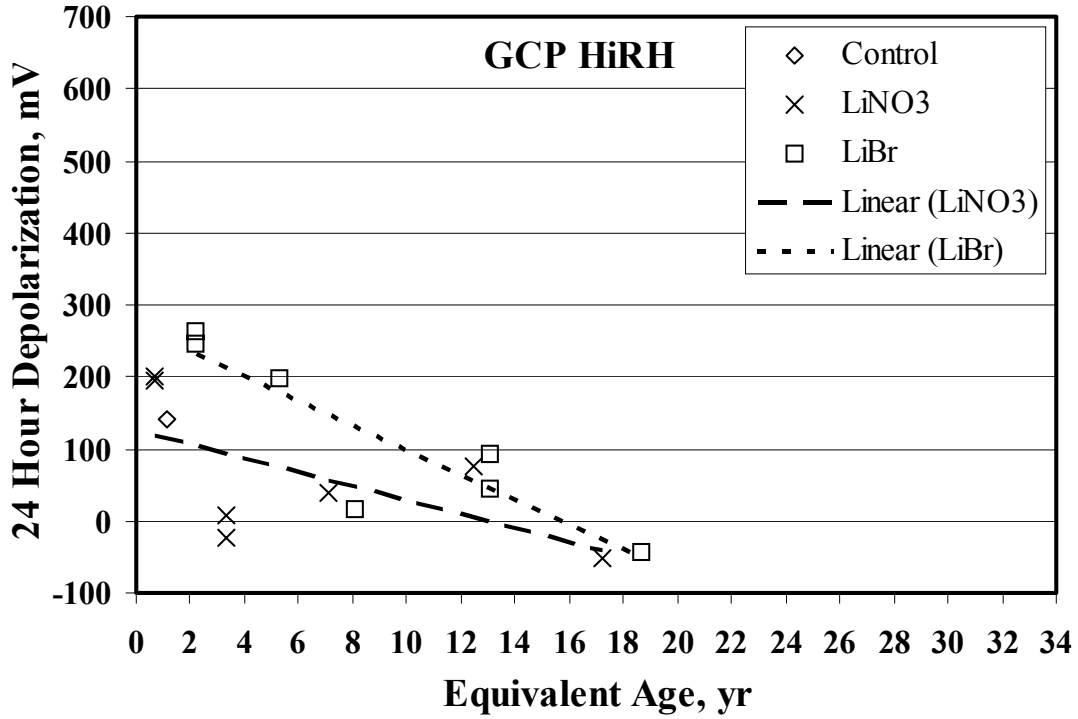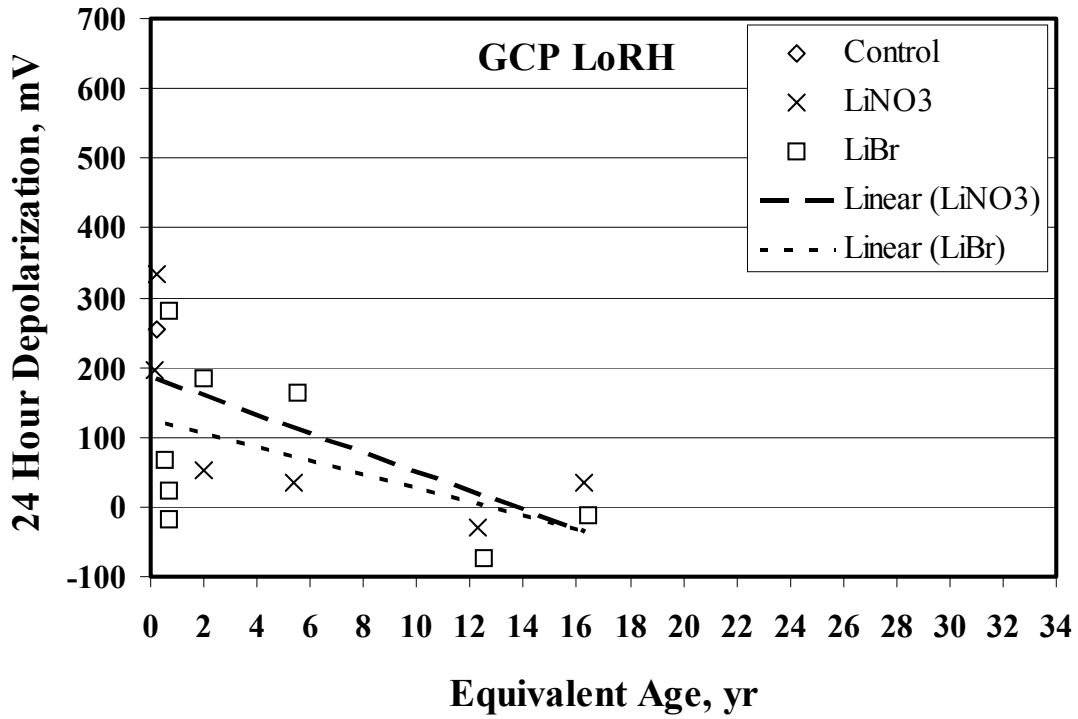
Figure 5.17: 24-hour depolarization voltages for long-term laboratory GCP samples in low RH (top) and high RH (bottom) conditions

5.1.5　Microscopy

5.1.5.1　Microscopy of Long-Term ICCP–LiNO₃

The structure of the LiNO$_3$-treated concrete-anode interface is shown in the BSE image and elemental x-ray maps; Figure 5.18 for high RH exposure, and Figure 5.19 for low RH exposure. The structure consists of three distinct layers or zones, which are typical of thermal-sprayed zinc CP systems (*Bullard, et al. 1998; Covino, et al. 1996a; Covino, et al. 1996b; Covino, et al 1997a; Covino, et al. 2002*). From top to bottom: the zinc anode, an anode-concrete reaction zone, and the undisturbed cement paste. The reaction zone can be further divided into three subzones or regions: 1) a layer of ZnO formed from and adjacent to the Zn anode; 2) a calcium-depleted, Zn-rich layer formed within the cement paste; and 3) cement paste containing low levels of Zn. The reaction zone resulted from the Zn anode oxidizing during ICCP. Zinc dissolution products migrated into the cement paste, interacted with moisture in the concrete, and replaced calcium within the cement paste (a secondary mineralization process). The rejected Ca migrated deeper into the reaction zone, where it deposited into and filled pores. The ZnO and the Ca-depleted, Zn-rich sublayers of the reaction zone were enriched in chloride, which migrated to the anode, under the influence of the CP potential gradient.
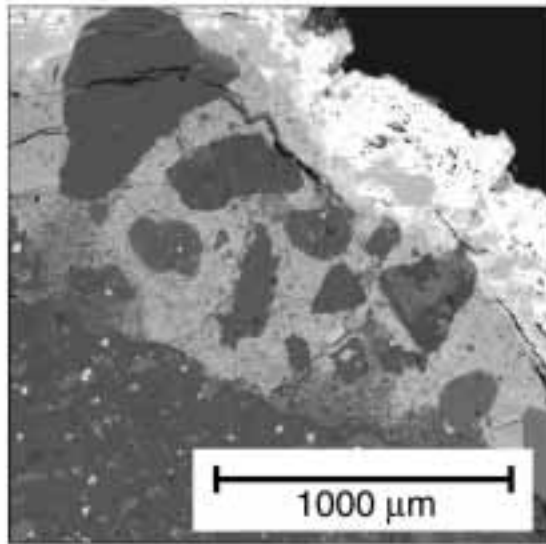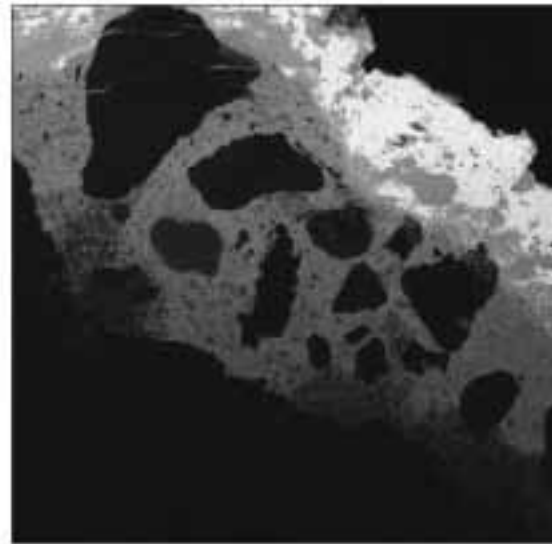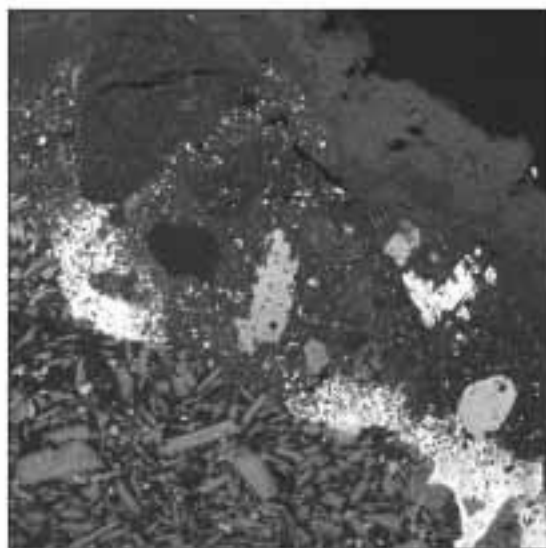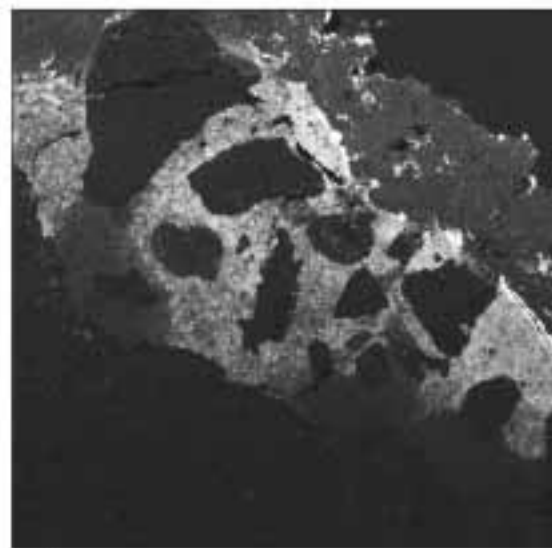
Figure 5.18: BSE and elemental x-ray maps of a LiNO$_3$-treated new slab exposed in the high-RH exposure after the equivalent of 5.3 years of ICCP. The zinc anode is at the top right and the unaltered concrete is at the bottom left of each cross section.

Figure 5.19: BSE and elemental x-ray maps of a LiNO$_3$-treated new slab exposed in the low-RH exposure after the equivalent of 6.1 years of ICCP. The zinc anode is at the top and the unaltered concrete is at the bottom of each cross section.

Element line scans obtained by ASEM were integrated and used to quantify the amount of selected elements in the various zones. Chloride results are presented in Table 5.1. The biggest distinctions between the high and low RH exposures were the larger reaction zone and the greater amount of Cl^- in the reaction zone for high RH conditions, indicating higher ion mobility under high RH conditions. The reaction zone was much larger in the high RH exposure (0.90 mm) than in the low RH exposure (0.21 mm), Table 5.1. The larger reaction zone in the high RH exposure shows the distinct reaction layer subzones (Figure 5.18) much clearer than in the low RH exposure (Figure 5.19). Table 5.1 also shows that there was much more Cl^- in the reaction zone for the high RH exposure.

Table 5.1: Long-term ICCP microanalyses

	LiNO₃		LiBr		
	High RH	**Low RH**	**High RH**	**Low RH**	**Low RH**
Initial electrochemical age[A], yr	0	0	0	0	19.0
Final electrochemical age[A], yr	5.3	6.1	5.3	6.1	19.8
Mean circuit resistance, $k\Omega\text{-}m^2$	0.13	0.95	0.28	2.45	3.68
Reaction zone thickness, mm	0.90	0.21	0.79	0.54	0.80
Retained Cl⁻, g Cl/m² (% of total)					
On surface	10.4	6.9	4.7	3.7	2.3
	(10.5)	(24.9)	(23.2)	(9.8)	(18.3)
In anode	1.3	2.2	5.7	4.7	0.6
	(1.3)	(8.1)	(28.0)	(12.5)	(4.7)
In reaction zone	82.9	15.7	9.3	21.7	9.5
	(83.9)	(56.3)	(45.8)	(57.5)	(75.6)
In cement paste beyond the reaction zone	4.3	3.0	0.6	7.6	0.2
	(4.4)	(10.8)	(2.9)	(20.2)	(1.4)
Total	98.9	27.8	20.2	37.8	12.6
Retained Br, g Br/m² (% of total)					
In anode			2.1	12.0	0.2
			(4.6)	(9.1)	(15.0)
In reaction zone			38.3	68.9	0.5
			(83.3)	(52.4)	(35.0)
In cement paste beyond the reaction zone			5.5	50.7	0.7
			(12.0)	(38.5)	(50.0)
Total[B]			46.0	131.6	1.4

[A]Years of service at the 0.2 mA/ft² (2.2 mA/m²) that Oregon DOT typically uses in coastal bridge ICCP systems.
[B]The LiBr application rate was 86 g LiBr/m², which corresponds to 79 g Br/m².

5.1.5.2   *Microscopy of Long-Term ICCP–LiBr*

The structure of the LiBr-treated concrete-anode interface is shown in the BSE image and elemental x-ray maps in Figure 5.20 for a new slab in the high RH enclosure, in Figure 5.21 for a new slab in the low RH enclosure, and in Figure 5.22 for an aged slab in the

low RH enclosure. The overall structure is similar to the LiNO$_3$-treated slabs as described above. The elemental x-ray line scans shown in Figure 5.23 for the new slab in the high RH enclosure illustrates the type of line scans that are obtained by ASEM. It also shows the different zones in terms of the atomic concentration of each element. The zones are most discernable from changes in the Zn and Ca concentrations.

The interface in Figure 5.22 delaminated during sample preparation, creating a gap within the reaction zone, between the ZnO layer and the Ca-depleted, Zn-rich layer formed within the cement paste.

The Br component of the humectant is detectable by x-rays. Figures 5.20-5.21 show the highest concentration of bromide to be in the ZnO portion of the reaction zone. However, Br was also found in the anode and in the rest of the reaction zone. Table 5.1 shows that in the high RH exposure, 83.3 percent of the Br was found in the reaction zone. In the low RH exposure, 52.4 percent of the Br was found in the reaction zone. In both cases much or all of the applied Br (79 g Br/m^2) was retained at the anode. Only 1.4 g/m^2 of Br was found in the aged slab (Table 5.1), much less than the applied amount.

The sulfur (S) x-ray maps in Figures 5.20 and 5.22 show that S from the concrete can also concentrate at the anode-concrete interface. Sulfate ions migrate to the anode under the influence of the CP potential gradient similar to chloride ions.

Unlike the LiNO$_3$-treated slabs, the reaction zone thickness in the LiBr-treated slabs did not differ much between the low and high RH exposures. As Table 5.1 shows, the high RH exposed reaction zone thickness was 0.79 mm compared to 0.54 mm for the low RH exposed reaction zone. The Zn x-ray maps for both humectants at both humidities, Figure 5.24, show the relative sizes of the reaction zones quite clearly. Figure 5.24 also shows that the reaction zone thickness was approximately the same, regardless of the humectant at high RH, but not at low RH.

A major difference between the LiBr- and LiNO$_3$-treated slabs was how the Cl$^-$ was distributed. The Cl x-ray map for both humectants, at both humidities, (Figure 5.25) shows that in the LiBr-treated slabs most of the Cl$^-$ was in the reaction zone nearest the Zn anode. This compares with the LiNO$_3$-treated slabs where there was a much broader Cl$^-$ distribution within the reaction zone.
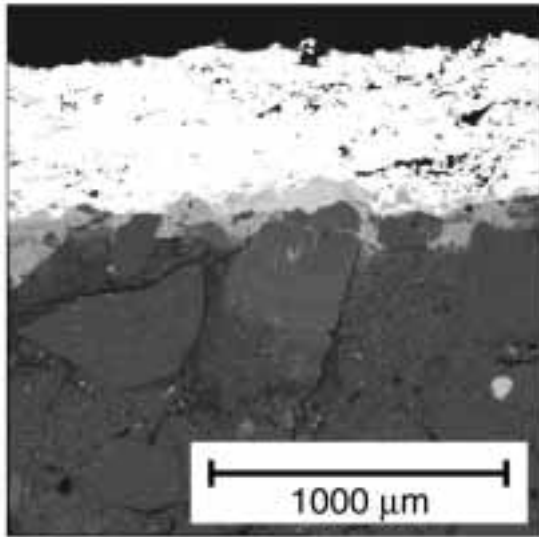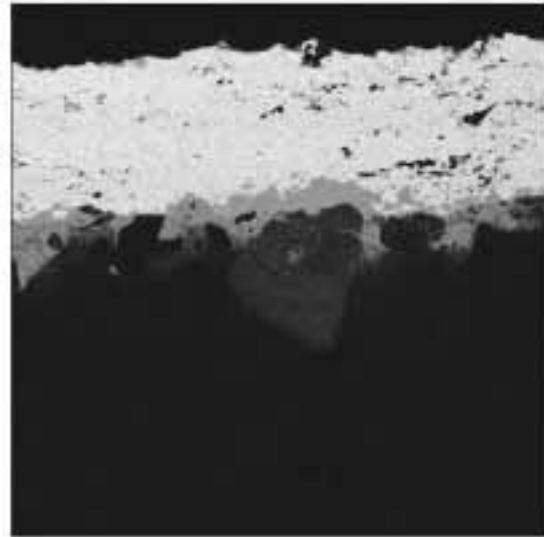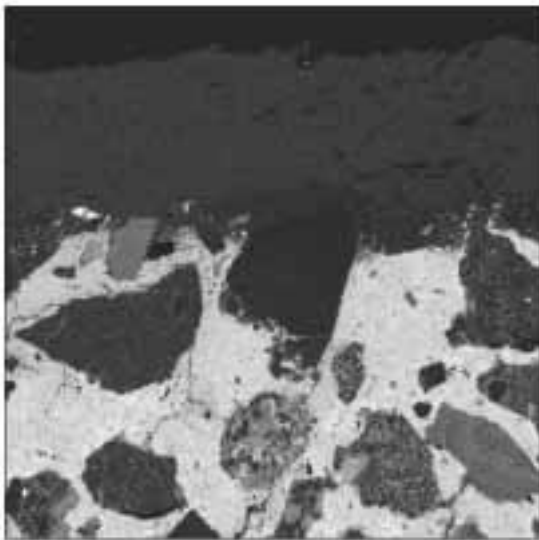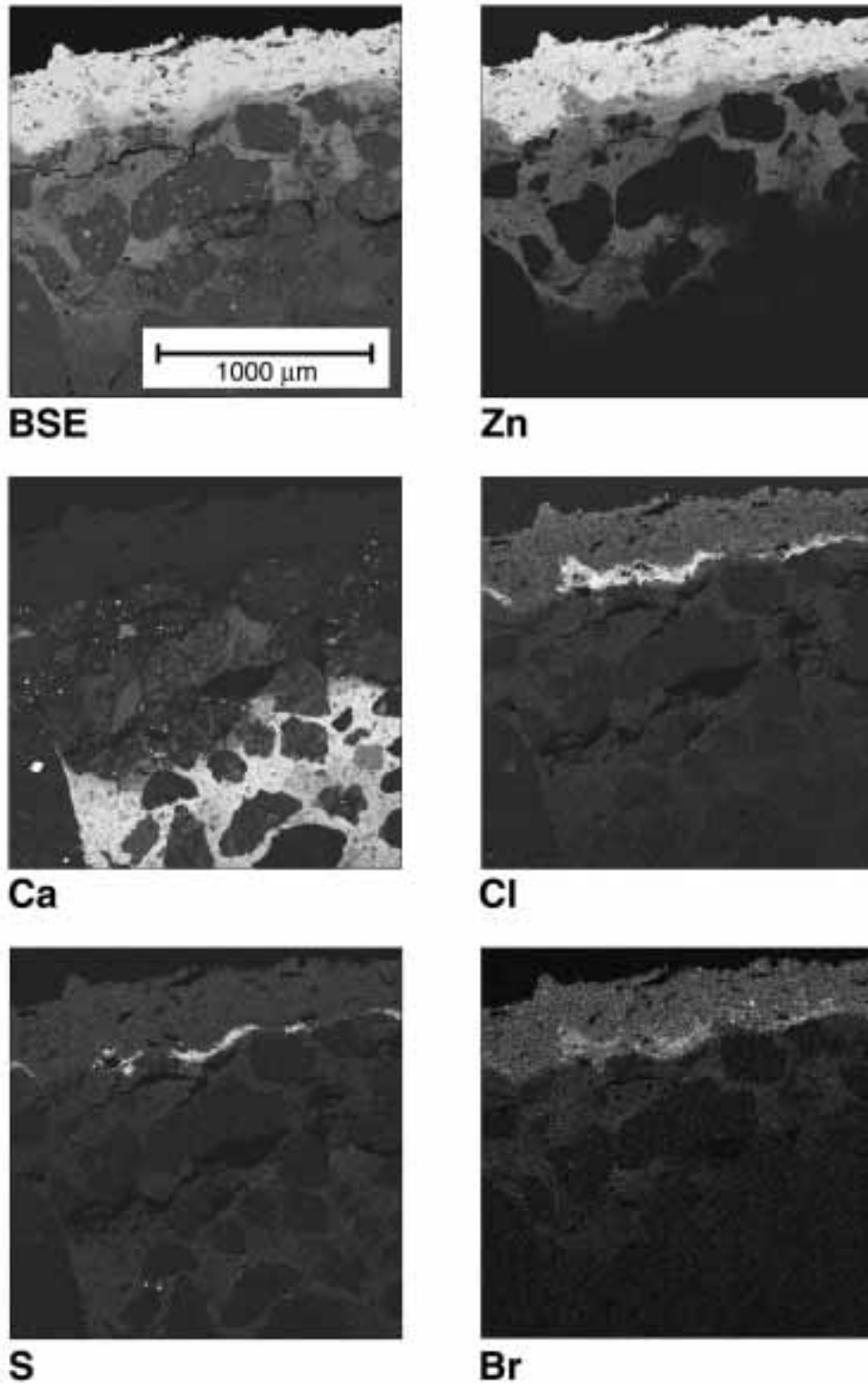
Figure 5.20: BSE and elemental x-ray maps of a LiBr-treated new slab exposed in the high-RH exposure after the equivalent of 5.3 years of ICCP. The Zn anode is at the top and the unaltered concrete is at the bottom of each cross section.
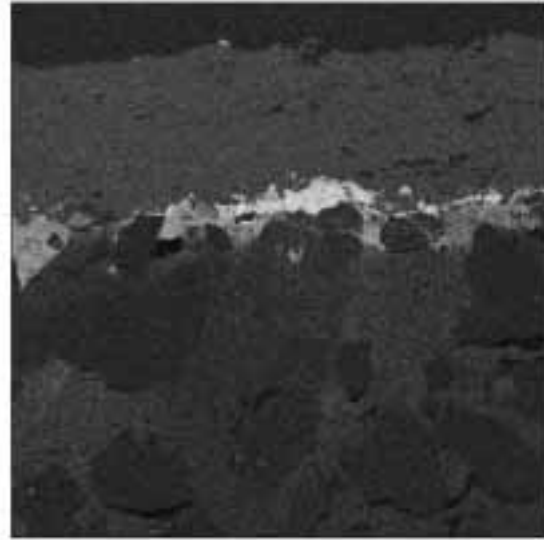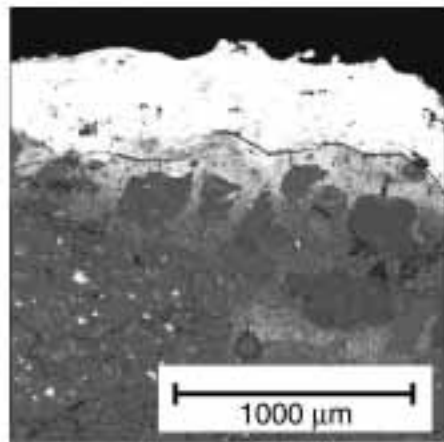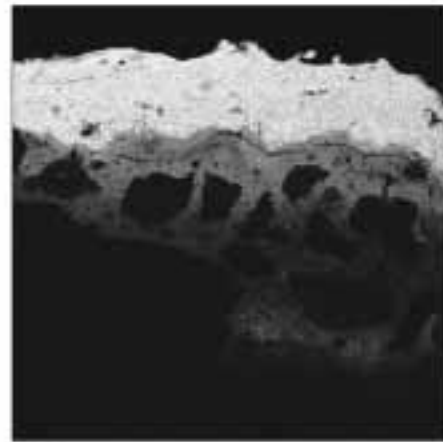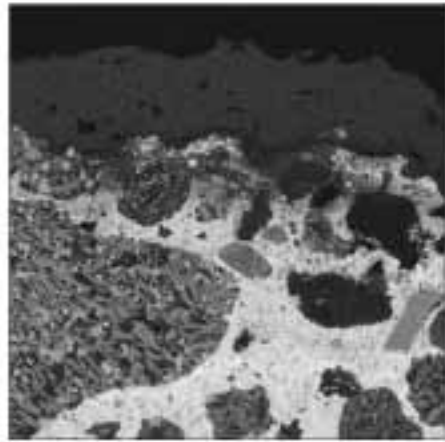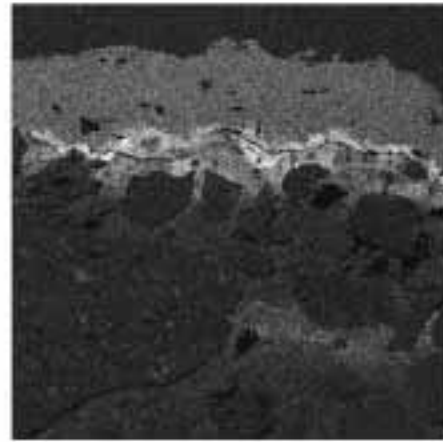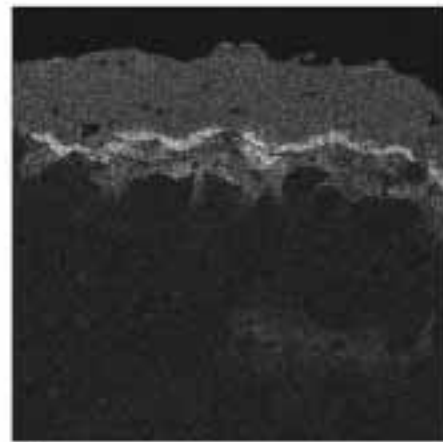
Figure 5.21: BSE and elemental x-ray maps of a LiBr-treated new slab exposed in the low-RH exposure after the equivalent of 6.1 years of ICCP. The Zn anode is at the top and the unaltered concrete is at the bottom of each cross section.
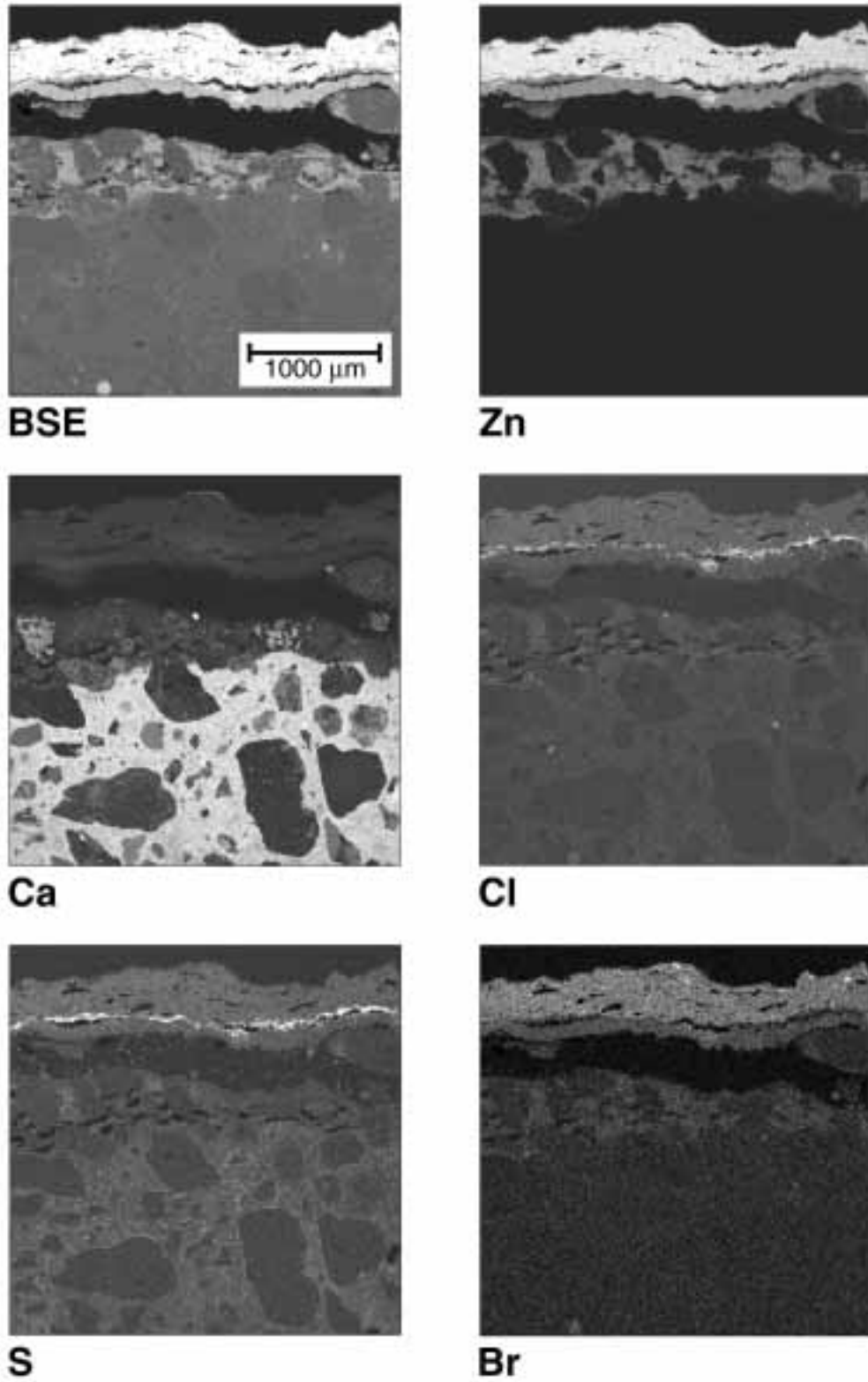
Figure 5.22: BSE and elemental x-ray maps of a LiBr-treated aged slab exposed in the low-RH exposure after the equivalent of 0.8 additional years of ICCP. The initial electrochemical age was 19 years. The Zn anode is at the top and the unaltered concrete is at the bottom of each cross section.
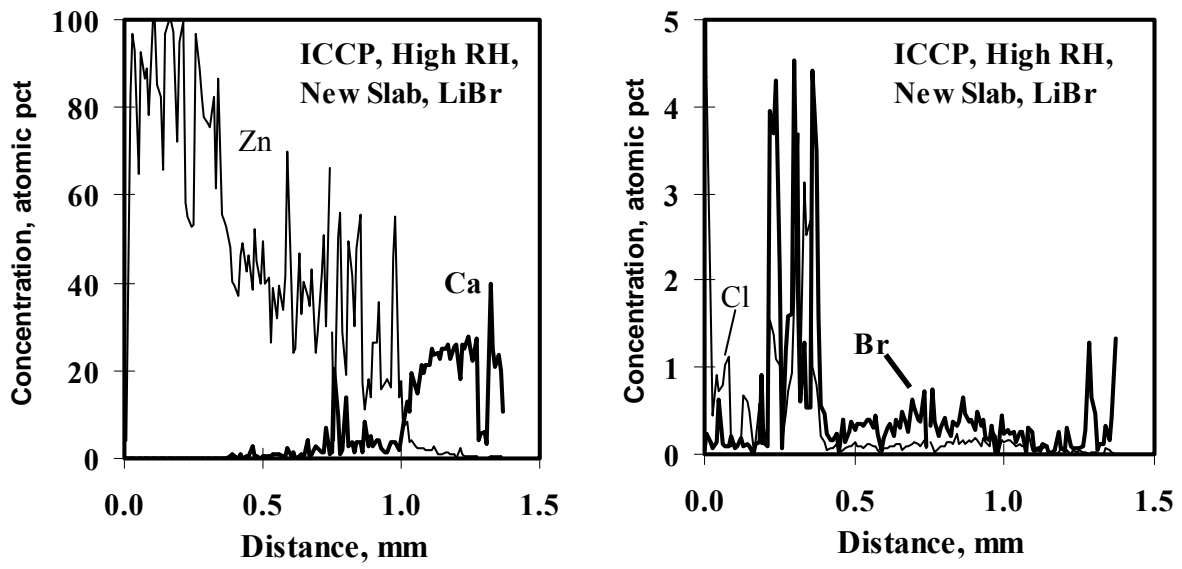
Figure 5.23: X-ray line scans of a LiBr-treated new slab exposed in the high-RH exposure after the equivalent of 5.3 years of ICCP
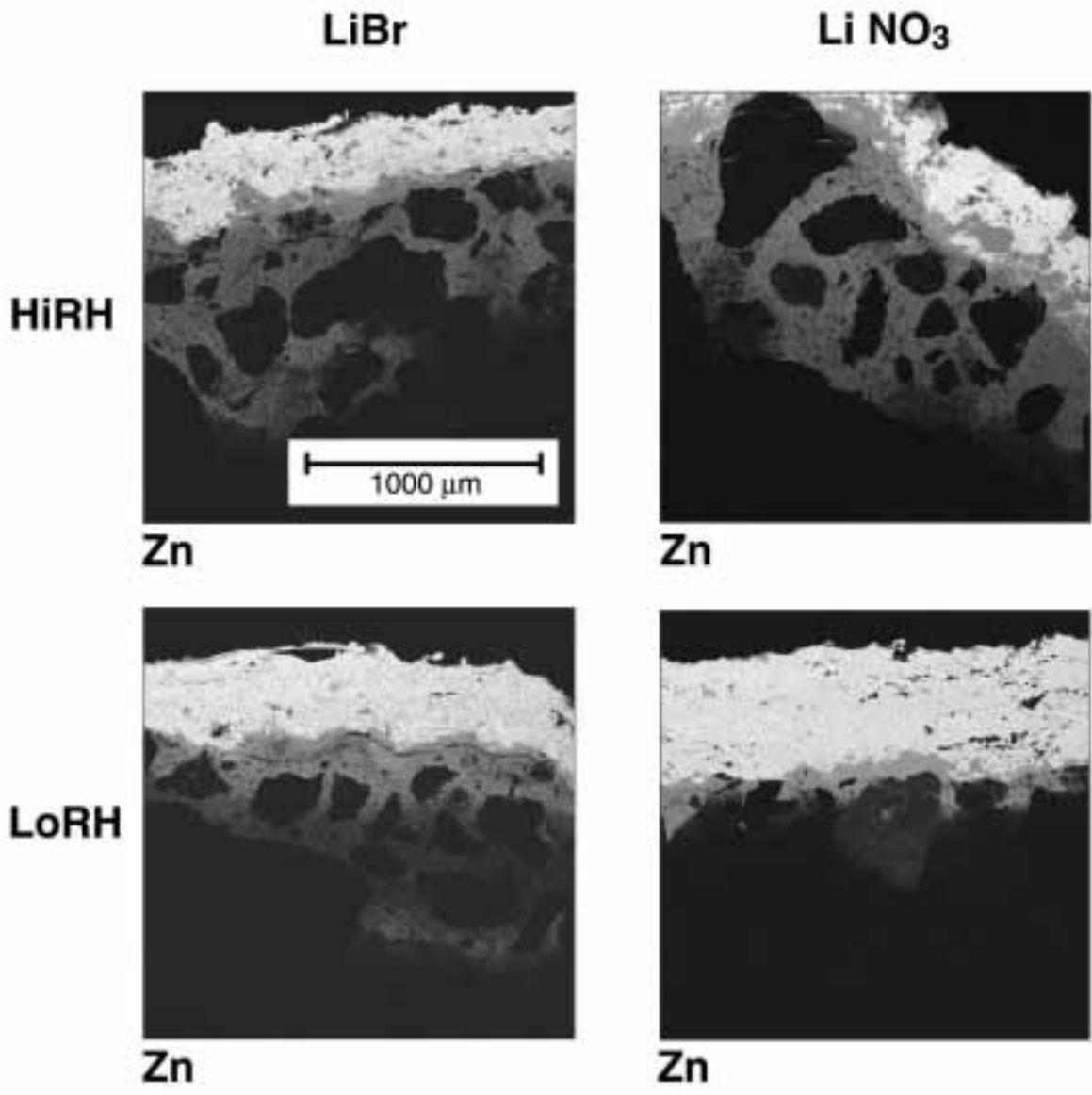
Figure 5.24: Elemental zinc x-ray maps for both humectants and both humidities after the equivalent of 5.3 years (high RH) and 6.1 years (low RH) of ICCP
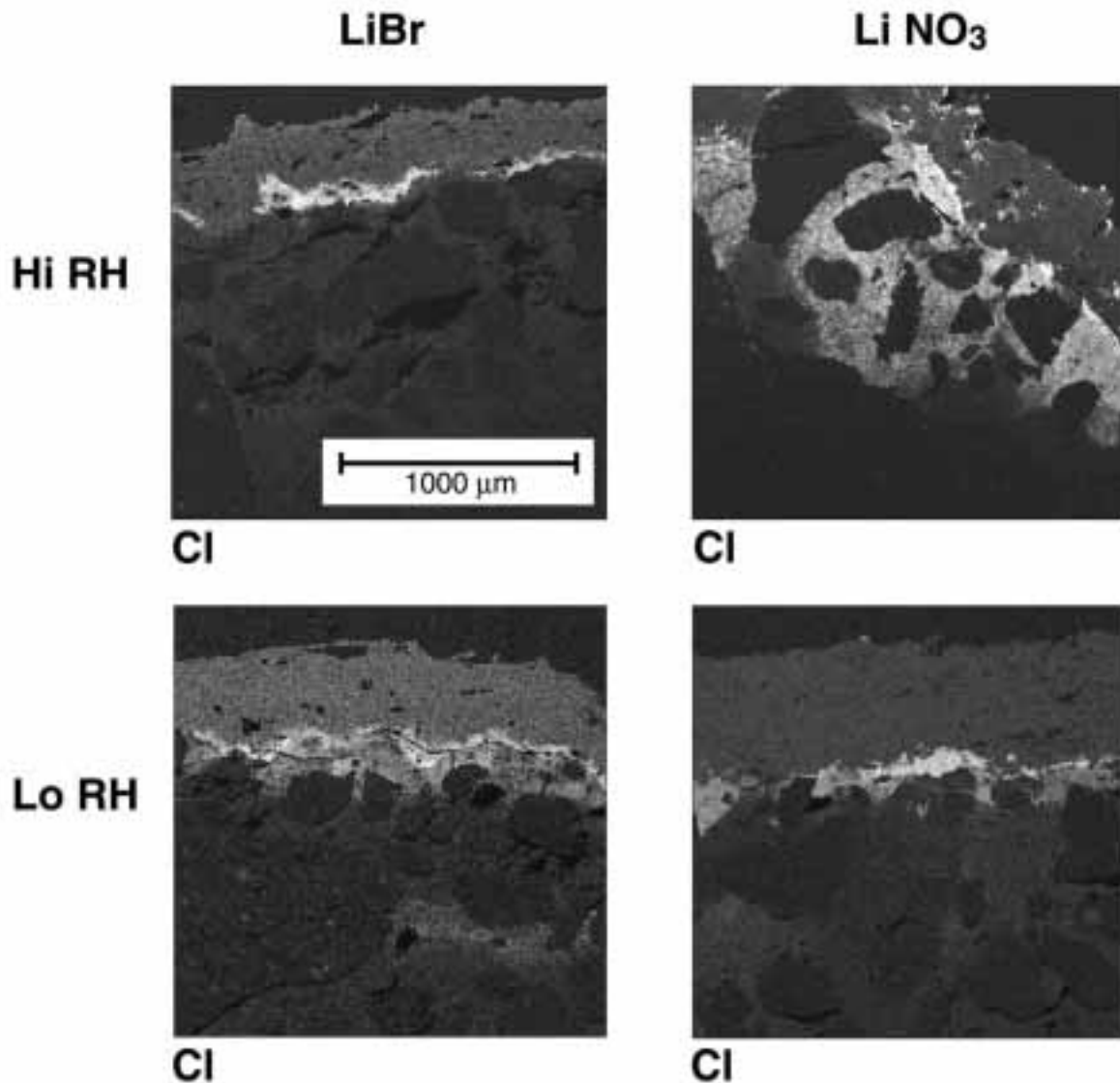
Figure 5.25: Elemental Cl x-ray maps for both humectants and both humidities after the equivalent of 5.3 years (high RH) and 6.1 years (low RH) of ICCP

5.1.6   AC Resistance and Circuit Resistance

AC Resistance measurements between anode and cathode are compared with circuit resistances in Figure 5.26. Linear regression resulted in a slope of 0.25 with a R^2 of 0.65. Even with the wide range of sample types, elapsed time between measurements, and differing current densities (the aged low RH slabs were at a lower impressed current density), a general trend emerges that circuit resistance tracks AC resistance. This means that circuit resistance, which can be obtained directly from ICCP operation parameters, should give useful information about the state of the Zn-concrete interface, where the buildup of corrosion products increases the ohmic resistance.

This is consistent with the successful use of circuit resistance calculations to track performance for CP zones of widely varying size and total current in both laboratory and field installations (*Bullard, et al. 1998; Covino, et al. 2000; Covino, et al. 2002*).
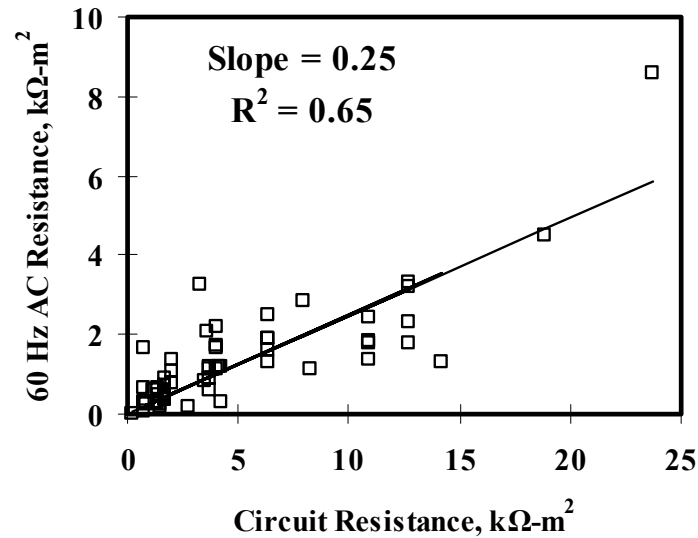
Figure 5.26: AC resistance compared with circuit resistance (defined as operating voltage divided by impressed current density)

5.1.7   Adhesion Strength

The adhesion strengths were measured at the conclusion of the CP test for each long-term ARC laboratory slab. In Figures 5.27-5.30, where bond strength is shown as a function of electrochemical age, the electrochemical age is the equivalent age based on the nominal current level of 2.2 mA/m^2 (0.2 mA/ft^2) used by Oregon DOT on Oregon coast ICCP systems. The conversion is that 100 kC/m^2 corresponds to 1.473 years of Oregon DOT coastal bridge service.

The fitted curved lines in Figures 5.27-5.30 are from the results of earlier adhesion strength experiments. The line reaching zero bond strength at 27 years is for environments with repeated wetting of the anode (*Covino, et al. 1996a; Covino, et al. 1996b; Covino, et al. 2002; Holcomb, et al. 1996*). This was essentially the same environment as used for the high RH conditions in this study. The curved line reaching zero bond strength at 5 years is for a much dryer environment with minimal wetting of the anode *(Bullard, et al. 1997a; Bullard, et al. 1998; Covino, et al. 2002).* This was a harsher environment than the low RH conditions used in this study because the anode was only infrequently wetted for the dryer environment measurements. However, the measurements from that work are illustrative of anode bond strengths from a dry environment.

The results for accelerated ICCP at low RH are shown in Figures 5.27. While there is significant scatter in the data, the general trend is much like the high RH wetted environment that had a lifetime of 27 years. In most cases the LiBr-treatments resulted in higher bond strengths than the LiNO$_3$ or KC$_2$H$_3$O$_2$ treatments. The new control and KC$_2$H$_3$O$_2$ slabs were pulled early from the experiment (Figures 5.2 and A5.2) because bond strengths were low. Consequently, their electrochemical ages are much lower than for the new LiBr or LiNO$_3$ slabs.

Figure 5.27: Bond strength results for accelerated ICCP in low RH environments. The aged slabs had initial equivalent ages of 3, 8, 13.1, and 19 years.

The aged slabs in Figures 5.27 have a mixed history. In the prior experiment they underwent accelerated ICCP at 27 mA/m^2 (2.5 mA/ft^2) in high RH conditions to equivalent ages of 3, 8, 13.1, and 19 years. After treatment with humectants they underwent accelerated ICCP at 10 mA/m^2 (0.9 mA/ft^2) in low RH conditions for approximately 5-6 more equivalent years. In Figures 5.27 these aged slabs showed poorer bond strengths as compared with the 27-year wet curve, but that could be expected from the low RH conditions.

The ranking of humectant treatments, in terms of bond strengths for new and aged ICCP slabs at low RH, was LiBr > LiNO$_3$ > KC$_2$H$_3$O$_2$.

The results for accelerated ICCP at high RH are shown in Figure 5.28. The bond strengths for the new slabs were very low, with some showing complete disbondment at the higher ages. The new KC$_2$H$_3$O$_2$ slabs had quite poor bond strengths even after as low as 3-5 equivalent years. The overall results for the new slabs were so poor that one could suspect that humectants were the cause. However, the control slab also had a very low bond strength that was consistent with the humectant-treated slabs. The cause for these low bond strengths has not been determined.
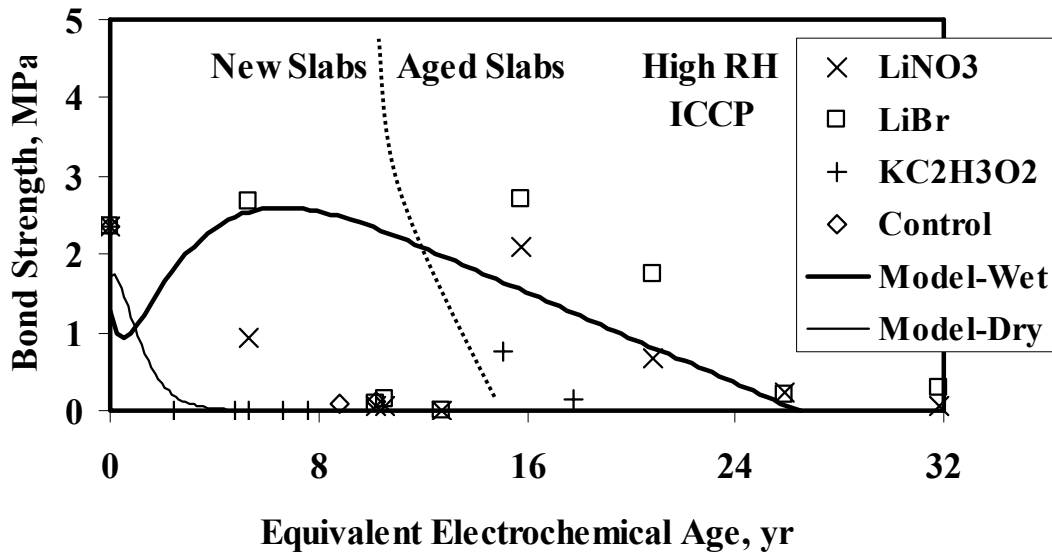
Figure 5.28: Bond strength results for accelerated ICCP in high RH environments. The aged slabs had initial equivalent ages of 3, 8, 13.1, and 19 years.

The aged slabs in Figure 5.28 started with electrochemical ages of 3, 8, 13.1, and 19 years. After treatment with humectants they underwent approximately 12-13 additional equivalent years of electrochemical aging. Since the environments of the prior and present experiments were very similar, these samples should show the effects of humectants more clearly than in Figure 5.27.

The ranking of humectant treatments, in terms of bond strengths for new and aged ICCP slabs at high RH, was LiBr > LiNO$_3$ > KC$_2$H$_3$O$_2$.

The results for GCP at low RH are shown in Figure 5.29. On this time scale the new slabs did not show much electrochemical age. They did show higher bond strengths than the ICCP lines from the prior experiments.
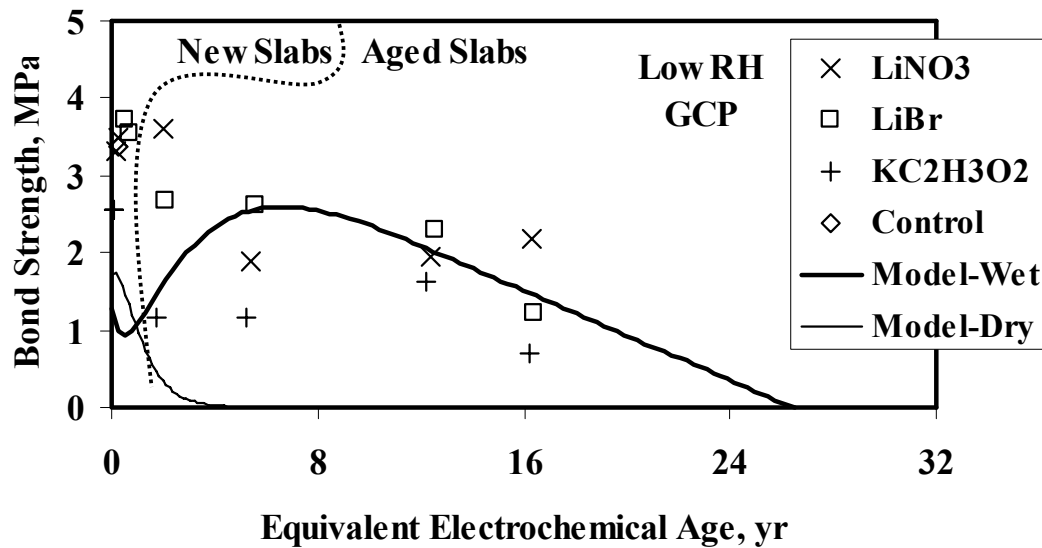
Figure 5.29: Bond strength results for GCP in low RH environments. The aged slabs had initial equivalent ages of 1.6, 5.1, 12, and 16.1 years.

The aged slabs in Figure 5.29 started with electrochemical ages of 1.6, 5.1, 12, and 16 years from accelerated ICCP. After treatment with humectants they underwent approximately 1 additional equivalent year of electrochemical aging. The bond strengths generally followed the 27 year wetted curve that the slabs had prior to the humectant treatments.

The ranking of humectant treatments, in terms of bond strengths for new and aged GCP slabs at low RH, was $LiBr = LiNO_3 > KC_2H_3O_2$.

The results for GCP at high RH are shown in Figure 5.30. The new slabs underwent electrochemical aging based on their current densities, which for LiBr were much larger than for the other treatments (Figure 5.14). The bond strengths were high for the $LiNO_3$ and control slabs. The bond strengths of the $KC_2H_3O_2$-treated slabs were very low.
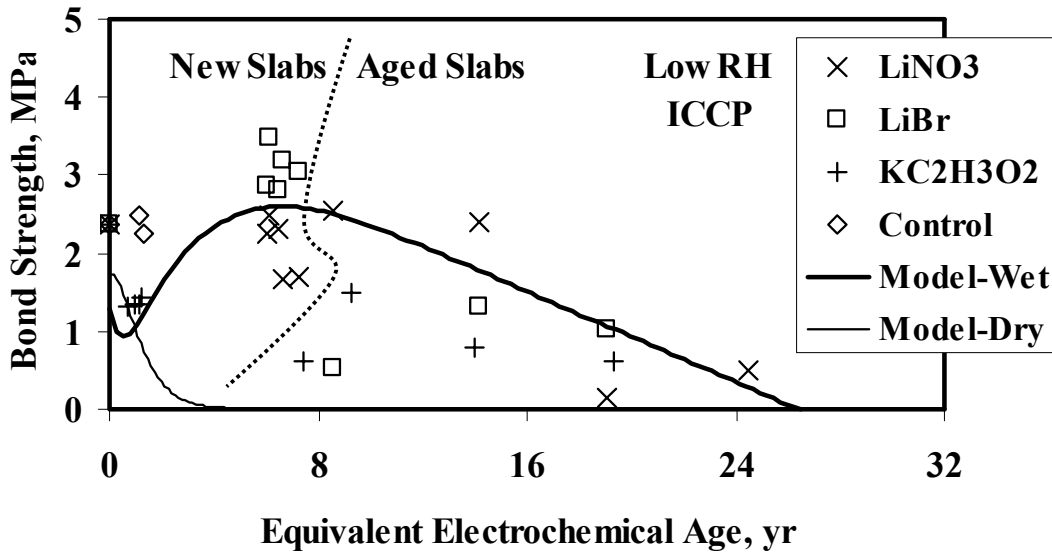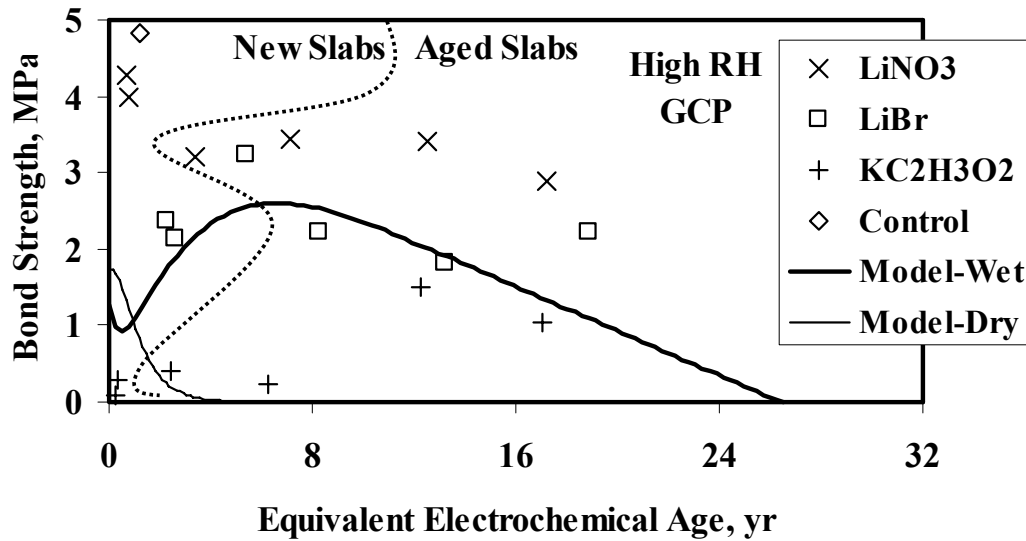
Figure 5.30: Bond strength results for GCP in high RH environments. The aged slabs had initial equivalent ages of 1.6, 5.1, 12, and 16.1 years.

The aged slabs in Figure 5.30 started with electrochemical ages of 1.6, 5.1, 12, and 16 years from accelerated ICCP. After the treatment with humectants the slabs underwent approximately 1-3 additional equivalent years of electrochemical aging. The LiNO$_3$ bond strengths were higher than the 27-year wetted curve. The LiBr bond strengths straddled the 27-year wetted curve. The results for the KC$_2$H$_3$O$_2$ slabs were mixed: two had very low bond strengths and two had bond strengths near the 27-year wetted curve.

The ranking of humectant treatments, in terms of bond strengths for new and aged GCP slabs at high RH, was LiNO$_3$ >LiBr >> KC$_2$H$_3$O$_2$.

The results in Figures 5.27-5.30 are compared with the model curves generated from the earlier study for wetted and dry conditions (*Covino, et al. 2002*). One more way to compare the results is by comparing the bond strengths for the aged slabs compared to the bond strengths measured from the same slab in the prior investigation, rather than to the fitted model curve. These comparisons are shown in Figures 5.31-5.32 for the ICCP tests in high and low RH environments. These results show that the additional aging follows the same trends as the model curve showed, with just the one LiBr-treated point in Figure 5.32 (low RH) showing a significant deviation.
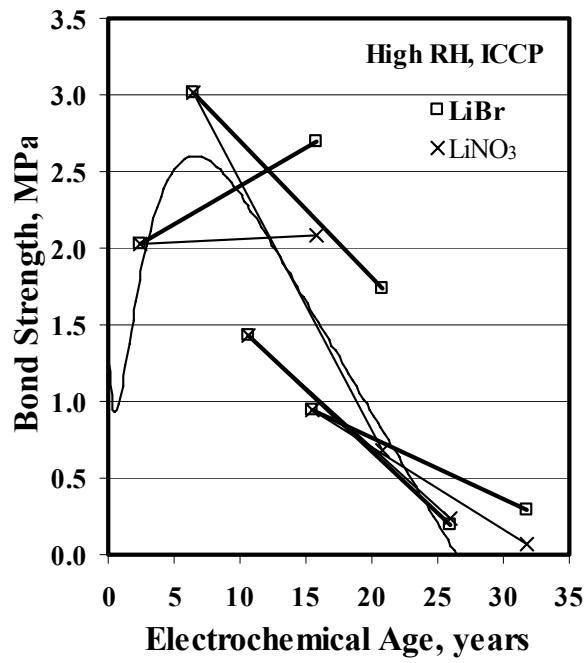
Figure 5.31: Bond strength results for ICCP aged slabs in high RH environments in comparison with their initial strength results
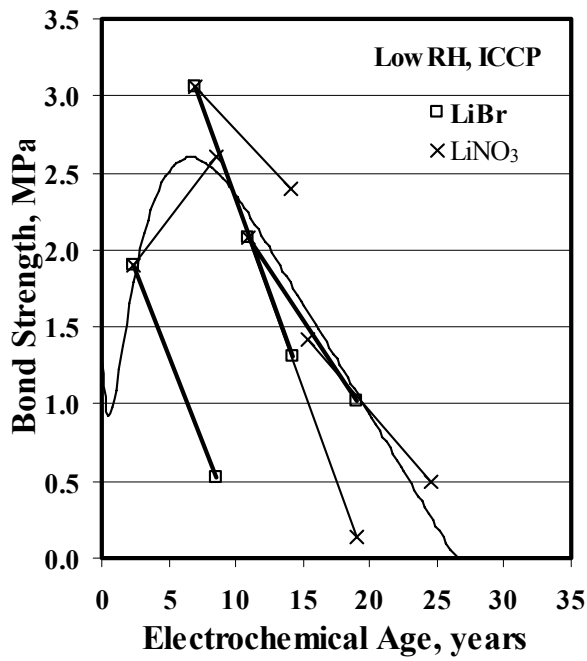
Figure 5.32: Bond strength results for ICCP aged slabs in low RH environments in comparison with their initial strength results

62

The results for different NaCl concentrations are shown in Figure 5.33 after accelerated electrochemical aging (to an equivalent electrochemical age of 17.9 years) in a high RH environment. Very little differences in bond strengths are seen for different NaCl concentrations. Note the closeness between the results at 1.2 kg/m^3 (2.0 1b/yd^3) for the control, and the blank. The blank received no treatment and the control received the same diluted surfactant solution that the humectants were dissolved into.
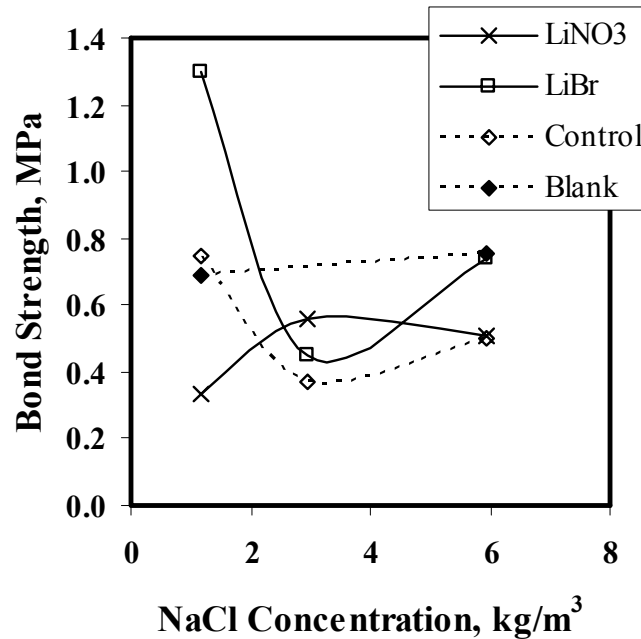
Figure 5.33: Bond strengths for different NaCl concentrations with accelerated ICCP (equivalent electrochemical age of 17.9 years) in high RH environments. The NaCl concentrations correspond to 2.0, 5.0, and 10.0 lb/yd^3.

5.2   SHORT-TERM CHAMBER EXPERIMENTS (ARC)

5.2.1   Mass Change Response to Temperature and Humidity

Results for mass change, as the slices equilibrated to the specific RH of the 90ºF (32.2ºC) humidity chamber are shown in Figure 5.34 for the LiNO$_3$- and LiBr- treated slices. Figure 5.35. shows the results for the slices with just the surfactant treatment and for the control. Results for KC$_2$H$_3$O$_2$-treated slices are in Appendix A. All of the plots are averages of 2 or 3 slices: 3 for LiNO$_3$- and LiBr-treated slices that have TS Zn, and 2 for all the remaining slices. All of the curves show the same general trends as the RH changes from 70%, 50%, 35%, and 80% RH.
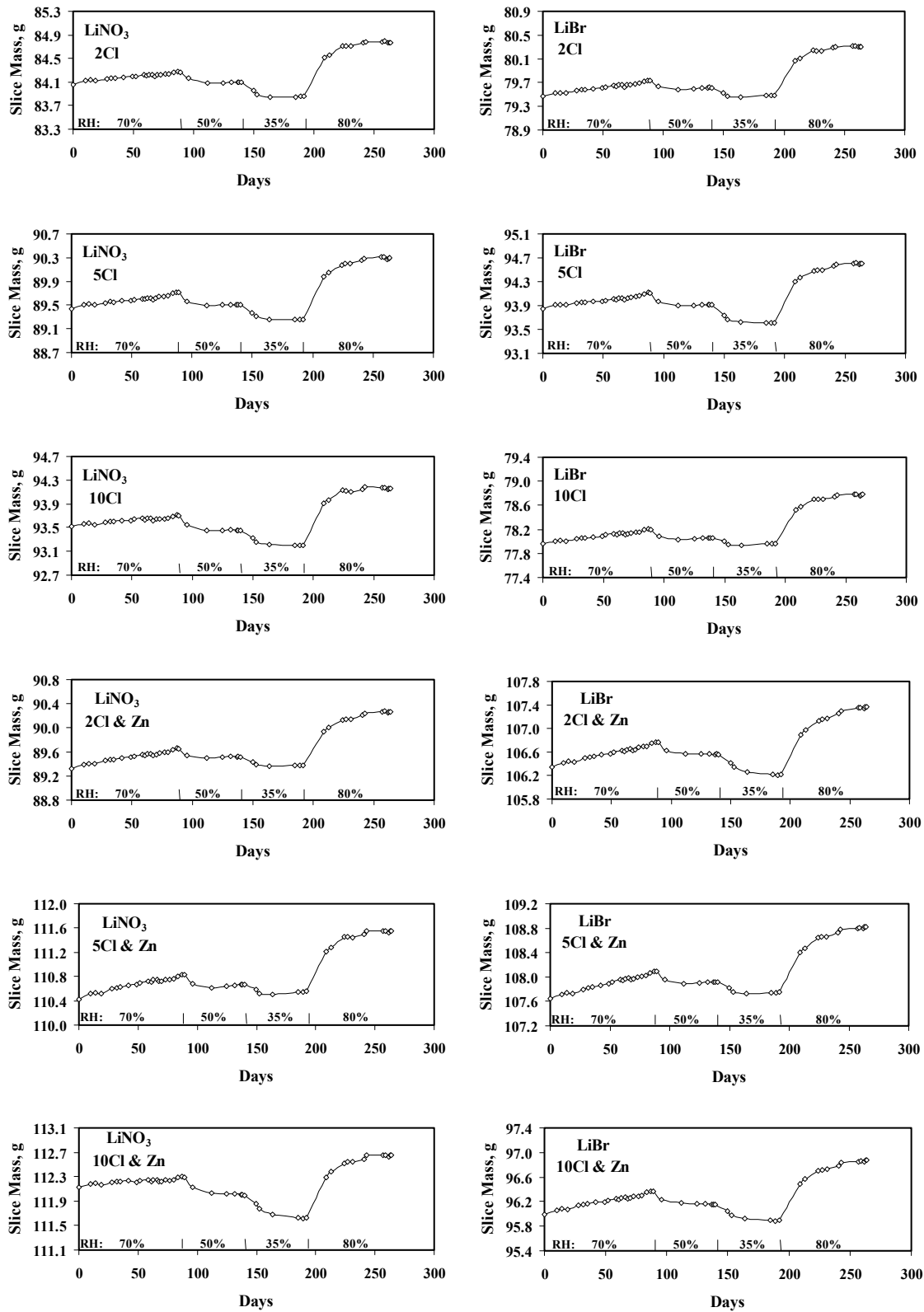
Figure 5.34: Mass change with exposure time of LiNO$_3$-treated and LiBr-treated slices at 90ºF (32.2ºC). The NaCl concentrations were 2.0, 5.0, and 10.0 lb/yd^3 (1.2, 3.0, and 5.9 kg/m^3).
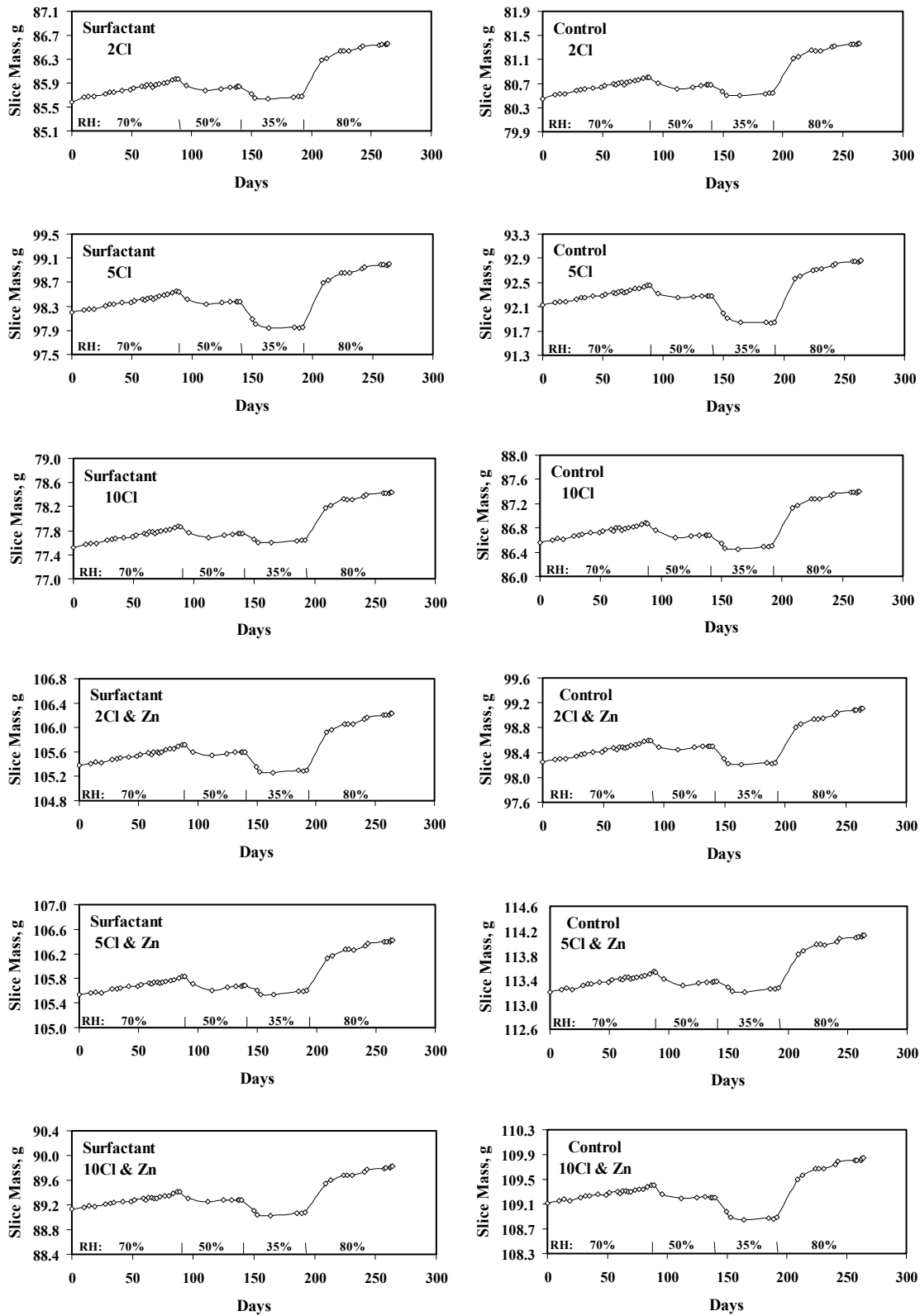
Figure 5.35: Mass change with exposure time of surfactant-treated and control slices at 90ºF (32.2ºC). The NaCl concentrations were 2.0, 5.0, and 10.0 lb/yd^3 (1.2, 3.0, and 5.9 kg/m^3).

The data in Figures 5.34 and 5.35 were examined by calculating the mass gain at 50%, 70%, and 80% RH with respect to the mass at 35% RH. The mass at each RH was the mean of the final 3 measurements at each RH. Table 5.2 shows the results of these calculations with the slices grouped together by humectant, NaCl level, and Zn.

Table 5.2: Equilibrated mass gain from a RH of 35%

CONDITION	50% RH, g	70% RH, g	80% RH, g	NUMBER OF SLICES
Humectant				
LiNO$_3$ (0.7854 g/slice + surfactant)	0.232	0.433	0.968	15
LiBr (0.7854 g/slice + surfactant)	0.220	0.390	0.966	15
Surfactant (1% of solution)	0.216	0.344	0.866	12
Control (no treatment)	0.247	0.398	0.901	12
NaCl				
2.0 lb/yd^3 (1.2 kg/m^3)	0.216	0.349	0.903	18
5.0 lb/yd^3 (3.0 kg/m^3)	0.240	0.408	0.978	18
10.0 lb/yd^3 (5.9 kg/m^3)	0.231	0.417	0.894	18
Thermal-Spray (TS)				
No TS Zn	0.229	0.391	0.912	24
TS Zn	0.228	0.392	0.938	30

As Table 5.2 shows, there is little difference between samples with or with out TS Zn. There are also no consistent trends with different levels of Cl$^-$ in the concrete mix. However, there are trends within the humectant group that seem significant. First, at each RH the slices with just the surfactant treatment all had smaller mass gains than either the controls or the humectant-treated slices. These differences in equilibrated mass gains between the surfactant treated slices and humectant treated slices increased as the RH increased. Secondly, the humectant-treated slices gained less mass than the control slices at a RH of 50%, gained more mass at a RH of 80%, and gained about the same at a RH of 70% (the LiNO$_3$-treated slices gained more than the control and the LiBr-treated slices gained just less than the control). It is as if the humectants need a certain amount of RH to overcome the effects of the surfactant. These results for the humectant group are summarized in Figure 5.36
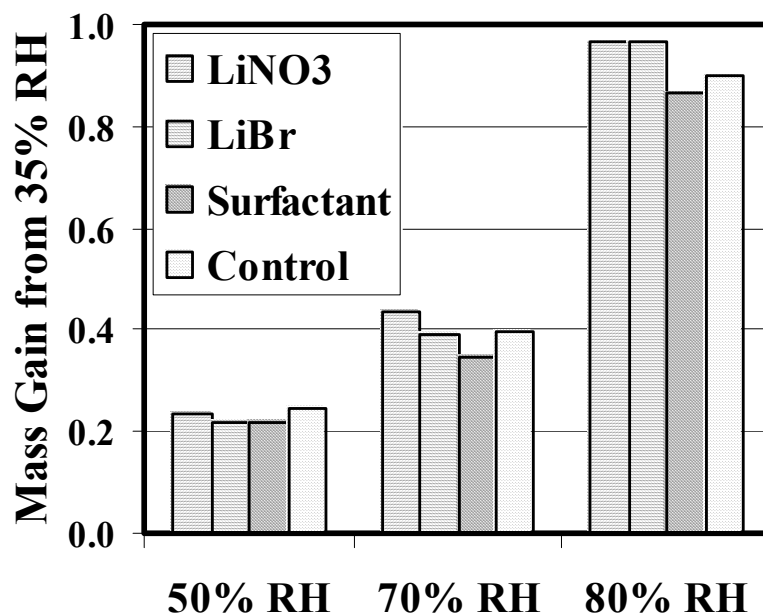
Figure 5.36: Mass gain of slices from an RH of 35% at 90ºF (32.2ºC)

A comparison was made between the measured mass gain and the mass gain calculated from the thermodynamics of binary mixtures of humectant and water (Table 3.2). The measured mass gain is found from the mass gain difference in Table 5.2 between humectant-treated slices and surfactant-treated slices. The calculated mass change is found from Equation 5-1:

$$Calculated\,MassGain(g) = \frac{1000 \times 0.7854}{M_i}\left(\frac{1}{m_i\left(RH = 50,70,80\right)} - \frac{1}{m_i\left(RH = 35\right)}\right) \qquad (5\text{-}1)$$

Where 0.7854 is the mass (grams) of humectant applied to each slice, M_i is the atomic weight of the humectant, and m_i is the molality of the humectant at a specific RH (Table 3.2). The results are shown in Table 5.3.

Table 5.3: Measured and calculated mass gain from 35% RH for LiNO$_3$ and LiBr humectant-treated slices

CONDITION	50% RH, g	70% RH, g	80% RH, g
Measured Mass Change			
LiNO$_3$	0.017	0.089	0.102
LiBr	0.005	0.046	0.100
Calculated Mass Change			
LiNO$_3$	0	0.188	0.603
LiBr	0.203	0.646	1.142

It is clear that the measured and calculated values in Table 5.3 do not agree. This disagreement is from the assumption of a binary humectant-water system used in the calculated mass change. The cement system is much more complicated, with many cement water interactions that already lower the activity of water. Thus, the introduction of the humectant does not lower the activity of water by as much in a binary humectant-water system.

5.2.2 Circuit Resistance Response to Temperature and Humidity

The results of applying low current (0.020 mA/ft^2) ICCP are shown in Figure 5.37 at the end of the five RH exposure periods. The plots are shown in order starting at the top with the first one tested. The time axis is shown on a log scale to expand the readings at the early portions of the experiment. For all five ICCP periods, the control had a much higher circuit resistance than either of the humectant-treated slabs. The circuit resistances of the humectant-treated slabs had values very close to one another, with the LiNO$_3$-treated slab having slightly lower values. For the 70% and 80% RH periods, and the first hour of the 50% RH period, the circuit resistances of the humectant-treated slabs were negative. This suggests that the current level was below what would have been the GCP current level, if the slabs were connected without the power supply.
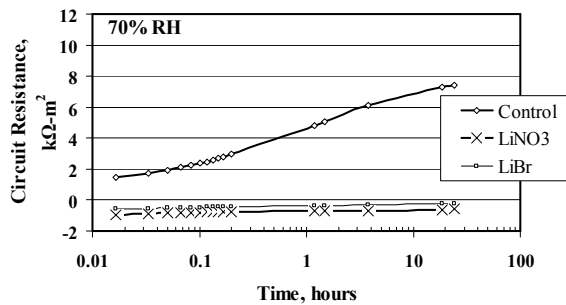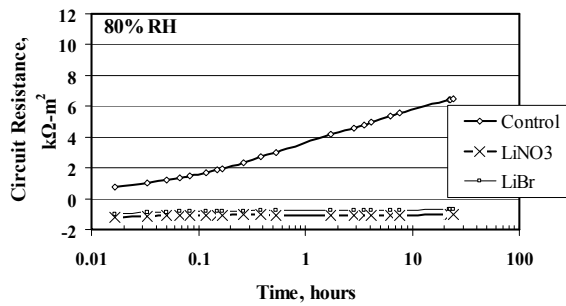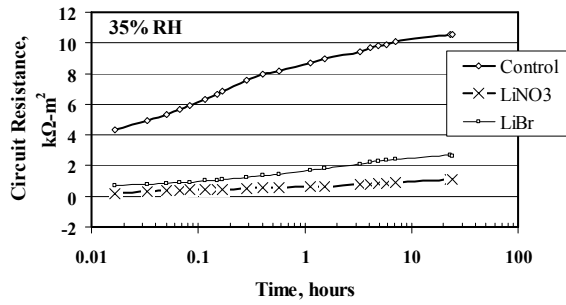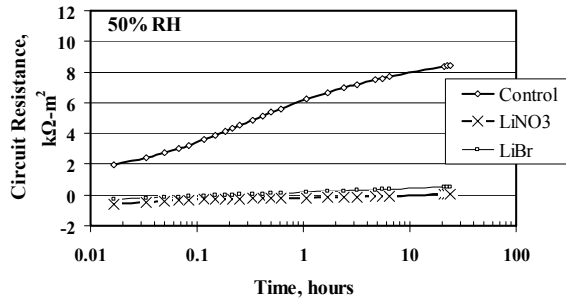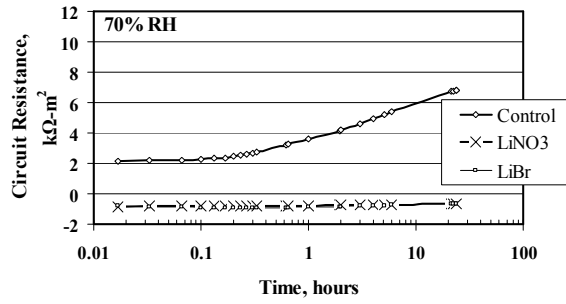
Figure 5.37: Circuit resistance as a function of time for 0.02 mA/ft^2 at 90ºF (32.2ºC)

The circuit resistances at the end of each 24-hour ICCP period are shown in Figure 5.38 as a function of RH. Circuit resistance decreases with increasing RH. The control and both humectant-treated slabs show the same general trends, but with the humectant-treated slabs having much lower circuit resistances.
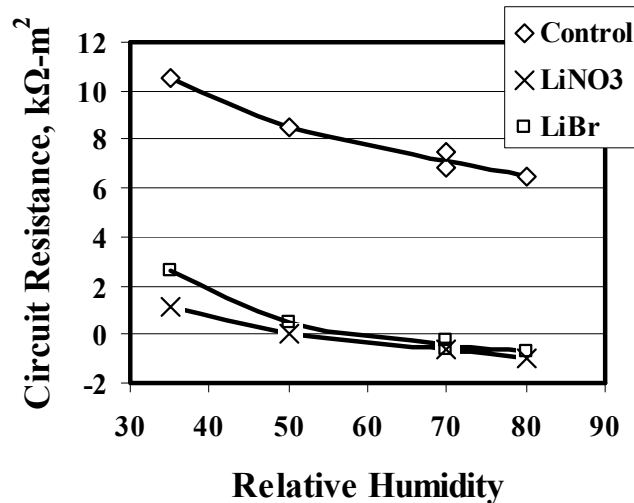
Figure 5.38: Circuit resistance after 24 hours of 0.02 mA/ft^2 ICCP at 90ºF (32.2ºC)

5.3 LONG-TERM LABORATORY GCP EXPERIMENTS (OHIO)

5.3.1 Original Blocks with 3.0 kg/m^3 (5.1 1b/yd^3) of NaCl

Galvanic current delivered by the untreated control blocks at 55% RH dropped to almost zero current within 3 weeks, Figures 5.39a and 5.40a. These blocks delivered virtually no protective current to the embedded steel. Galvanic current delivered by the blocks treated with potassium acetate dropped to nearly zero in less than 100 days, Figure 5.39a. Block 19, which was retreated with potassium acetate after 230 days, experienced only a brief increase in current. Galvanic current delivered by the lithium nitrate treated blocks, Figure 5.39a, remained relatively high initially (about 1 mA/m^2 after 6 months), dropping to 0.2 to 0.5 mA/m^2 after 720 days on line. Current delivered by the retreated block remained the highest throughout the test period. Galvanic current delivered by the lithium bromide treated blocks, Figure 5.40a, was also relatively high initially, but dropped to near zero after one year on line. This holds true except for current delivered by the retreated block, which was still at 0.5 mA/m^2 after 720 days. Performance in the 55% RH environment was as follows: LiNO$_3$ > LiBr >> KC$_2$H$_3$O$_2$ > Control.
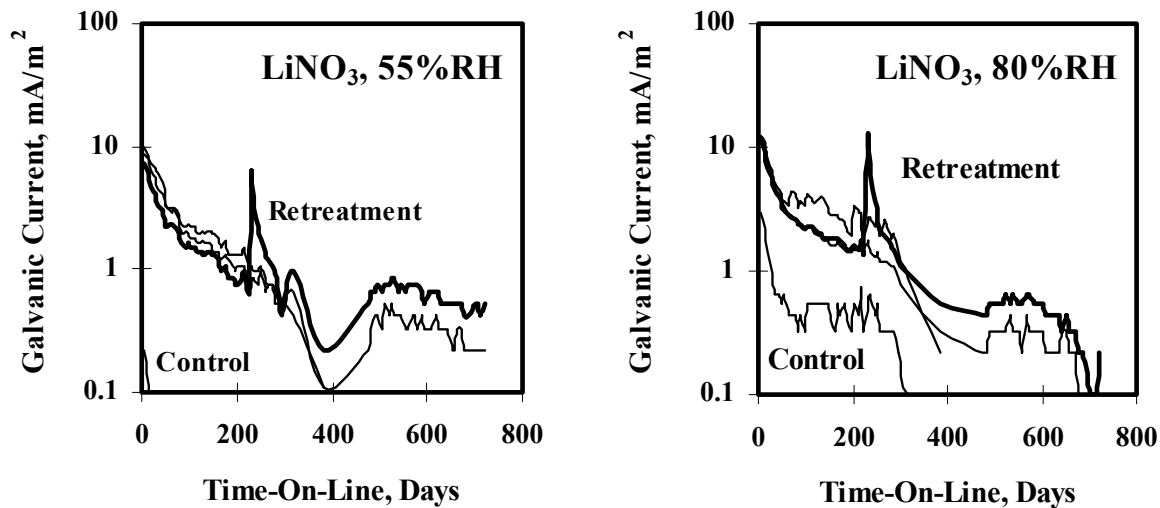
Figure 5.39: Galvanic current for LiNO$_3$-treated blocks with 3.0 kg/m^3 (5.1 1b/yd^3) NaCl. Retreatment of one block after about 200 days (shown in bold). The environments were a) 55% RH (left) and b) 80% RH (right).

In the 80% RH environment, the untreated control blocks (Figures 5.39b and 5.40b) were able to maintain a higher galvanic current at first (about 0.4 mA/m^2 up to 300 days), but after one year current had dropped to essentially zero. Current delivered by the potassium acetate treated blocks was higher than the control blocks at first, but approached that of the control blocks after approximately 250 days on line, Figure A5.39b. After nearly 300 days on line, the metallized Zn treated with KC$_2$H$_3$O$_2$ began to delaminate and operation of those blocks was discontinued. Galvanic current delivered by the LiNO$_3$-treated blocks (Figure 5.39b), was much higher than the control blocks (about 1.5 mA/m^2 after 250 days), and remained significant throughout most of the test period. Only after 700 days did the current decrease to near zero. The LiBr-treated blocks (Figure 5.40b), were the best performers in the 80% RH environment (about 2 mA/m^2 after 250 days), and were still delivering 0.4 to 0.8 mA/m^2 at the conclusion of the 720-day test. Performance in the 80% RH environment was as follows: LiBr > LiNO$_3$ > KC$_2$H$_3$O$_2$ >> Control.
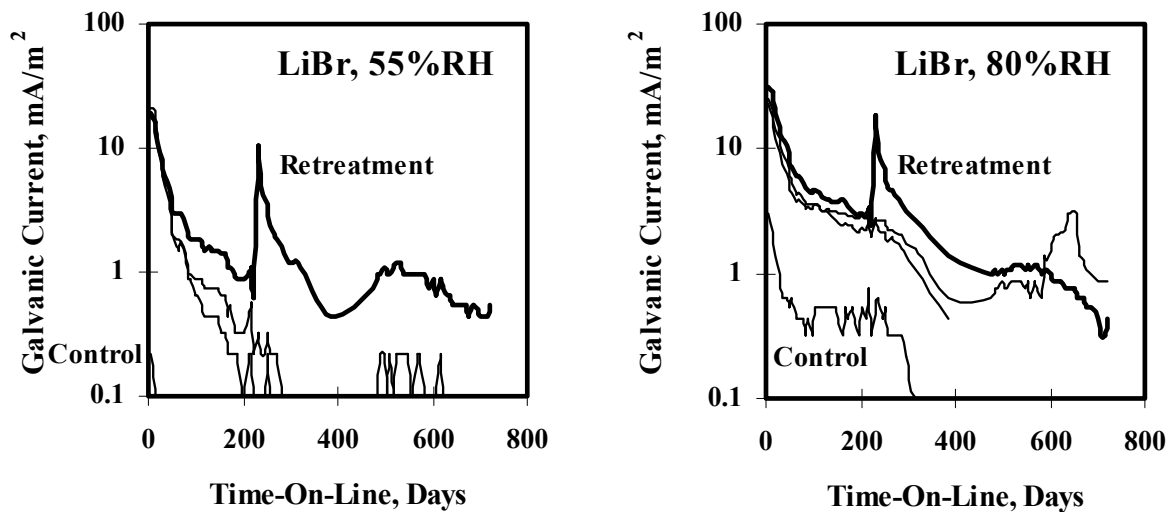
Figure 5.40: Galvanic current for LiBr-treated blocks with 3.0 kg/m^3 (5.1 lb/yd^3) NaCl. Retreatment of one block after about 200 days (shown in bold). The environments were a) 55% RH (left) and b) 80% RH (right).

Performance in the outdoor environment (Figure 5.41) was very irregular due to excursions in temperature, humidity, and moisture content. Current irregularities were most pronounced for the untreated control blocks. The LiBr-treated blocks delivered the highest galvanic current while outdoors, both for the covered blocks and for those with direct exposure. Current delivered by the outdoor LiBr-treated blocks remained well above 1 mA/m^2 throughout the 500-day test period. Current delivered by the LiNO$_3$-treated blocks also remained well above the level delivered by the control blocks, with exception for those with direct exposure for which current dropped to near zero at the end of the test. Performance in the outdoor environment was: LiBr > LiNO$_3$ > Control (except after 350 days, for which LiBr > Control > LiNO$_3$).
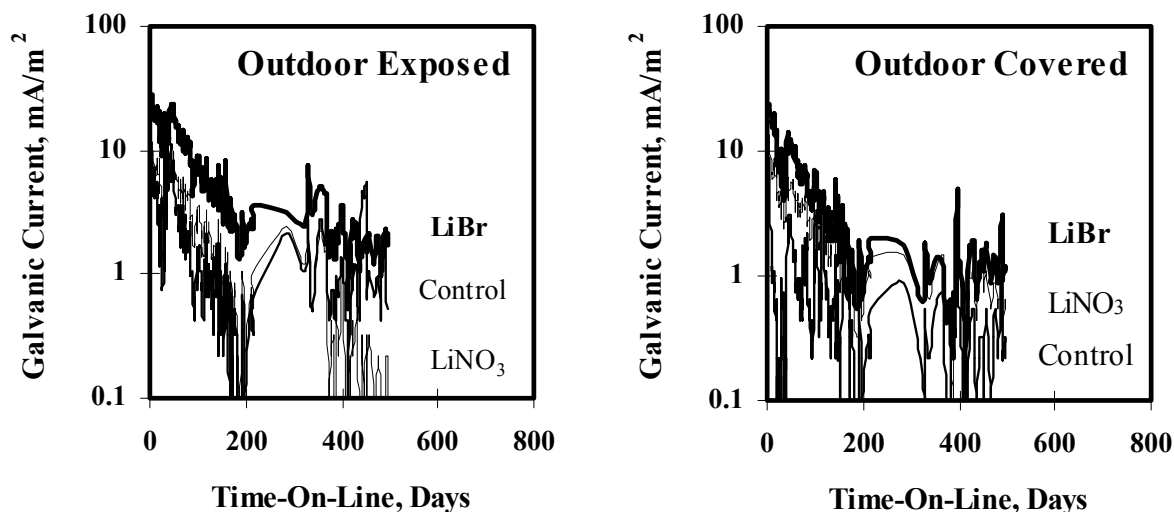
Figure 5.41: Galvanic current for humectant-treated blocks with 3.0 kg/m³ (5.1 lb/yd³) NaCl. The environments outdoors in the Cleveland Ohio area in a) Exposed (left) and b) Covered (right) conditions.

5.3.2   Additional Blocks with 4.9, 7.3 and 9.8 kg/m³ of NaCl

In the 55% RH environment (Figure 5.42), galvanic current for the untreated control blocks constructed with 4.9, 7.3, and 9.8 kg/m³ (8.2, 12.4, and 16.5 lb/yd³) of NaCl still decreased to nearly zero in less than 50 days while on-line at 55% RH. Blocks constructed with 4.9 and 7.3 kg/m³ of NaCl and treated with LiNO₃ or LiBr solutions behaved similarly to those in the original study with 3.0 kg/m³ of NaCl. Current was approximately 0.8 to 1 mA/m² at the end of the 250-day test period. Treated blocks constructed with 9.8 kg/m³ of NaCl delivered approximately 20% higher current in the 55% RH environment. Performance for the high Cl⁻ blocks in the 55% RH environment was: LiBr = LiNO₃ >> Control.

In the 80% RH environment (Figure 5.43), galvanic current for the untreated control blocks constructed with higher chloride content was much greater, increasing significantly with Cl⁻ content. In fact, the untreated control block with 9.8 kg/m³ of NaCl was still producing 0.6 mA/m² of current after 250 days. In this case, the Cl⁻ admixture itself is acting as a humectant to increase protective current. Nevertheless, the LiNO₃- and LiBr-treated blocks still delivered much higher current than the untreated controls, particularly early in the test period. Performance for the high Cl⁻ blocks in the 80% RH environment was: LiBr = LiNO₃ >> Control.

In the outdoor environment (Figure 5.44), both LiBr- and LiNO₃-treated blocks delivered significantly higher current than the untreated control blocks. Galvanic current delivered by the treated blocks was much more consistent, whereas current for the untreated control blocks cycled wildly with changes in moisture content. As noted for the 80% RH environment, the untreated control block with 9.8 kg/m³ of NaCl delivered significantly higher current than control blocks

with lower Cl⁻ content. Performance for the high Cl⁻ blocks in the outdoor environment was: LiBr = LiNO$_3$ >> Control.

Comparisons of the 55% and 80% RH environments as a function of the NaCl content are found in Figure 5.45. For this comparison, average galvanic currents are used from 150 to 250 days of time on-line. Data for the same time period range, with NaCl contents of 3.0 kg/m^3 (5.1 1b/yd^3), as shown in Figures 5.39 and 5.40, are also included. This comparison shows that the presence of humectants, and the RH of the environment influence the mean galvanic current much more than the Cl⁻ level in the concrete.
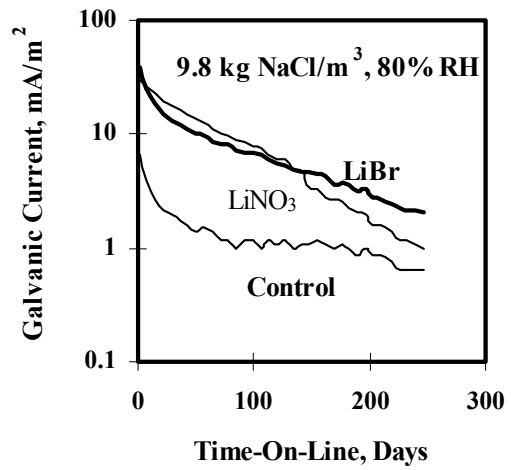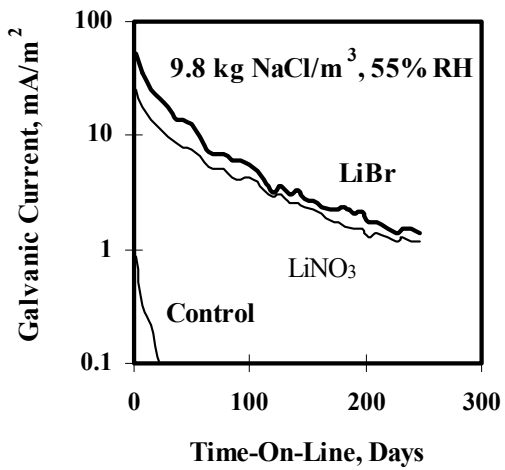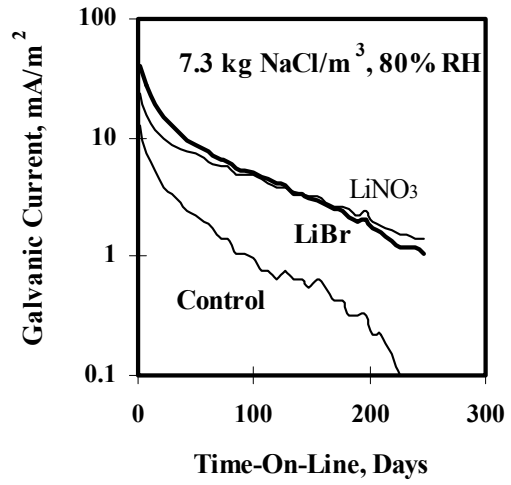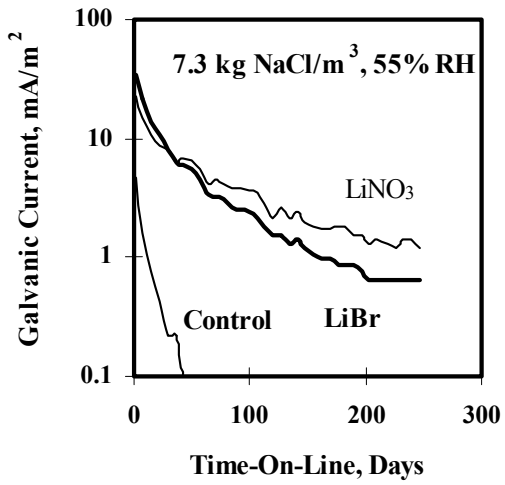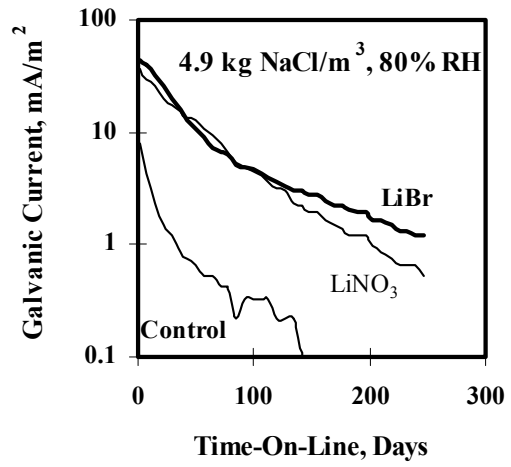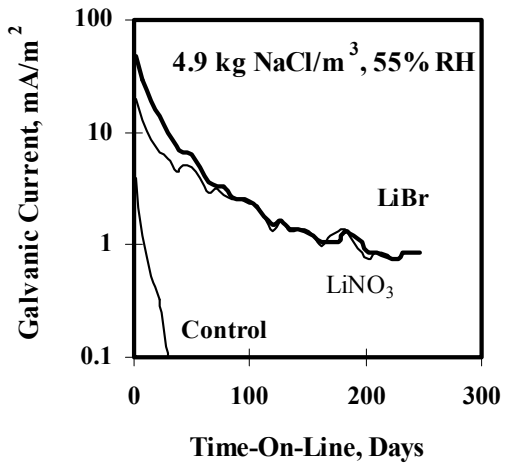
Figure 5.42: Galvanic currents for blocks with 4.9, 7.3, and 9.8 kg/m³ NaCl in 55% RH conditions

Figure 5.43: Galvanic currents for blocks with 4.9, 7.3, and 9.8 kg/m³ NaCl in 80% RH conditions
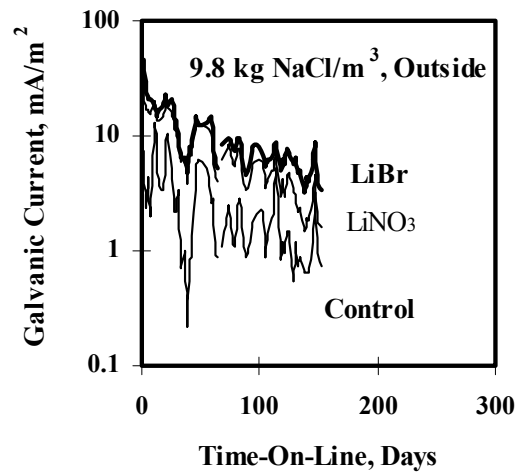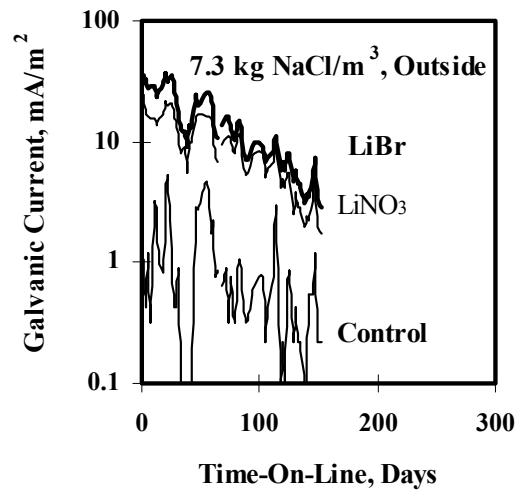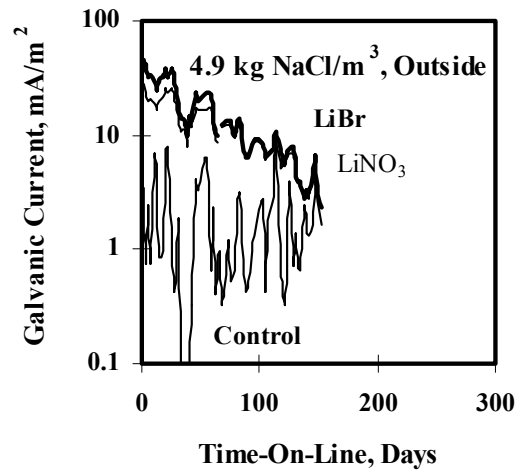
Figure 5.44: Galvanic currents for blocks with 4.9, 7.3, and 9.8 kg/m³ NaCl in covered outdoor exposures
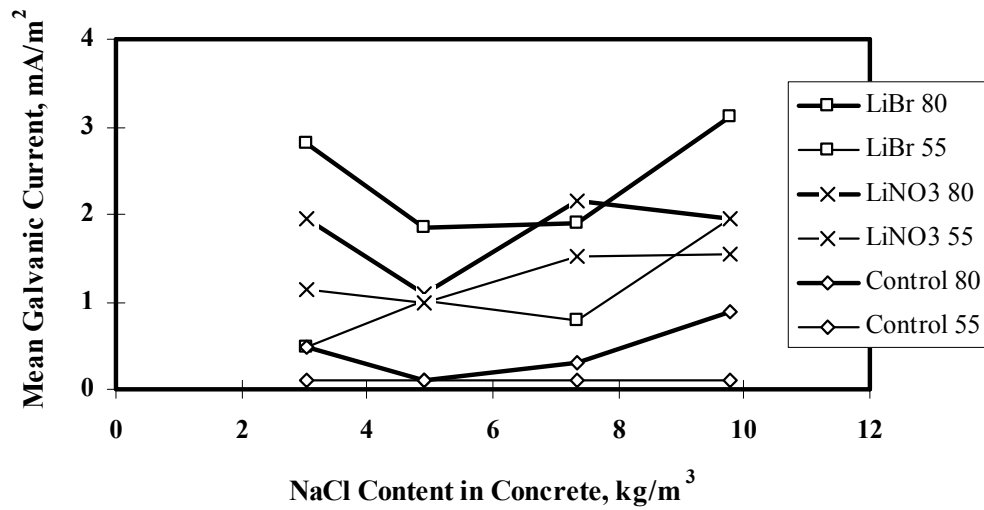
Figure 5.45: Mean galvanic currents (over 150-240 days) as a function of concrete NaCl contents

5.4 YAQUINA BAY BRIDGE FIELD EXPERIMENT

5.4.1 Chloride Depth Profiling

The results from chloride profiling, prior to humectant application, for the soffits of the four ICCP test zones are shown in Figure 5.46. All of the profiles show the diffusion of Cl⁻ in from the concrete surface. Zones 11, 13, and 14 show the effects of washing at the surface, a decrease in Cl⁻ concentration right at the surface. Figure 5.46 also shows an increase in Cl⁻ levels, the closer the zone is to the ocean. All four zones have Cl⁻ concentrations above the corrosion threshold to a depth of at least 4 cm (1.6 inches).
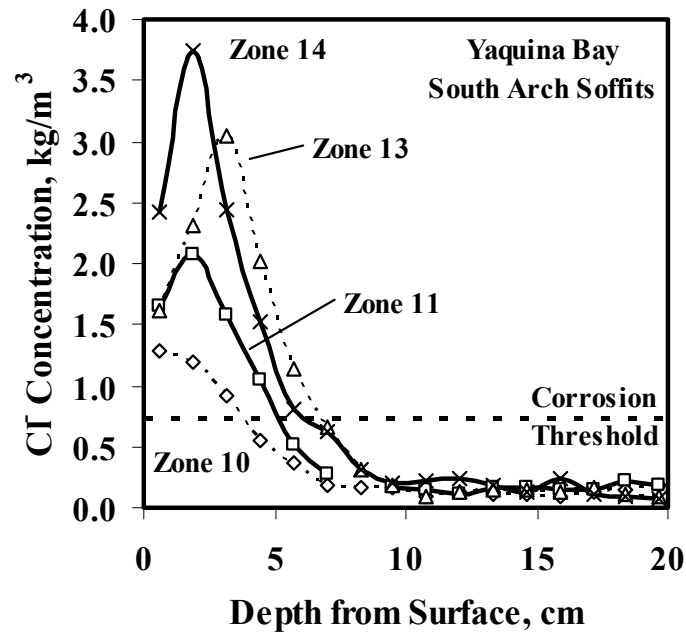
Figure 5.46: Chloride profiles from the soffits of the four ICCP test zones on the Yaquina Bay Bridge south arches

The results from chloride profiling on the west side base, of Bent 3N, on the north part of the Yaquina Bay Bridge are shown in Figure 5.47. The contrast between the north and south faces in Figure 5.47, illustrates the strong effect precipitation washing has on reducing chloride levels in the concrete. There is greater washing from the prevailing late fall and winter rains, on the more exposed south face, than on the more sheltered north face. The chloride levels are substantially lower on the south face compared to the north face.
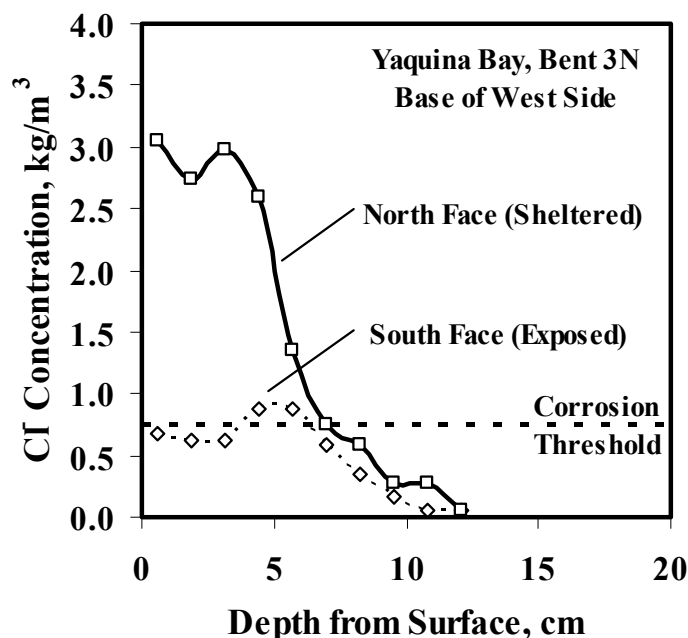
Figure 5.47: Chloride profiles from the west side of the base of bent 3N on the north side of the Yaquina Bay Bridge

Figures 5.46 and 5.47 show the differences in chloride levels and washing effects that can occur on the same structure. This is consistent with results from other bridges on the Oregon coast (*Cramer, et al. 2002b*). Presumably, washing effects would also be found in humectant-treated zones where a multitude of microclimates exist. Washing effects would then affect the frequency of humectant reapplications.

The profiles in Figure 5.46 were examined with *Fick's First Law*, for the 63-year-old concrete to obtain effective diffusion coefficients, D, and surface Cl^- concentrations (without the washing decrease), C_o. The results are in Table 5.4. These values are generally lower than those found on either the Rocky Point Viaduct or the Brush Creek Bridge (*Cramer, et al. 2002b*). The differences arise because the concrete at the bridges have different properties (different D values) and the deposition of salt on the concrete surface is different in each microclimate (different C_o values).

Table 5.4: Diffusion parameters for the ICCP field test zones on the Yaquina Bay Bridge

ICCP Zone	Distance to Bay, m	C_o, kg Cl^-/m^3	$C_o{}^a$, kg $NaCl/m^3$	D, cm^2/s
10	131	1.67	2.75	7.03×10^{-9}
11	113	3.34	5.51	4.86×10^{-9}
13	94	6.63	10.93	4.50×10^{-9}
14	73	5.41	8.92	4.49×10^{-9}

[a] Assuming all of the Cl^- was from NaCl.

5.4.2   Microscopy

SEM photomicrographs and x-ray maps of the anode-concrete cross-sections, exposed in core samples taken from CP Zones, 10, 11, 13, and 14, showed many of the same features as seen in earlier work (*Covino, et al. 2002*) and in the long-term laboratory experiments (Section 5.1, Figures 5.18-5.25). These include mineral zones representing the unreacted anode, a reaction zone containing anode dissolution products, and the unaltered cement paste. The reaction zone can be further divided into three subzones or regions: 1) a growing mineral layer characterized largely as ZnO or $Zn(OH)_2$ adjacent to the Zn anode, 2) a calcium-depleted, Zn-rich layer formed within the cement paste, and 3) cement paste containing low levels of Zn. These features are a consequence of the anode reaction and the consequent acidification of the anode-concrete interface, as well as the complex mineral interaction between the anode dissolution products, moisture, and the cement paste.

ASEM line scans for anode-concrete interfaces from Zones 10, 11, 13, and 14, are shown in Figures 5.48-5.51. The results are for cores taken from the zones immediately after humectant treatment (10-22-99). In terms of general features, the line scan for Zone 10, representing the driest environment, shows a sharply defined interface with little secondary mineralization, as would be indicated by a more complex mineral structure at the interface. Moving towards Zone 14, the Zn mineral structure at the interface broadens and becomes more varied, with evidence of a ZnO layer and Zn diffused into the cement paste. The reaction zone width increases substantially, moving from Zone 10 to Zone 14. The trend in reaction zone widths is similar to that for the chloride profiles (Figure 5.46), and C_o values (Table 5.4): the closer to the bay, the greater the impact that moisture and salt deposition have on zone properties, which can affect the service life of the structure and the CP zone.
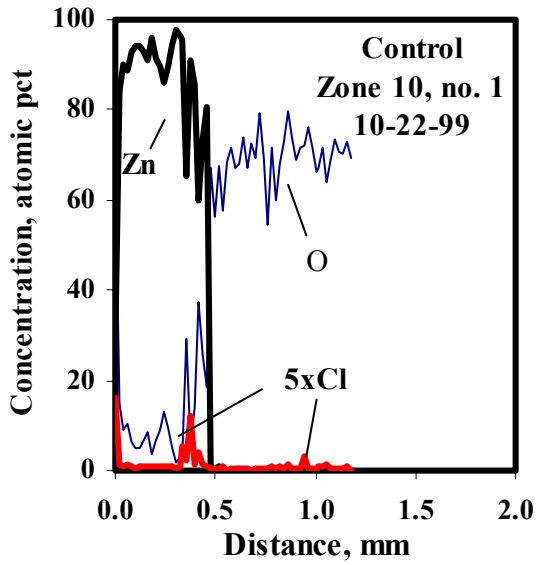
Figure 5.48: X-ray line scans across a cross-section of control Zone 10 of the Yaquina Bay Bridge, immediately after humectant application of bridge zones.
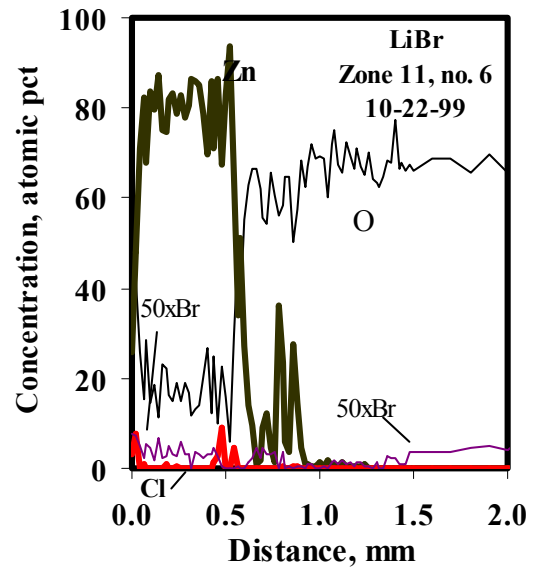
Figure 5.49: X-ray line scans across a cross-section of LiBr-treated Zone 11 of the Yaquina Bay Bridge, immediately after humectant application.
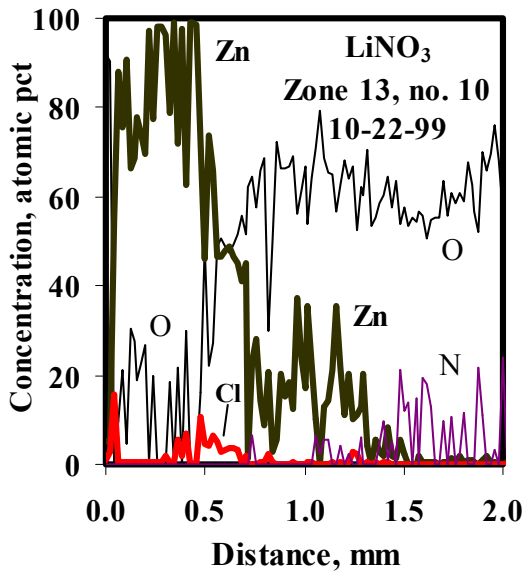
Figure 5.50: X-ray line scans across a cross-section of LiNO$_3$-treated Zone 13 of the Yaquina Bay Bridge, immediately after humectant application.
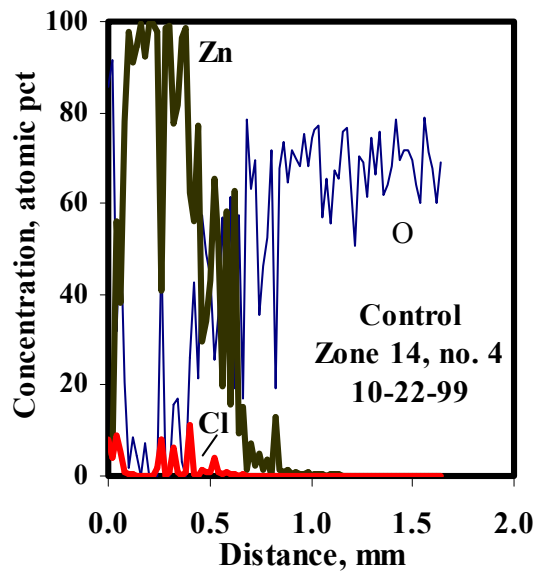
Figure 5.51: X-ray line scans across a cross-section of control Zone 14 of the Yaquina Bay Bridge, immediately after humectant application to bridge zones.

Figures 5.48-5.51 all provide evidence that Cl⁻ accumulate at the anode-concrete interface, most likely as a zinc hydroxylchloride (*Covino, et al. 2002*). The lowest Cl⁻ levels at the anode-concrete interface were in zone 10, where there was less moisture to aid penetration of Cl⁻ into and transport them through the concrete.

Figure 5.49 for Zone 11 contains a curve for the Br L_β line. Analysis of the spectra for the KBr standard and for the Zone 11 cross-section indicates that the values shown represent background. The levels of Br in the core sample from Zone 11 are not detectable by the sample preparation and analytical methods used. Consequently, the Br curve in Figure 5.52 also represents background. There were no significant changes between the line scans for the as-treated sample (Figure 5.49), and the aged sample (Figure 5.52). This suggests little modification of the anode-concrete interfacial chemistry by the presence of the LiBr humectant for Zone 11. Chloride accumulation at the interface was greater for the aged sample. The zone representing zinc oxide was also broadened, which could be interpreted as evidence of increased ion mobility. However, sampling statistics (there was only one as-treated and one aged sample examined) suggest caution in generalizing this result.

Figure 5.50, for Zone 13, contains a curve for the N K_α line. Analysis of the spectra for the BN standard and for the Zone 13 cross-section indicates that the values shown are real. They also indicate the presence of $LiNO_3$ in the cement paste. The line scan for the aged sample (Figure 5.53) also indicates the presence of $LiNO_3$, but at a substantially reduced level. This would suggest that $LiNO_3$ was leached from the sample over the course of the roughly 2-year aging experiment. In other respects, the line scans for the as-treated and aged samples were similar.
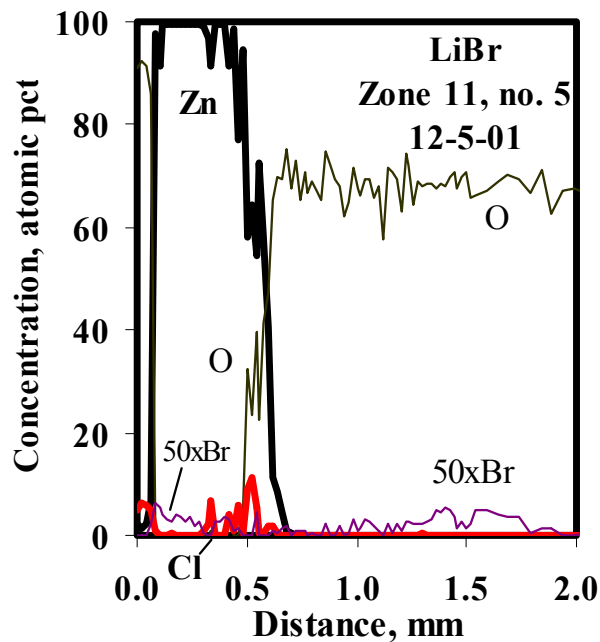
Figure 5.52: X-ray line scans across a cross-section of LiBr-treated Zone 11 of the Yaquina Bay Bridge, after 2 years of ICCP.
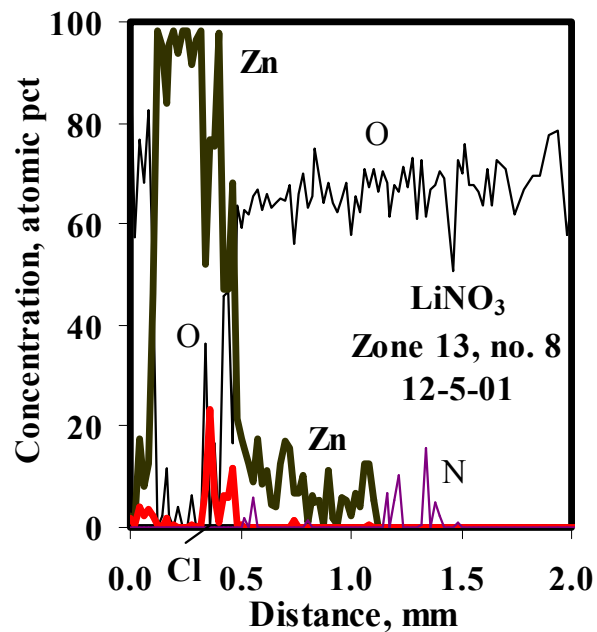
Figure 5.53: X-ray line scans across a cross-section of LiNO$_3$-treated Zone 13 of the Yaquina Bay Bridge, after 2 years of ICCP.

5.4.3   Operation

The operating data, in terms of circuit resistance, for the Yaquina Bay Bridge field trial are shown in Figure 5.54. During the field trial there were gaps in the collection of data and significant changes in the current level. As a result, Figure 5.54 is broken down into six time periods (I-VI).
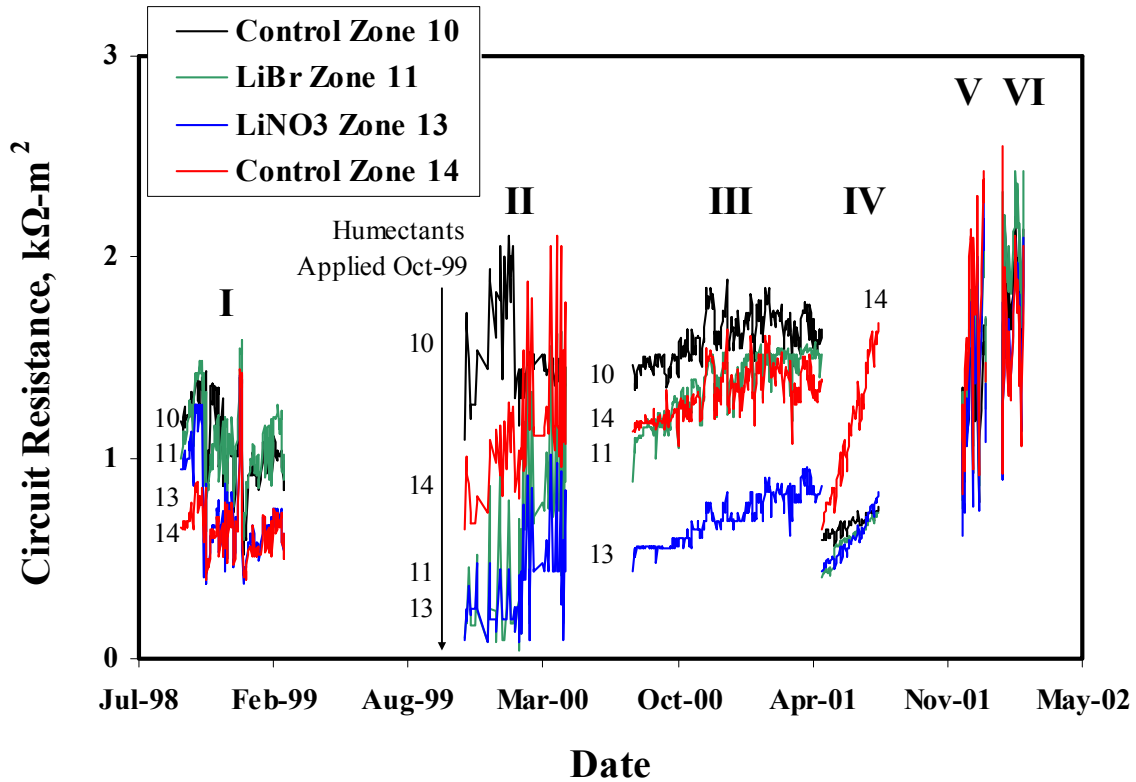
Figure 5.54: Circuit resistance data from the Yaquina Bay Bridge field trial

Period I was prior to humectant application. Periods II and III were after humectant application and were at a nominal current density of 2.2 mA/m^2. The difference in the noise between II and III results from the number of decimal places with which the voltage and current data were stored (the "ON" and "SRP" data as described in Section 4.4.5). Period II data was stored with only 1 voltage and 2 current decimal places; period III data was stored with 4 decimal places for both voltage and current. Due to this variation, the Period II data shows much more noise in circuit resistance. During Periods IV and V the nominal current density jumped up to 13 mA/m^2. The increase was a result of failures in the potentiometers in the rectifiers, which caused the voltages and currents to drift upward. The ICCP zones were at this accelerated level for approximately 8 months, which resulted in premature electrochemical aging of the anodes by about four years. In period VI the current levels dropped back to normal levels. The data for each of the six time periods are given in Table 5.5.

Table 5.5: Summary of Yaquina Bay Bridge field trial

Time Period	I	II	III	IV	V	VI
Start Date	09/25/98	11/20/99	07/26/00	05/03/01	11/26/01	01/24/02
End Date	02/25/99	04/18/00	05/02/01	07/25/01	12/29/01	02/26/02
Mean Current Density, mA/m^2						
10 – Control	3.0	2.0	2.4	13.9	13.5	2.2
11 – LiBr	2.3	2.4	2.6	17.0	16.6	2.5
13 – LiNO$_3$	2.5	2.2	2.3	16.2	15.9	2.5
14 – Control	2.7	2.2	3.0	13.3	13.6	2.5
Mean Voltage, V						
10 – Control	3.2	3.0	3.8	9.3	16.8	4.1
11 – LiBr	2.5	1.4	3.6	10.0	24.5	5.1
13 – LiNO$_3$	1.9	0.8	1.6	9.6	22.2	4.0
14 – Control	1.8	2.5	4.0	15.0	22.6	4.0
Mean Circuit Resistance, kΩ-m^2						
10 – Control	1.07	1.51	1.60	0.67	1.25	1.83
11 – LiBr	1.08	0.58	1.37	0.59	1.48	2.02
13 – LiNO$_3$	0.74	0.38	0.70	0.59	1.40	1.63
14 – Control	0.65	1.11	1.33	1.13	1.67	1.62

The effects of humectants can be seen in Figure 5.55, where the mean circuit resistance values in Table 5.5 are shown for the time periods where the current densities were nominally 2.2 mA/m^2. The control zones show gradually increasing circuit resistances, with Zone 10 (farther from the bay) having higher values than Zone 14 (closer to the bay). Without humectant treatments one would expect the circuit resistances in Zones 11 and 13 to follow the same trends and be bounded by the Zone 10 and Zone 14 data. The dip in circuit resistances in Period II for LiBr and LiNO$_3$ zones show the benefits of the humectant treatment. However, by time Period III the benefits of LiBr have disappeared. After the accelerated aging in time Periods IV and V the benefits of using LiNO$_3$ have also disappeared. Figure 5.55 shows that the benefits of LiNO$_3$ were present for 2-3 years.
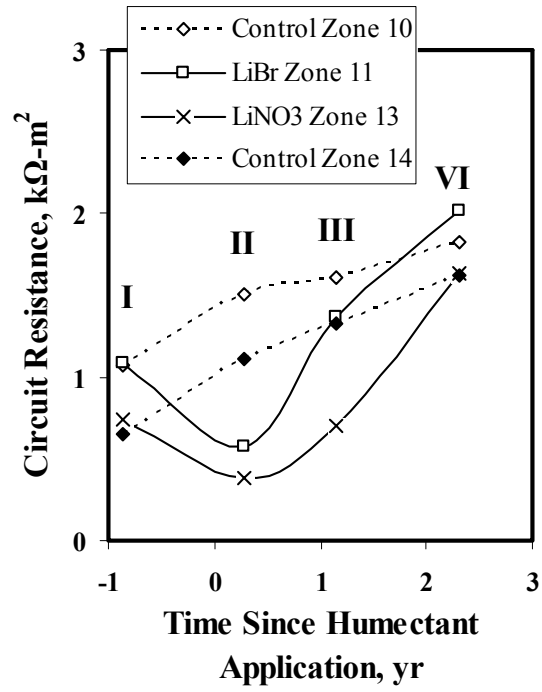
Figure 5.55: Mean circuit resistance data from periods with nominal current of 2.2 mA/m^2. Period I was prior to humectant application.

6.0   DISCUSSION

The main goals of this project (humectant effectiveness, increased service life, and life cycle considerations) are discussed along with the appropriateness of accelerated laboratory tests and the importance of collecting and examining operating data.

6.1   HUMECTANT EFFECTIVENESS

A summary of all of the different experiments is shown in Table 6.1, along with a ranking of the relative effectiveness of the humectants and the control. The ranking reflects circuit resistance and depolarization results for ICCP and long-term galvanic current for GCP. According to Figure 3.1, LiBr should lower the activity of water more than $LiNO_3$, especially in environments with a RH below 50%. All things being equal, one would expect better results with LiBr. For GCP, LiBr is generally more effective than $LiNO_3$, and both are generally more effective than the control. However, for ICCP, $LiNO_3$ is generally more effective than LiBr, and both are generally more effective than the control. The same basic electrochemical processes occur in both GCP and ICCP, so the question arises as to what is causing the humectant rankings to change between GCP and ICCP.

Table 6.1: Summary of humectant rankings for each CP experiment

CP Type	APPLIED CURRENT mA/m^2	DURATION[A]	ENVIRONMENT	NOTE	RANK
ICCP	0.22	Short	Variable RH	Equilibrated at RH	LiBr = LiNO$_3$ > Control
ICCP	27	Long	High RH	New Slabs	LiNO$_3$ > LiBr = Control
ICCP	27	Long	High RH	Aged Slabs	LiNO$_3$ > LiBr >> Control[B]
ICCP	27	Long	Low RH	New Slabs	LiNO$_3$ > LiBr > Control
ICCP	10	Long	Low RH	Aged Slabs	LiNO$_3$ > LiBr
ICCP	27/2.2	Long	High RH	Cyclic Current	LiNO$_3$ > LiBr > Control
ICCP	27/2.2	Long	Low RH	Cyclic Current	LiNO$_3$ = LiBr > Control
ICCP	2.2	Long	Yaquina Bay	Before High Currents	LiNO$_3$ > LiBr > Control
ICCP	13	Long	Yaquina Bay	After High Currents	LiNO$_3$ = LiBr = Control
GCP	--	Long	High RH	New Slabs	LiBr > LiNO$_3$ = Control
GCP	--	Long	High RH	Aged Slabs	LiBr > LiNO$_3$
GCP	--	Long	Low RH	New Slabs	LiBr > LiNO$_3$ > Control
GCP	--	Long	Low RH	Aged Slabs	LiBr > LiNO$_3$
GCP	--	Long	55% RH	Never Wetted	LiNO$_3$ > LiBr >> Control
GCP	--	Long	80% RH	Never Wetted	LiBr > LiNO$_3$ >> Control
GCP	--	Long	Cleveland OH	Covered	LiBr > LiNO$_3$ > Control
GCP	--	Medium	Cleveland OH	Exposed	LiBr > LiNO$_3$ > Control
GCP	--	Long	Cleveland OH	Exposed	LiBr > Control > LiNO$_3$
GCP	--	Medium	55%	4.9, 7.3 & 9.8 kg/m^3 NaCl	LiBr = LiNO$_3$ >> Control
GCP	--	Medium	80%	4.9, 7.3 & 9.8 kg/m^3 NaCl	LiBr = LiNO$_3$ >> Control
GCP	--	Medium	Cleveland OH	4.9, 7.3 & 9.8 kg/m^3 NaCl , Exposed	LiBr = LiNO$_3$ >> Control

[A]Duration: Short < 1 month < Medium < 1 year < Long
[B]Control comparison from untreated data in Bullard. (1998).

One possibility is that the GCP results reflect a much smaller electrochemical age than the ICCP results. The electrochemical ages in the GCP tests, in the high humidity enclosure, averaged 92 kC/m^2 for the LiNO$_3$-treated slabs, and 185 kC/m^2 for the LiBr-treated slabs. In the low humidity enclosure, the GCP ages were quite small and averaged 19 kC/m^2 for the LiNO$_3$-treated slabs, and 31 kC/m^2 for the LiBr-treated slabs. These compare with average ICCP electrochemical ages of 741 kC/m^2 in the high humidity enclosure and 379 kC/m^2 in the low humidity enclosure. However, the separation between the LiNO$_3$- and LiBr-treated slabs had already appeared in the 100 to 200 kC/m^2 range in the ICCP experiments in the high RH exposure (Figure 5.1). Thus, the reversal of humectant rankings does not appear to be a function of electrochemical age.

Another possibility is that the higher voltages experienced in ICCP caused the rankings to change. Since the humectants appear to reside in the reaction zone (Br in Figures 5.20-5.23), and this is the region of the highest voltage drop (*Orlova, et al. 1999*), it is possible that the bromide ions are being oxidized (the nitrate ions are already fully oxidized). Bromide oxidation reactions were discussed in Section 3.2. It is possible that the high voltages in the accelerated ICCP tests eliminated bromide as a humectant and not the nitrate. Bromide oxidation would also explain the very low bromide levels found in the aged, low RH cross-section (Table 5.1). If bromide

oxidation occurs by Equation 3-3, then $Br_2(g)$ evolution would produce very low bromide concentrations.

To summarize, both humectants are more effective than the control. LiBr is inherently more effective as a humectant since it lowers the activity of water more than $LiNO_3$. LiBr was found to be more effective in GCP, while $LiNO_3$ was more effective in ICCP. It is probable that LiBr is less effective in ICCP because of the loss of humectant from the oxidation of Br^- and subsequent Br_2 evolution or conversion to oxygen derivatives of Br.

6.2   INCREASED SERVICE LIFE

The service life of TS Zn anodes can be limited in a variety of ways. Failures can occur from faulty application of the anode, incorrect operation of the CP system, or from limitations of the anode. Humectants are aimed at the third type—anode limitations.

6.2.1   Reduced Anode Bond Strength and Delamination

Insertion of a weak intermediate layer of anode reaction products between the anode and concrete has been shown to reduce bond strength with increasing electrochemical age. In addition, stresses develop within the reaction product layer as the layer grows. This can cause micro-cracking or delamination of the coating along the anode-concrete interface and also reduce anode bond strength. Zinc oxide reaction products accumulate along the highly uneven interface between the TS zinc anode and the concrete during ICCP. Zinc oxide occupies a greater volume than zinc, which creates stresses at sharp bends in the interface. This will eventually lead to micro- cracking or delamination of the anode from the concrete. This appears as minute cracks across the uneven topography of the interface, with cracks both in the zinc reaction product and in the cement paste.

Zinc ions have been shown to migrate into the cement paste and displace calcium ions, a process that is facilitated by the increased ion mobility associated with moister concrete. This results in secondary mineralization of the cement paste and of the original zinc reaction products to form new mineral species and chemical bonds. To some extent this reduces the damaging effects of zinc oxide formation. It improves the mixing of cement and zinc reaction product minerals at the interface and can result in a stronger bond than the original mechanical bond between anode and concrete. This also helps to dissipate the zinc reaction products, thereby delaying the development of the reaction product layer and the associated stresses that lead to micro-cracking and delamination along the interface. Accelerated ICCP tests have predicted service lives of 27 years in environments with periodic wetting (*Covino, et al. 1996a; Covino, et al. 1996b; Covino, et al. 2002; Holcomb, et al. 1996*) and just five years without wetting (*Bullard, et al. 1997a; Bullard, et al. 1998; Covino, et al. 2002*). Secondary mineralization improves with increased wetting and humidity and to a large extent accounts for the much greater predicted service life for the periodically wetted anodes.

This project used two measurements of how humectants might extend the service life based on adhesion strength and delamination. The first was the adhesion strength tests. The second was

the use of microscopy to examine the zinc anode-concrete structure for evidence of increased secondary mineralization, which should lead to less micro-cracking and delamination.

The effects on service life from adhesion strength changes were inconclusive, in large part because of the inherent variation that accompanies such measurements. However, when a comparison is made with prior results without humectants, as was done in Figures 5.27-5.30, a few points can be made:

- With the exception of some $KC_2H_3O_2$-treated slabs, the bond strengths after GCP were much higher than was found with ICCP in either prior experiments or this investigation. This large increase in bond strength with GCP is consistent with the observations from the Richmond-San Rafael Bridge (*Bullard, et al. 1997b; Covino, et al. 2002*), where the bond strength of the GCP anode was greater than the field test equipment could measure.

- In the case where the best comparison with prior experiments can be made (i.e., with the same conditions, ICCP current levels, and slabs), the aged slabs in Figure 5.28 show perhaps a 0 to 3 year advantage with LiBr and $LiNO_3$. Note that 12-13 years of the equivalent age for the aged samples in Figure 5.28 occurred while treated with the humectants.

- Casting doubt on the benefits shown above for the aged slabs in Figure 5.28, are the results for the new slabs in Figure 5.28. The bond strength of the new slabs plummeted to near zero. However, the control slab also had very low bond strength. This indicates that something besides humectants was probably the cause.

6.2.2   Anode-Concrete Interface Chemistry

The driest environments show little secondary mineralization of Zn dissolution products. In wetter environments, the interfacial chemistry becomes more complex, with evidence of a ZnO layer adjacent to the anode and of Zn ions diffused into the cement paste. For CP zones with similar operating histories, the reaction zone width increases substantially, moving from driest to the wettest environment. The trend in reaction zone width is similar to that for chloride profiles and concrete surface salt concentrations (C_o values), i.e., the closer to the bay, the greater the impact that moisture and salt deposition have on zone properties that can affect the service life of the structure and the CP zone. Cl^- accumulate at the anode-concrete interface, most likely as a zinc hydroxychloride. The lowest Cl^- levels at the anode-concrete interface occur where there is less moisture to aid penetration of Cl^- into and transported through the concrete.

6.2.3   Loss of Rebar Protection

Galvanic CP anodes can fail by not providing enough galvanic current to protect the rebar. As Table 6.1 shows, LiBr always provided better long-term galvanic current than without a humectant for all of the experiments, and in most cases performed better than $LiNO_3$ as well.

The minimum required current is an empirically derived value and may well be different for different climates and chloride levels. For example, Oregon DOT has found that 0.2 mA/ft^2 (2.2 mA/m^2) is sufficient for their coastal thermal-sprayed zinc ICCP systems (*Bullard, et al. 1998;*

Covino, et al. 1997a; Covino, et al. 2002), while Fontana and Greene (*1978, p. 207*) give 0.1-0.5 mA/ft^2 (1.1-5.4 mA/m^2) as sufficient for protecting reinforcing bars in concrete.

Table 6.2 shows the long-term currents for the GCP tests in this report. In many cases, LiBr supplied sufficient galvanic current (~2 mA/m^2) to protect the rebar even after a year. In most cases LiNO$_3$ did not supply enough galvanic current, while none of the controls did either.

Table 6.2: Summary of medium and long term galvanic current densities

DURATION[A]	ENVIRONMENT	NOTE	LONG-TERM GALVANIC CURRENT DENSITY[B], mA/m^2		
			LiBr	LiNO$_3$	Control
Long	Low RH	New Slabs	0.3	0.2	0.04
Long	Low RH	Aged Slabs	0.5	0.3	
Long	High RH	New Slabs	0.8	0.2	0.3
Long	High RH	Aged Slabs	2.9	1.2	
Long	55% RH	Never Wetted, 3.0 kg/m^3 NaCl	0.5	1.1	< 0.1
Medium	55% RH	Never Wetted, 4.9 kg/m^3 NaCl	1.0	1.0	< 0.1
Medium	55% RH	Never Wetted, 7.3 kg/m^3 NaCl	0.8	1.5	< 0.1
Medium	55% RH	Never Wetted, 9.8 kg/m^3 NaCl	2.0	1.5	< 0.1
Long	80% RH	Never Wetted, 3.0 kg/m^3 NaCl	2.8	1.9	0.5
Medium	80% RH	Never Wetted, 4.9 kg/m^3 NaCl	1.8	1.1	< 0.1
Medium	80% RH	Never Wetted, 7.3 kg/m^3 NaCl	1.9	2.2	0.3
Medium	80% RH	Never Wetted, 9.8 kg/m^3 NaCl	3.1	1.9	0.8
Long	Cleveland OH	Covered	1.2	0.9	0.4
Medium	Cleveland OH	Exposed	3.1	0.9	0.6
Long	Cleveland OH	Exposed	2.0	0.3	1.3

[A]Duration: 1 month < Medium < 1 year < Long.
[B]Mean current density after 1 year for long duration tests and after 150 days for medium duration tests.

It appears that treatment with LiBr should increase the protective power and service life of the GCP anode. With the exception of the Cape Perpetua Viaduct, Oregon has only installed ICCP systems on coastal bridges. Occasionally zones have been converted to GCP because of shorts between the rebar and the anode, or because of power supply failures. In these cases, application of LiBr to the anode should help in providing sufficient protection current.

Another measure of the effectiveness of a CP system is depolarization. A common standard is that depolarization, after the IR drop has occurred, should be at least 100 mV. Figure 5.16 for ICCP tests shows that in most cases the 100 mV depolarization was achieved in both the high and low RH environments and without much dependence upon electrochemical age. Figure 5.17 for GCP tests shows that in many cases 100 mV was not achieved, especially as the equivalent electrochemical age increased. The large spread of the depolarization data, combined with very few measurements on control samples, results in no conclusions as to the effectiveness of humectants to achieve 100 mV of depolarization.

6.2.4 Excessive Required Voltage or Circuit Resistance

One way that ICCP anodes can fail is by excessive circuit resistance. This translates to voltage requirements above the ability of the providing power supplies. For example, this was the primary reason that the ICCP test on the Richmond-San Rafael Bridge was ended (*Bullard, et al. 1997b; Covino, et al. 2002*).

Circuit resistance, for a constant current, is proportional to voltage. So reductions in circuit resistance would alleviate the problem of elevated voltage requirements. The rankings, Table 6.1, for ICCP tests are primarily based on long-term values in circuit resistance. In all cases, the use of $LiNO_3$ reduced the circuit resistances as compared to controls. In nearly all of the cases, the use of LiBr also reduced the circuit resistances. Therefore, application of $LiNO_3$ should help to extend the service life of ICCP systems with excessive voltage requirements. The use of LiBr is suspect in this case because the high voltage may lead to oxidation of Br^-, which would limit the time period that this humectant would be effective. However, bridge systems have voltages on the order of 10V, instead of the 100-300V sometimes found in the accelerated laboratory tests, so the proposed mechanism of Br^- oxidation may or may not be applicable.

6.3   LIFE CYCLE CONSIDERATIONS

There are two types of benefits for using humectants described in Section 6.2. The first involves increased time, until adhesion strength loss, results in delamination. This is a long-term benefit and would require repeated applications of a humectant over the lifetime of the anode. The second type involves prolonging the usefulness of the anode when there is a specific problem, such as insufficient protection current in GCP or too high of a voltage in ICCP. These would require spot applications of humectants in problem areas, with reapplication dependant upon the measured success of the humectant to address the problem. It is the first type of humectant use, (the scheduled reapplication of humectant for long-term benefits), which is most amenable to life cycle calculations.

One such life cycle calculation involves translating future costs, *F*, into what those would represent in today's dollars, *P*, given a constant annual interest rate, *i*, for *n* years in the future (*Newnan 1980*), Equation 6-1.

$$P = F(1+i)^{-n} \qquad\qquad \textbf{(6-1)}$$

If one considers two recurring future costs, the cost of ICCP re-installation, *C*, and the cost of humectant application, *H*, then Equation 6-1 can be repeatedly used with various assumptions for *H*, *C*, *i*, and *n*. The values for *n* would come from y_C (the years until ICCP re-installation is required without the use of humectants), y_H (the years between humectant applications), and y_L (the years of added anode lifetime from the humectant). For example, the future cost of the fifth humectant application, with applications occurring every 2 years (y_H=2) would be $H(1+i)^{-10}$. Each of these terms is discussed below.

The cost of ICCP re-installation, *C*, can be estimated from the initial application costs. It should in principle be lower, since part of the initial costs involved restoration of damaged concrete,

assurance of rebar continuity, and elimination of surface metal *(Holcomb and Cryer 1998)*, which should all be lower during reinstallation. Offsetting these cost reductions would be the removal and disposal of the existing zinc anode. In the calculations that follow, the benefits of humectant use will be given in terms of a percentage of, C. A positive benefit is a net gain in present value. A negative benefit is a net loss in present value.

The cost of humectant application, H, should in some respects correlate with the cost of ICCP re-installation, C. This is because both H and C are functions of the size of the anode and the difficulty of access to the concrete surfaces. With little surface preparation and fast application rates, humectant application costs should be relatively lower in ICCP zones that are easily accessible than those that are not easily accessible. In the calculations that follow, H will be given a value of some small percentage of C.

The annual interest rate, i, is assumed to be a constant even though it is very likely to change over time. Examining the consequences of changes in i with time is beyond the scope of this simple life cycle analysis.

The years until ICCP re-installation, y_C, depends on the conditions (corrosion rate and Cl$^-$ content) and microclimate (including humidity, temperature, and rainfall) of the bridge. For relatively wet conditions, 27 years is a reasonable estimate *(Covino, et al. 1996a; Covino, et al. 1996b; Covino, et al. 2002; Holcomb, et al. 1996)*. For dry conditions this will be much lower, and could be as little as 5 years *(Bullard, et al. 1997a; Bullard, et al. 1998; Covino, et al. 2002)*. The benefit of using humectants, in additional years before ICCP re-installation, y_L, can be estimated from changes in adhesion strength and secondary mineralization with humectant use. This investigation was inconclusive as far as bond strength results. However, the possible adhesion strength increases shown for the aged slabs in Figure 5.28, combined with increased Zn infusion into the concrete paste, Figure 5.24, indicate that some increase is probable.

The determination of the time between humectant applications, y_H, was not an emphasis of this study. However, humectants were reapplied in the GCP tests shown in Figures 5.39-5.40. In Figures 5.39 and 5.40b there was a small, but measurable, long-term benefit from the re-treatment that was done after 200 days of the initial GCP. This indicates that the original humectants were still effective. However, in Figures 5.40a, there was a major benefit from reapplication. The results from these particular tests at 55% RH were a bit odd in that these were the only ones that resulted in LiNO$_3$ being superior to LiBr during GCP. Overall, one could surmise that reapplication periods of 1 to 3 years would be appropriate. Data from the field trial, Figure 5.55, indicate a similar period of effectiveness of 2-3 years for LiNO$_3$. One would expect increasing exposure of the treated anode to the washing effects of precipitation would decrease y_H. The more exposed the anode, the higher the expected humectant losses from runoff effects (and thus smaller values for y_H). The field trial zones were a mix of sheltered and boldly exposed areas within each ICCP zone, Figure 4.4. Overall one could surmise that reapplication periods of 1 to 5 years would be appropriate. The microclimate of both the bridge location and location on the bridge can affect the amount of exposure and precipitation runoff. Humectants may be washed from the surface in a similar manner as chlorides are washed from the surface, as illustrated by Figures 5.46 and 5.47. The amount of washing that a surface experiences is a function of rainfall, wave splash, dew formation, wind, and fog.

The results of some sample calculations using Equation 6-1 are shown in Figures 6.1-6.3. In these calculations a time frame of 40 years was considered. In Figure 6.1, with $y_C = 27$ years and an interest rate of 4%, the case when the humectants increased the lifetime of the anode by 9 years (a) and 6 years (b) were considered. The importance of the cost to apply the humectants (H, x-axis) and the time between reapplications (y_H) are apparent in that the benefit of applying humectants are positive with small H and large y_H values, and negative with large H and small y_H values. In dryer conditions, when the time until ICCP installation is reduced (y_C), the benefits of humectants are increased, Figure 6.2. In Figure 6.2: $y_C = 15$ years, $i = 4\%$, and humectants increase the lifetime of the anode by 5 years (a) and 3 years (b).
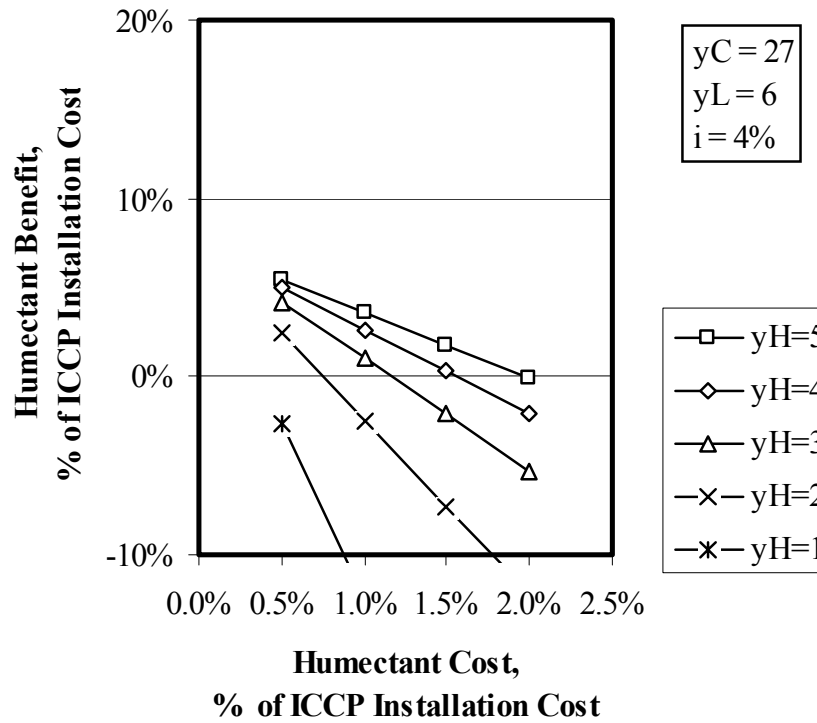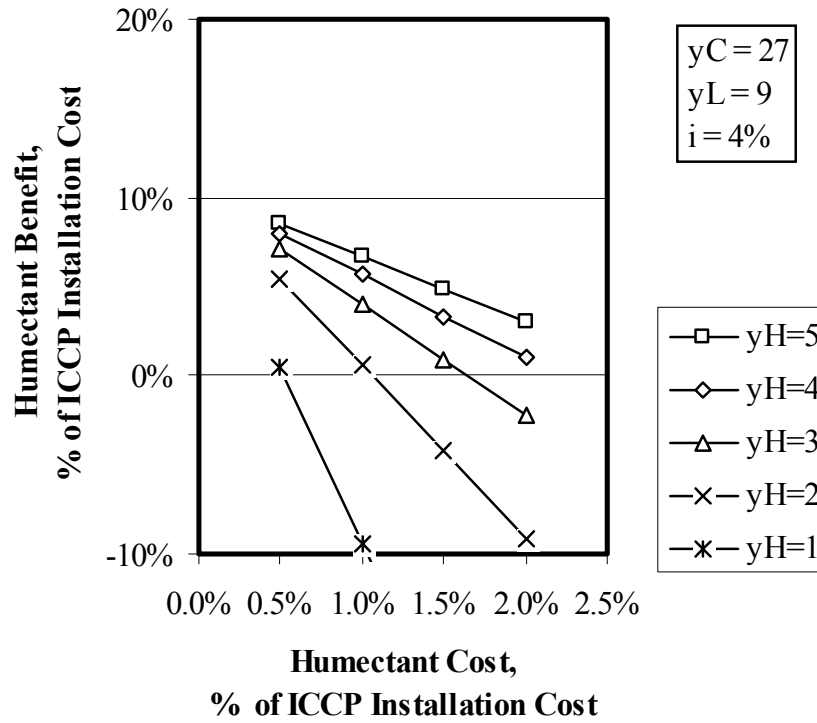
Figure 6.1: Benefits of using humectants, as a % of ICCP installation costs as functions of humectant application costs and cycle times (y_H) for 27 years of anode life (without humectants), an interest Rate of 4%, and an anode life extension of a) 9 years (top) and b) 6 years (bottom). Calculations cover 40 years.
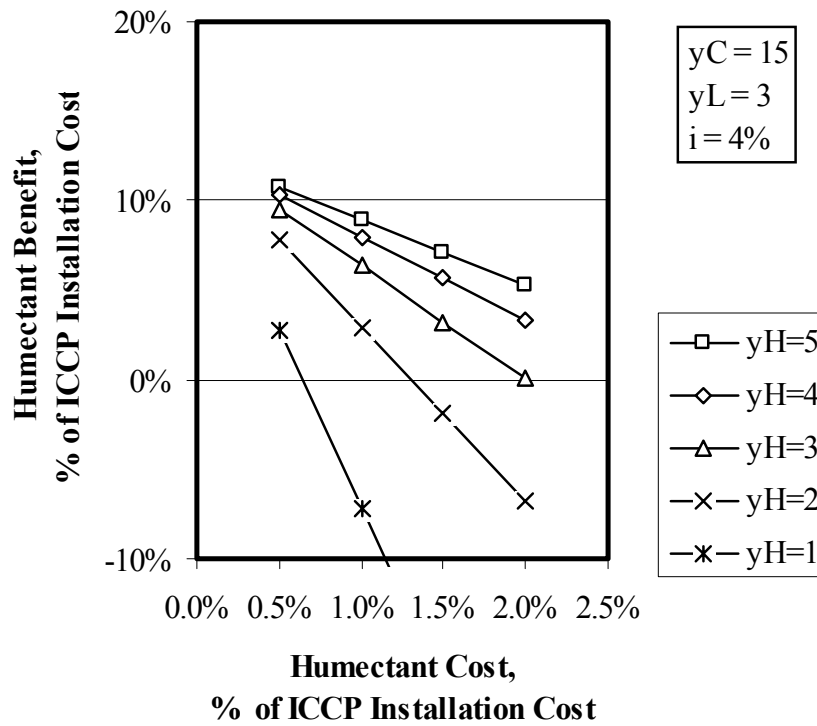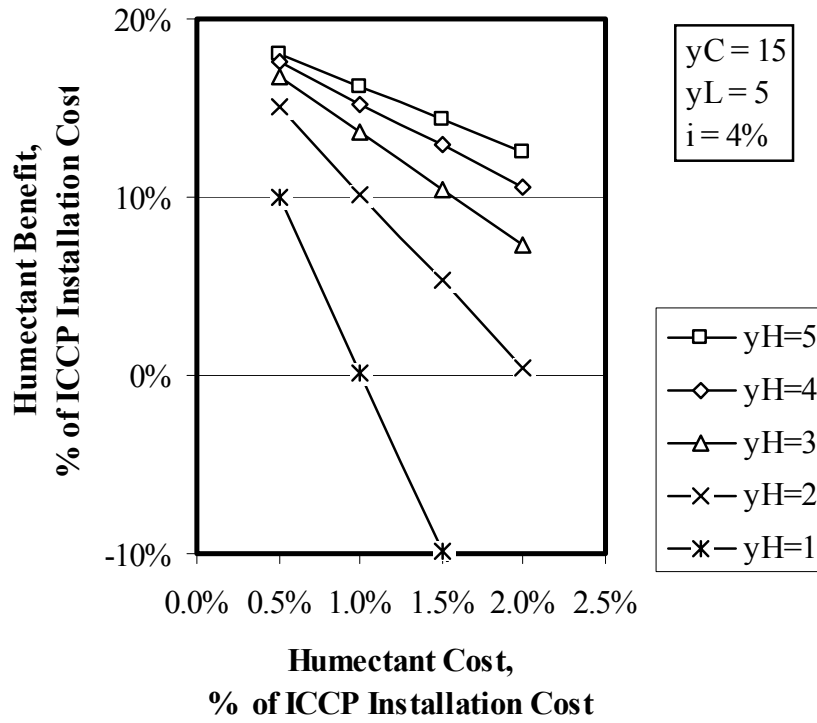
Figure 6.2: Benefits of using humectants, as a % of ICCP installation costs as functions of humectant application costs and cycle times (y_H) for 15 years of anode life (without humectants), an interest Rate of 4%, and an anode life extension of a) 5 years (top) and b) 3 years (bottom). Calculations cover 40 years.

The influence of interest rates are shown in Figure 6.3 for the case of $y_C = 27$ years, $y_L = 9$ years, $y_H = 3$ years and $H/C = 1\%$. At very low interest rates the additional costs of applying the humectants (H) overrides any benefits. In the limit of 0% interest the "benefit" is –13% (13 applications of humectant each costing 1% of C). At high interest rates the earlier costs of applying humectants every 3 years becomes more important. In Figure 6.3 the benefit would become negative at an interest rate of 11.5%.
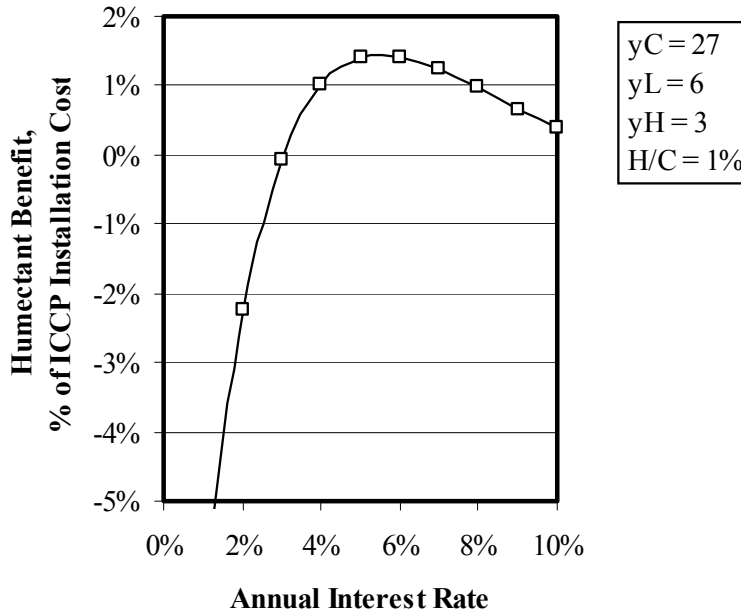

Figure 6.3: Benefits of using humectants, as a % of ICCP installation costs as a function of interest rate for 27 years of anode life (without humectants), a lifetime extension of 6 years, 3 years between humectant applications, and the cost of applying humectants equal to 1% of the ICCP installation costs. Calculations cover 40 years.

To summarize, the five parameters used to obtain Figures 6.1-6.3 were:

- **H/C** – the ratio of the cost of humectant application to the cost of ICCP reinstallation. Values from 0.005 to 0.02 were used.

- **y_C** – the expected lifetime of the anode without humectant treatment. Values of 27 years (normal wet conditions) and 15 years (dryer conditions) were used.

- **y_L** – the expected lifetime gain from humectant use. Values of 9 and 6 years were used for y_C=27; values of 5 and 3 years were used for y_C=15.

- **y_H** – the time between humectant applications. Values between 1 and 5 years were used.

- **i** – the interest rate. Most calculations used a value of 4%.

6.4   ACCELERATED LABORATORY TESTS

The usefulness of accelerated ICCP tests for ICCP applications was demonstrated by producing similar rankings in humectant effectiveness and in producing similar microscopic reaction zones in the zinc/concrete interface.

The use of circuit resistance allows ICCP applications with different current levels to be compared. The cyclic tests between accelerated and non-accelerated ICCP, at low RH, showed similar results in terms of circuit resistance with that found after the period of high impressed currents on the Yaquina Bay Bridge. In both cases (Figures 5.7 and 5.54) the higher current levels produced lower circuit resistances than the low current levels. This was the case even though circuit resistance normally tracks the same, regardless of current levels (as in Figure 5.6).

The different results between those found with LiBr and $LiNO_3$ in GCP and ICCP tests showed how one must be careful when using accelerated tests. Most of the electrochemical processes between GCP and ICCP are the same. So both humectants could be expected to respond with the same rankings in GCP as in ICCP. However, the higher voltages in ICCP may have led to the oxidation of Br^- ions in the LiBr treated samples, which did not occur in GCP.

6.5   COLLECTING AND EXAMINING OPERATING DATA

The CP systems on the Oregon coast are well instrumented in terms of recording current levels and voltages, and in delivering that data to off-site locations. However, there has not been a systematic approach that allows for the data to be readily examined or interpreted. As Figure 5.54 shows, gaps in data can result from inoperative equipment or loss of collected data. Differences in the noise levels in Figure 5.54 showed the importance of gathering the data to a sufficient number of decimal places (more than the 1 and 2 decimal places for voltage and current used to calculate the circuit resistance during time Period II).

Besides collecting operating data, the data also need to be regularly examined for defective equipment or for errors in operating the equipment. Examples of this would be current levels being set too low (for insufficient corrosion protection) or too high (for unnecessary aging of the anode, Periods IV-V in Figure 5.54).

Beyond examining current density and voltage, circuit resistance offers a measurement that relates to the electrochemical age of the anode and to more readily compare structures with different current levels. It should be noted that increases in current density are also apparent in circuit resistance data, as seen in the transition between Periods II and III in Figure 5.54.

7.0 CONCLUSIONS

Humectant Mechanisms

- Humectants bring moisture into the Zn anode and concrete by their affinity for water (i.e., lowering the activity of water).

- From a thermodynamic argument, LiBr should be a more effective humectant than $LiNO_3$, since it lowers the activity of water more than $LiNO_3$, especially in environments with an RH below 50%.

Humectant Effectiveness

- $LiNO_3$ and LiBr were both effective in lowering the long-term circuit resistance in ICCP, raising the long-term galvanic current density in GCP, and in keeping the depolarization voltage above 100 mV in laboratory ICCP tests.

- LiBr was more effective than $LiNO_3$ in GCP. This was consistent with the lower water activity expected with LiBr as compared with $LiNO_3$.

- $LiNO_3$ was more effective than LiBr in ICCP.

- Based on literature sources, the low Br levels found in aged ICCP anodes was consistent with higher voltages leading to Br^- oxidation and the subsequent evolution of Br_2 or conversion to oxygen derivatives of Br. $LiNO_3$ is already fully oxidized and is not susceptible to further oxidation.

- $KC_2H_3O_2$ was not effective as a humectant and was especially detrimental in terms of loss of adhesion strength. It was dropped from consideration after poor early results.

- Application of LiBr and $LiNO_3$ to aged anodes was just as effective as applications to new anodes.

- The field trial suggests that the chemistry of the anode-concrete interface was modified somewhat by the presence of the humectant, leading to improved ion mobility as evidenced by greater chloride accumulation at the interface and broadening of the zinc oxide reaction product layer.

- Significant leaching of $LiNO_3$ from the treated zone on the Yaquina Bay Bridge occurred over a two-year test period.

Increased Service Life

- Humectant treatment increased the protection current in GCP. Spot application of humectants would prolong the useful life of GCP zones that were not achieving sufficient galvanic current.

- Long-term increases in circuit resistances occur during ICCP. Spot applications of humectants lower the circuit resistance, retarding the effects of electrochemical aging on the anode and extending its service life.

- Increased service life, based on bond strength results, was inconclusive. However, a case can be made for small increases of 0-3 years based on treatments to anodes with prior ICCP aging.

- Increased service life was apparent from circuit resistance results from the Yaquina Bay Bridge field trial. Service life extensions of 2-3 years are possible by treatment with $LiNO_3$. Longer service life extension may have been indicated by these results if the anode had not been aged at a greatly accelerated rate during the field trial.

Life Cycle Considerations

- A life cycle cost model was developed for humectant application and its effects on delaying anode replacement.

- The usefulness of the model is limited by uncertainties in the expected lifetime gains due to humectants (y_L) and by the years between humectant reapplication (y_H).

- Humectant treatments are expected to be most beneficial, in terms of life cycle costs, when the ratio of the cost of humectant application to the cost of ICCP reinstallation (*H/C*) is small (likely in ICCP zones with easy access), or when the time between humectant applications (y_H) is large (likely in sheltered ICCP zones with less humectant loss due to washing).

Accelerated Laboratory Tests

- Accelerated tests proved useful in producing similar humectant rankings as found in the Yaquina Bay Bridge field trial.

- The increased voltages used in accelerated ICCP tests, as compared with GCP, may have caused the differences in humectant rankings between ICCP and GCP. This illustrated one of the hazards in using accelerated tests.

Other Conclusions About CP Systems

- Bond strengths of GCP anodes were much greater than those of ICCP anodes for equivalent electrochemical ages.

- Circuit resistance arises from a variety of bulk and interfacial resistances, and from polarization at the anode and cathode. The 60-cycle AC resistance accounts for an average of 25% of the total circuit resistance.

- Operating data from field installations of CP need to be regularly examined for equipment malfunctions and changes in operating parameters that adversely impact the service life of ICCP anodes.

8.0   RECOMMENDATIONS

- Spot applications of LiBr should allow GCP zones that are not achieving enough galvanic current to remain useful and to prolong their useful life.

- Spot applications of $LiNO_3$ should allow ICCP zones that are becoming voltage limited to remain useful and to prolong their useful life.

- The decision to use $LiNO_3$ in ICCP zones for increased service life needs to be examined further, on a case-by-case basis, in terms of H/C (the ratio of the cost of humectant application to the cost of ICCP reinstallation), y_C (the expected lifetime of the anode without humectant treatment), y_L (the expected lifetime gain from humectant use), and y_H (the time between humectant applications).

- In cases where H/C is expected to be small (i.e., ICCP zones with easy access) and y_H is expected to be large (sheltered ICCP zones with less humectant loss due to washing) the use of $LiNO_3$ is expected to be cost effective.

- Operating data from CP field installations need to be regularly examined for malfunctions of operating equipment and changes in system operating conditions that may have detrimental consequences for the service life of coastal bridge ICCP systems. Out of specification operating conditions must be corrected in a timely manner to preserve Oregon's investment in these systems.

9.0   REFERENCES

AASHTO. 1995. Sampling and Testing for Chloride Ion in Concrete and Concrete Raw Materials. Standard Specifications for Transportation Materials and Methods of Sampling and Testing, 17th ed., part II. no. T 260-94. Washington, DC.

Bennett, J. 1998. Chemical Enhancement of Metallized Zinc Anode Performance. CORROSION/98, paper 98640. Houston: NACE International.

Bennett, J.E., Schue, T.J., Clear, K.C., Lankard, D.L., Hartt, W.H., and Swiat, W.J. 1993. *Electrochemical Chloride Removal and Protection of Concrete Bridge Components: Laboratory Studies*. Report SHRP-S-657, Washington D.C.: Strategic Highway Research Program, National Research Council.

Bennett, J.E., Bushman, J.B., Costa, J., and Noyce, P. 2000. Field Application of Performance Enhancing Chemicals to Metallized Zinc Anodes. Corrosion/2000, paper 00790. Houston: NACE International.

Bullard, S. J., Covino, B. S., Jr., Holcomb, G. R., Cramer, S. D., and McGill, G. E. 1997a. Bond Strength of Thermal-Sprayed Zinc on Concrete During Early Stages of Electrochemical Aging. CORROSION/97, paper 97232. Houston: NACE International.

Bullard, S. J., Cramer, S. D., Covino, B. S., Jr., Holcomb, G. R., McGill, G. E., Cryer, C. B., Reis, R. 1997b. Thermal Sprayed Zinc Anodes: Laboratory and Field Studies. In *Expanding Coatings Knowledge Worldwide*, Proceedings of the SSPC 1997 Seminars, pp. 309-319. Pittsburgh: Steel Structures Paint Council.

Bullard, S. J., Cramer, S. D., Covino, B. S., Jr., Holcomb, G. R., McGill, G. E., and Reis, R. 1998. Thermal-Sprayed Anodes for Cathodic Protection of Reinforced Concrete Bridges. In *Concrete Under Sever Conditions: Environment and Loading*, Proceedings of the Second International Conference on Concrete Under Severe Conditions, eds. O. E. Gjørv, K. Sakai, and N. Banthia, pp. 959-969. London: E&FN Spon.

Bullard, S. J., Covino, B. S., Jr., Cramer, S. D., Holcomb, G. R., Russell, J. H., Bennett, J. E., Cryer, C. B. 2000. Performance Of Thermal-sprayed Zinc Anodes Without and with Humectants in Impressed Current Cathodic Protection Systems. In *Corrosion Control as a Base for a Suitable Development*, Proceedings of LATINCORR: 2000, 7th Ibero-American Congress of Corrosion and Protection and 4th NACE Latin-American Region Corrosion Congress. Cartagena de Indias, Columbia.

Bullard, S. J, Covino, B. S., Jr., Cramer, S. D., Holcomb, G. R., Russell, J. H., Bennett, J. E., Milius, J. K., Cryer, C. B., Soltesz, S. M. 2001. Performance of Thermal-Sprayed Zinc Anodes Treated with Humectants in Cathodic Protection Systems. In Concrete Under Severe Conditions: Environment and Loading, Proceedings of the Third International Conference on Concrete Under Severe Conditions, Vol. 2, eds. N. Banthia, K. Sakai, and O. E. Gjørv, pp. 1801-1808. Vancouver BC, Canada: The University of British Columbia, 2001.

Covino, B. S., Jr., Bullard, S. J., Holcomb, G. R., Cramer, S. D., McGill, G. E., and Cryer, C. B. 1995. Factors affecting the bonding of arc-sprayed zinc to concrete. *In Balancing economics and compliance for maintaining protective coatings*, p. 115. Pittsburgh, PA: Steel Structures Painting Council.

Covino, B. S., Jr., Cramer, S. D., Bullard, S. J., Holcomb, G. R., McGill, G. E., and Cryer, C. B. 1996a. Factors Affecting Thermal-Sprayed Zinc Anodes on Concrete. In *Proceedings of 13th International Corrosion Congress*, Vol. II, paper 173. Clayton, Australia: Australasian Corrosion Association.

Covino, B. S., Jr., Cramer, S. D., Holcomb, G. R., Bullard, S. J., McGill, G. E., and Cryer, C. B. 1996b. Thermal-Sprayed Zinc Anodes for Cathodic Protection of Reinforced Concrete Structures. In *Materials for the New Millennium*, Proceedings of the 4th Materials Conference, Vol. 2, ed. K. P. Chong, pp. 1512-1521. New York: American Society of Civil Engineers.

Covino, B. S., Jr., Bullard, S. J., Cramer, S. D., Holcomb, G. R., McGill, G. E., Cryer, C. B., Stoneman, A., and Carter, R. R. 1997a. Interfacial Chemistry of Zinc Anodes for Reinforced Concrete Chemistry. CORROSION/97, paper 97233. Houston: NACE International.

Covino, B. S., Jr., Bullard, S. J., Holcomb, G. R., Cramer, S. D., McGill, G. E., and Cryer, C. B. 1997b. Bond strength of electrochemically-aged arc-spray coatings on concrete. Corrosion 53(5): 399-411.

Covino, B. S., Jr., Bullard, S. J., Holcomb, G. R., Russell, J. H., Cramer, S. D., Bennett, J. E., and Laylor, H. M. 1999a. Chemical Modification of Thermal-Sprayed Zinc Anodes for Improved Cathodic Protection of Reinforced Concrete. In *Proceedings of the 14th International Corrosion Congress*, paper 33.0. Kelvin, South Africa: Corrosion Institute of Southern Africa.

Covino, B. S., Jr., Bullard, S. J., Holcomb, G. R., Russell, J. H., Cramer, S. D., Bennett, J. E., and Laylor, H. M. 1999b. Chemically-Modified Thermal-Spray Zinc Anodes for Galvanic Cathodic Protection. *Materials Performance*. 38(12): 28-32.

Covino, B. S., Jr., Holcomb, G. R., Bullard, S. J., Russell, J. H., Cramer, S. D., Bennett, J. E., and Laylor, H. M. 1999c. Electrochemical Aging of Humectant-Treated Thermal-Sprayed Zinc Anodes for Cathodic Protection. CORROSION/99, paper 99548. Houston: NACE International.

Covino, B. S., Jr., Russell, J. H., Bullard, S. J., Holcomb, G. R., and Cramer, S. D. 2000. Nondestructive Evaluation of Thermal Spray Cathodic Protection Anodes. CORROSION/2000, paper 00811, Houston: NACE International.

Covino, B. S., Jr., Cramer, S. D., Bullard, S. J., Holcomb, G. R., Russell, J. H., Collins, W. K., Laylor, H. M., and Cryer, C. B. 2002. *Performance of Zinc Anodes for Cathodic Protection of Reinforced Concrete Bridges.* Final Report, SPR 364 (FHWA-OR-RD-02-10), Washington, DC: Federal Highway Administration.

Cramer, S. D., Bullard, S. J., Covino, B. S., Jr., Holcomb, G. R., Russell, J. H., Cryer, C. B., and Laylor, H. M. 2002a. Carbon Paint Anode for Reinforced Concrete Bridges in Coastal Environments. CORROSION/2002, paper 02265, Houston: NACE International.

Cramer, S. D., Covino, B. S., Jr., Bullard, S. J., Holcomb, G. R., Russell, J. H., Nelson, F. J., Laylor, H. M., and Soltesz, S. M. 2002b. Corrosion Prevention and Remediation Strategies for Reinforced Concrete Coastal Bridges. *Cement & Concrete Composites* 24:101-117.

Fontana, M. G., and Greene, N. D. 1978. *Corrosion Engineering.* 2nd ed. New York: McGraw-Hill.

Holcomb, G. R., Bullard, S. J., Covino, B. S., Jr., Cramer, S. D., Cryer, C. B., and McGill, G. E. 1996. Electrochemical Aging of Thermal-Sprayed Zinc Anodes on Concrete. In *Thermal Spray: Practical Solutions for Engineering Problems*, Proceedings of the 9th National Thermal Spray Conference, ed. C. C. Berndt, pp. 185-192. Metals Park, OH: ASM International.

Holcomb, G. R., and Cryer, C. B. 1998. Cost of Impressed Current Cathodic Protection for Coastal Oregon Bridges. *Materials Performance* 37(7): 22-26.

Holcomb, G. R., Covino, B. S., Jr., Russell, J. H., Bullard, S. J., Cramer, S. D., Collins, W. K., Bennett, J. E., and Laylor, H. M. 2000a. Humectant Use in Cathodic Protection of Reinforced Concrete. CORROSION/2000, paper 00812. Houston: NACE International.

Holcomb, G. R., Covino, B. S., Jr., Russell, J. H., Bullard, S. J., Cramer, S. D., Collins, W. K., Bennett, J. E., and Laylor, H. M. 2000b. Humectant Use in Cathodic Protection of Reinforced Concrete. *Corrosion*. 56: 1140-1157.

Koch, G. H., Brongers, M. P. H., Thompson, N. G., Virmani, Y. P., and Payer, J. H. 2002. *Corrosion Cost and Preventive Strategies in the United States*, FHWA-RD-01-156, Washington, DC: Federal Highway Administration, U.S. Department of Transportation.

Mehta, P. K. 1991. *Concrete in the Marine Environment*. NewYork, NY: Elsevier Applied Science, pp. 73-100.

Newnan, D. G, 1980. *Engineering Economic Analysis*. San Jose, CA: Engineering Press. pp. 45, 286.

Orlova, N. V., Westall, J. C., Rehani, M., and Koretsky, M. D. 1999. *The Study of Chloride Ion Migration in Reinforced Concrete under Cathodic Protection*, Salem, OR: Oregon Department of Transportation. FHWA-OR-RD-00-03.

Pourbaix, M. 1974. *Atlas of Electrochemical Equilibria*. Houston: NACE International. pp. 99, 604-610.

Powers, R., Sagues, A., and Murase, T. 1992. Sprayed-Zinc Galvanic Anodes for the Cathodic Protection of Reinforcing Steel in Concrete. In *Materials: Performance and Prevention of Deficiencies and Failures*, ed. T.D. White, pp. 732-747. New York: American Society of Civil Engineers.

Robinson, R. A., and Stokes, R. H. 1959. *Electrolyte Solutions*. 2nd ed. London: Butterworths Publications. p. 510.

Sagues, A., Powers, R., Murase, T., and Lasa, I.. 1994. *Low-Cost Sprayed Zinc Galvanic Anode for Control of Corrosion of Reinforcing Steel in Marine Bridge Substructures*. Final Report, Contract No. SHRP-88-ID024, Washington D.C.: Strategic Highway Research Program, National Research Council.

Scannell, W. T., Sohanghpurwala, A. A., and Powers, R. G. 1995. Sacrificial Cathodic Protection of Prestressed Concrete Bridge Pilings in a Marine Environment. *1995 Conference on Corrosion and Infrastructure: Practical Applications and Case Histories*. Conference Abstracts. pp. 91-94. Houston, TX: NACE International.

Sugino, K. 1964. Bromates, Electrolytic Production. *The Encyclopedia of Electrochemistry*, ed. C.A. Hampel, pp. 127-130. New York: Reinhold Publishing Corp.

Stokes, R. H., and Robinson, R. A. 1949. Standard Solutions for Humidity Control at 25°C. *Industrial & Engineering Chemistry* 41:2013.

Wagner, J. 1992. *Cathodic Protection—Design I Course*. Houston: NACE International. p. 3:15.

Weast, R. C., ed. 1979. *Handbook of Chemistry and Physics*. 59th ed. Boca Raton, FL: CRC Press. pp. B131-B132.

Zaytsev, I. D., and Aseyev, G. G. 1992. *Properties of Aqueous Solutions of Electrolytes*. Boca Raton, FL: CRC Press. pp. 1691, 1721

APPENDIX

POSTASSIUM ACETATE RESULTS

APPENDIX

RESULTS FOR POTASSIUM ACETATE (KC$_2$H$_3$O$_2$)

During the course of the project it was decided by the researchers and the technical advisory committee to drop potassium acetate, KC$_2$H$_3$O$_2$, from further study. The initial laboratory results (both indoor and outdoor) showed that KC$_2$H$_3$O$_2$ was detrimental to the Zn anode in terms of ICCP circuit resistance and GCP protection current. This appendix presents the data that was collected on the KC$_2$H$_3$O$_2$-treated samples prior to eliminating it from the study (and that was not presented in the main body of the report). The figure caption numbers are used for referring back to equivalent figures in the main body of the report for comparison with LiBr- and LiNO$_3$-treated samples.
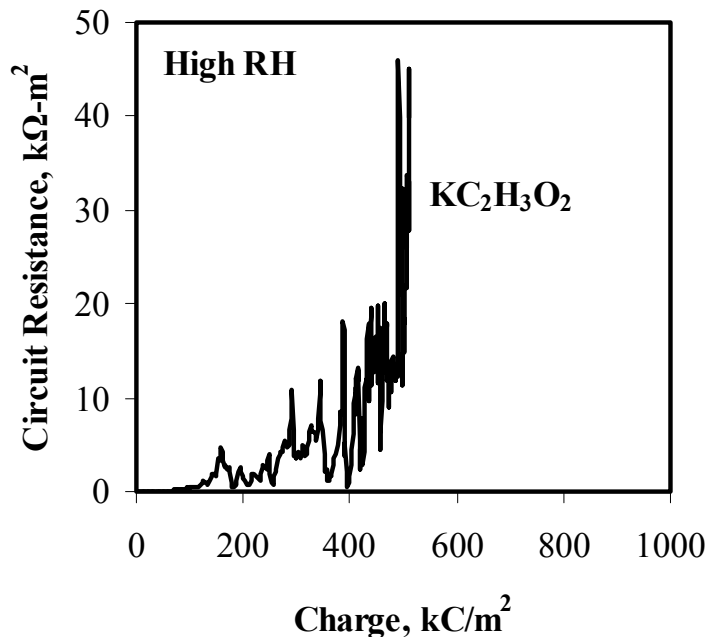
Figure A5.1: Circuit resistances of new ICCP slabs in high RH conditions
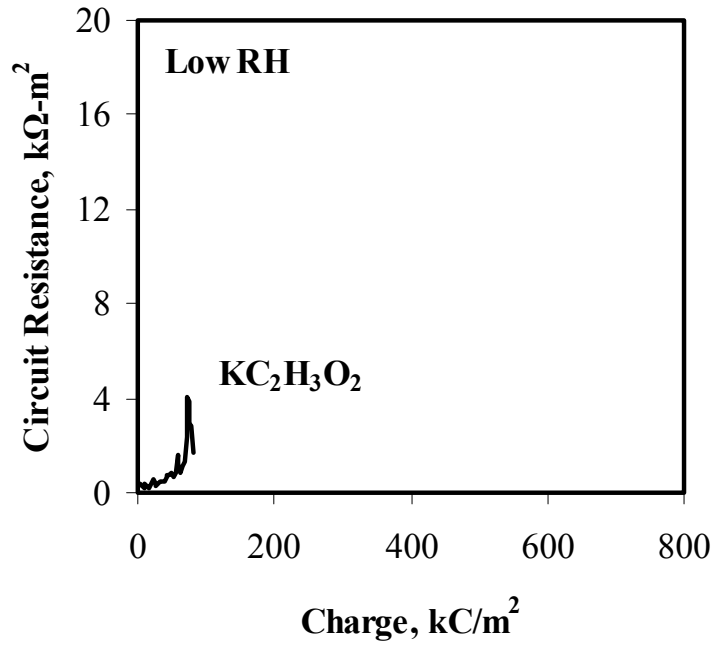
Figure A5.2: Circuit resistances of new ICCP slabs in low RH conditions
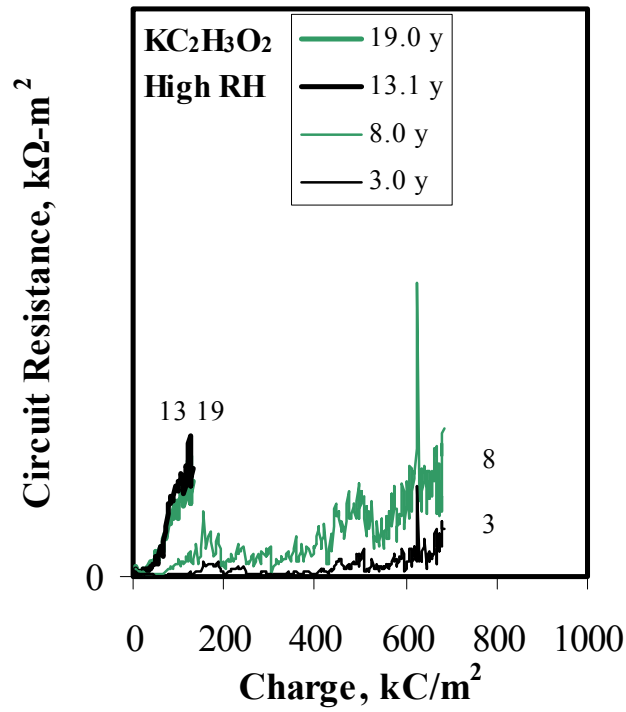
Figure A5.3: Circuit resistances of aged ICCP slabs in high RH conditions
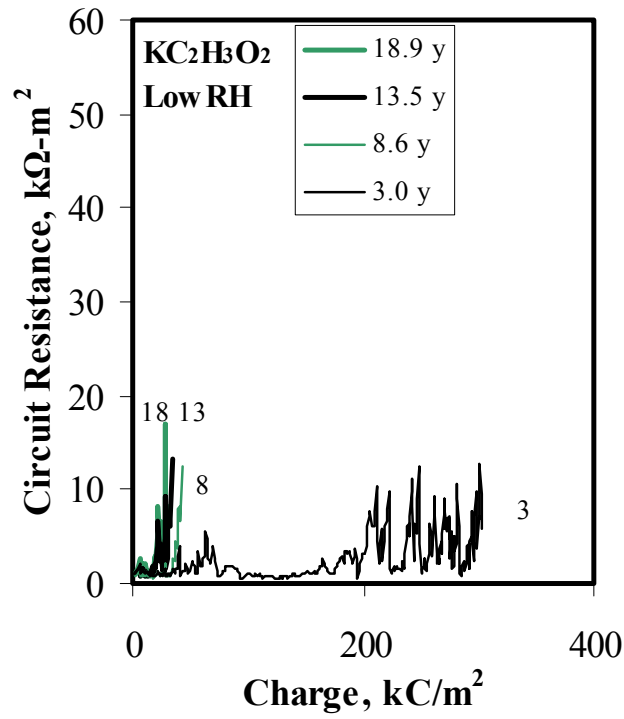
Figure A5.4: Circuit resistances of aged ICCP slabs in low RH conditions
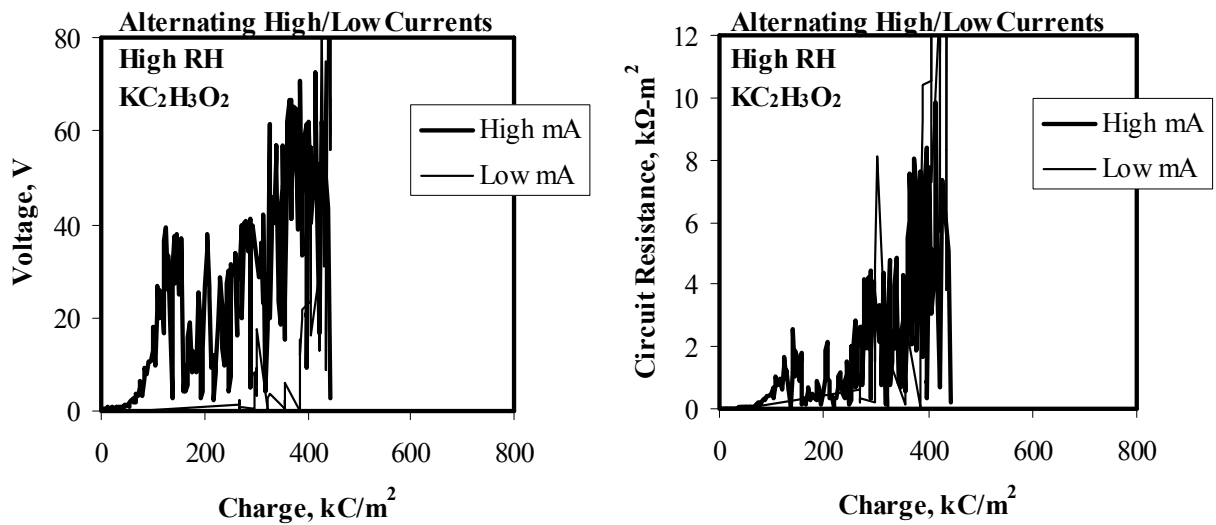
Figure A5.6: Cyclic ICCP voltages (left) and circuit resistances (right) in high RH conditions
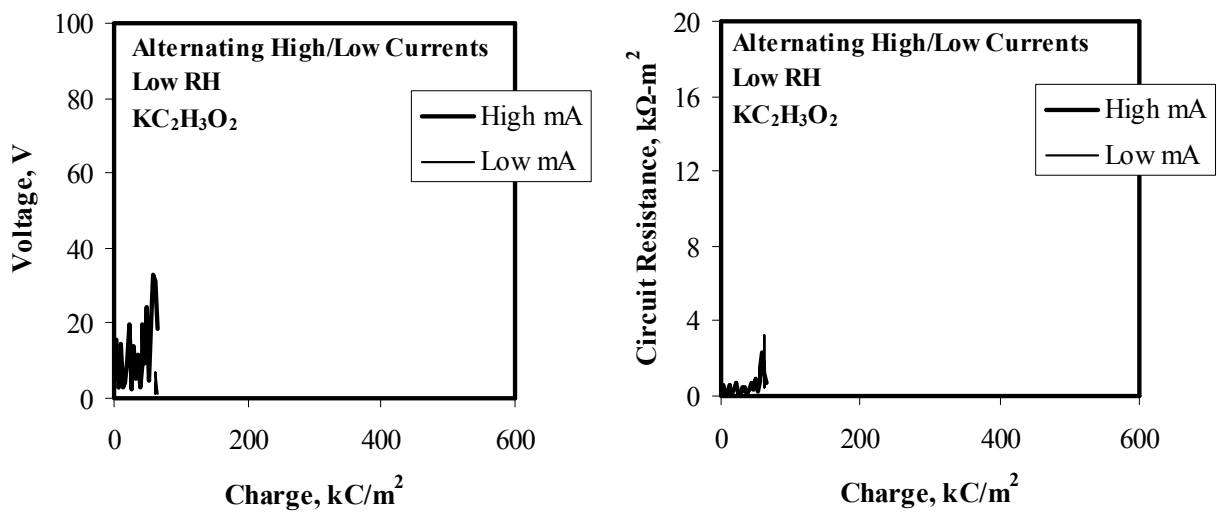
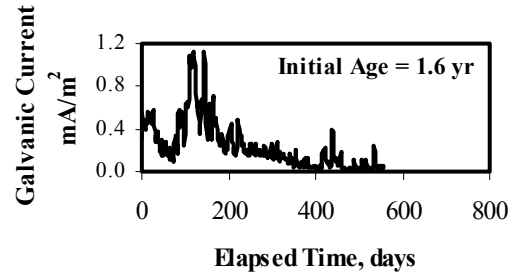Figure A5.7: Cyclic ICCP voltages (left) and circuit resistances (right) in low RH conditions
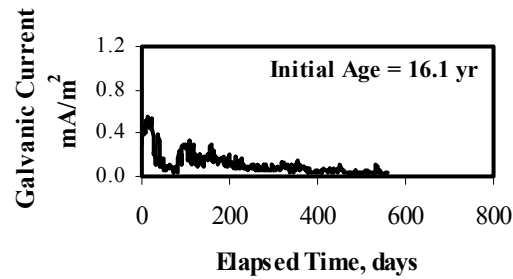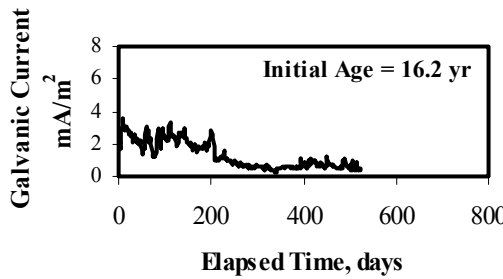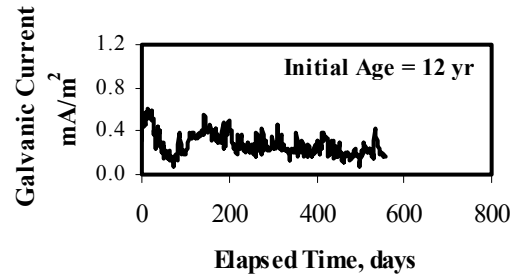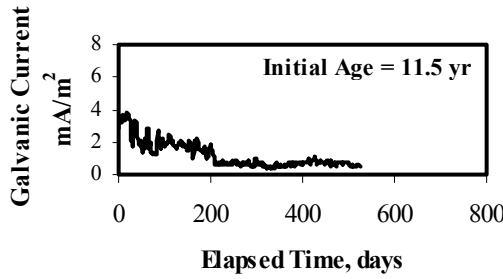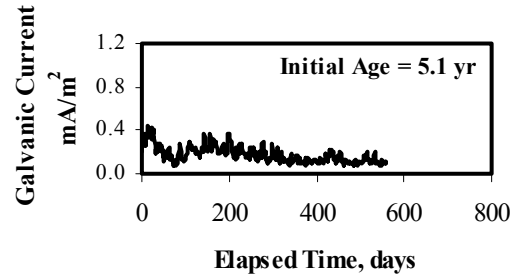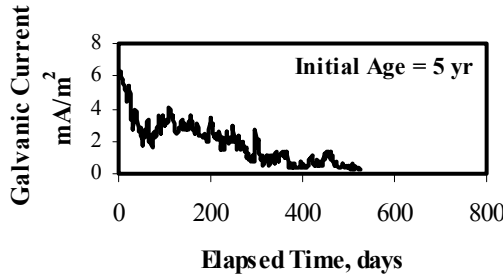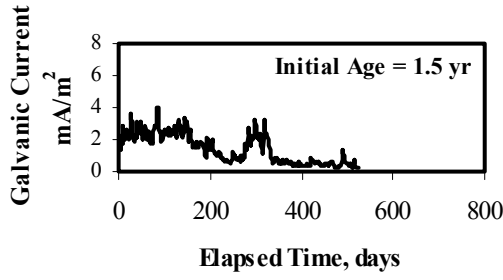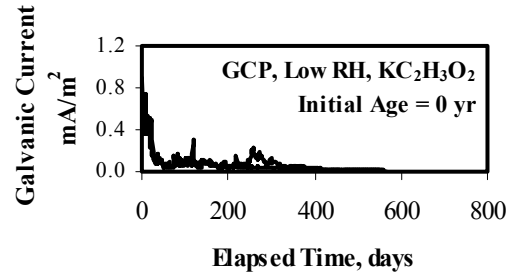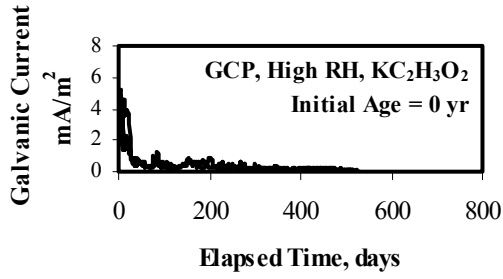
Figure A5.8: Galvanic currents for new and aged slabs with $KC_2H_3O_2$ in high RH conditions

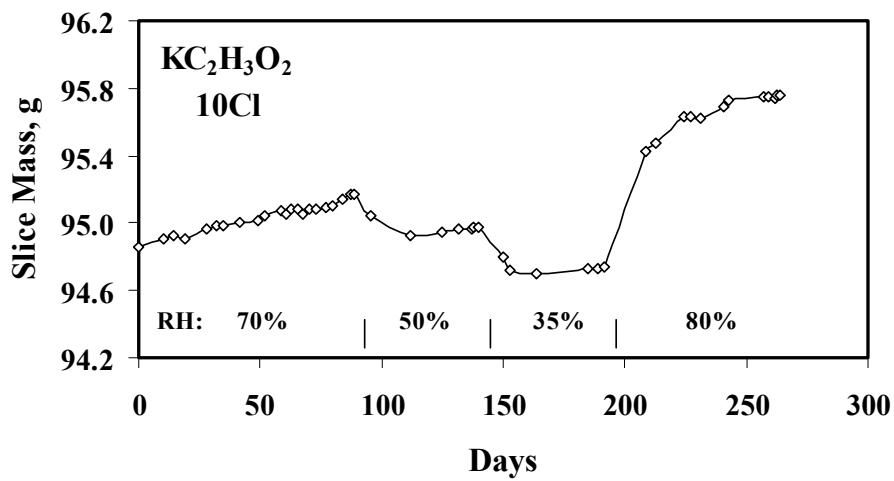Figure A5.10: Galvanic currents for new and aged slabs with $KC_2H_3O_2$ in low RH conditions
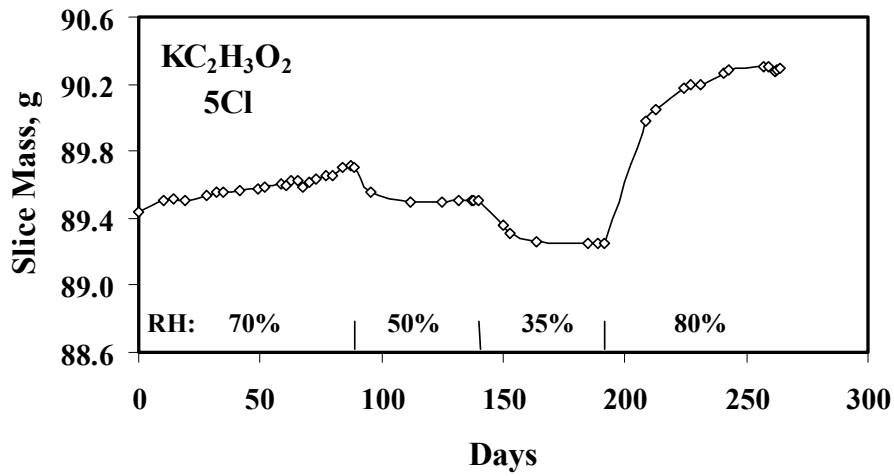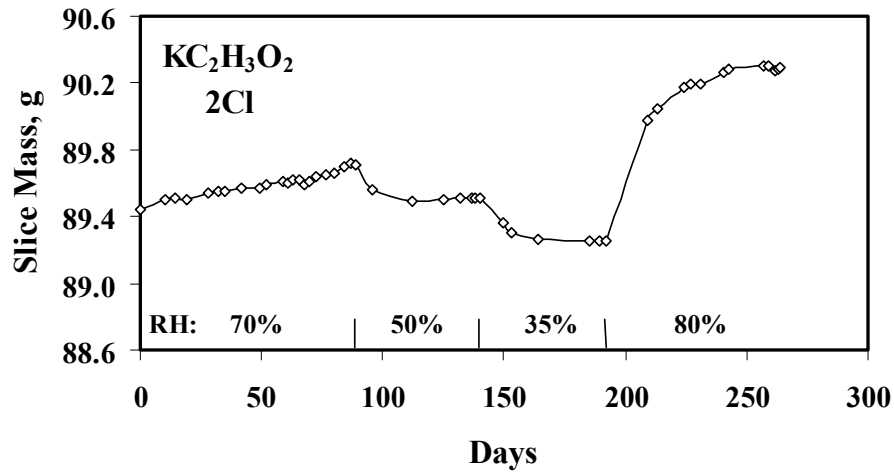
Figure A5.34: Mass change with exposure time of $KC_2H_3O_2$-treated slices at 90ºF (32.2ºC). The NaCl concentrations were 2.0, 5.0, and 10.0 lb/yd^3 (1.2, 3.0, and 5.9 kg/m^3).
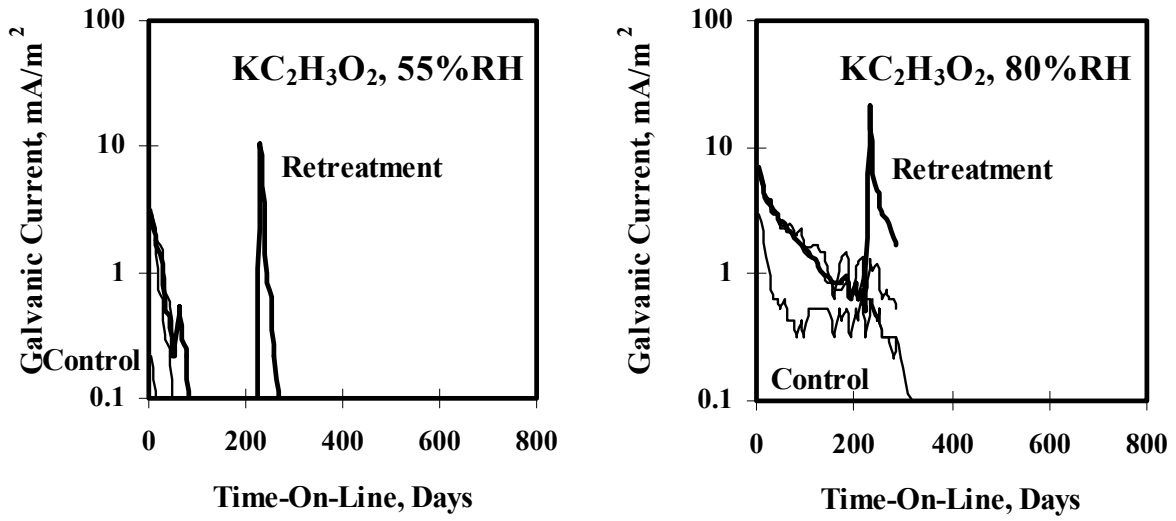
Figure A5.39: Galvanic current for KC$_2$H$_3$O$_2$-treated blocks (with 3.0 kg/m^3 NaCl). Retreatment of one block after about 200 Days (shown in bold). The environments were a) 55% RH (left) and b) 80% RH (right).